PTEN *in Vitro* and *in Silico*: Implications in Cancer and Autism

By
Sean B. Johnston

A dissertation submitted in partial fulfillment of the requirements for the degree of

Doctor of Philosophy
(Biochemistry)

at the

UNIVERSITY OF WISCONSIN – MADISON

2015

Date of final oral examination: 4/21/2015

This dissertation is approved by the following members of the Final Oral Committee:
Ronald T. Raines, Professor, Departments of Biochemistry and Chemistry
Richard A. Anderson, Professor, School of Medicine and Public Health
Laura L. Kiessling, Professor, Departments of Biochemistry and Chemistry
David J. Pagliarini, Assistant Professor, Department of Biochemistry
Alessandro Senes, Associate Professor, Department of Biochemistry

"Optimism is the faith that leads to achievement. Nothing can be done without hope and confidence."

Helen Keller

UNIVERSITY OF WISCONSIN – MADISON

Abstract

Department of Biochemistry

Doctor of Philosophy

PTEN *in Vitro* and *in Silico*: Implications in Cancer and Autism

by Sean B. Johnston

Compared to most other tumor suppressors known to be crucial to cancer development, PTEN was relatively recently discovered. Current estimates put defects in the *PTEN* gene as the cause of 50–80% of sporadic tumors (including glioblastoma and prostate cancer) and 30–50% of breast, colon, and lung cancers. Mutations in *PTEN* in the human germline result in tumor syndromes like Cowden syndrome, which is associated with a much greater risk of cancer in all tissues. PTEN has a central antagonistic role in a crucial development and proliferation pathway. Given the centrality of this protein in cancer and proliferation pathways, additional information concerning the biochemical mechanisms by which PTEN performs its roles is crucial. In this thesis, I focus on biochemical aspects of the PTEN protein and explore mechanisms by which PTEN function can be compromised.

In Chapter 2, I develop a new continuous assay for PTEN phosphatase activity and provide the first in-depth characterization of activity of a novel isoform of PTEN, PTEN-L. I also present an explanation for the enhanced activity of PTEN-L and confirm previous findings of activation of PTEN by monodisperse product. In Chapter 3, I develop an assay to measure the thermodynamic stability of PTEN and use this to analyze a number of variants of PTEN that are linked to cancer, PTEN hamartoma tumor syndromes, and autism spectrum disorders. In Chapter 4, I develop a machine-learning algorithm specific to predicting harmful PTEN amino acid variations. Last, in Chapter 5, I propose future directions for the continuation of this work, as well as present additional data on the way to elucidating more about PTEN and its function.

Acknowledgements

I would like to express my deepest gratitude to everyone who has helped me along this long and sometimes challenging path to where I am today. First, I would like to thank my thesis advisor, Professor Ronald T. Raines. While I was considering which lab to join years ago, I was struck by Ron's optimism and enthusiasm for the many projects and opportunities in his lab. The project he pitched—the one that would eventually transform into this body of work—offered me an opportunity to be very independent and self-motivated. I was excited to start working on such an important protein with an excited and helpful guide. The Raines Lab, with its focus on protein biochemistry alongside an extremely capable team of organic chemists, has been the perfect place for me to become the scientist I am today. The interdisciplinary nature of the lab has allowed me to become accustomed to seeing topics from different perspectives, able to see possibilities for projects that wouldn't be possible in other settings. Ron is also a fantastic writer—his expert editing of manuscripts has been crucial to the clear communication of the science contained in this document.

I would like to thank my committee members for their support and guidance over the years: Professors Richard Anderson, Paul Bertics, Laura Kiessling, David Pagliarini, and Alessandro Senes. I am also grateful for the scientific discussions with Dr. Darrell McCaslin at the Biophysics Instrumentation Facility early in my career. I have had many discussions with and support also from Dr. David Aceti, with whom I was able to talk to a fair amount about topics concerning differential scanning fluorimetry and

graciously allowed access to crucial instrumentation. I also want to thank my undergraduate advisors: Professor Robert Hanson, who helped me launch my love of scientific computation, and Professor Greg Muth, who inspired my interest in biochemistry.

I do not think I would be where I am today were it not for support from Dr. Kelley Harris-Johnson. I met Kelley when I was a teacher's assistant for Biochemistry 501, where I was able to assist with students' understanding of introductory biochemistry concepts. Her support and guidance has been indispensable.

An immense part of the Raines Lab experience is the people that are part of it. I was immediately drawn to the sense of togetherness that this lab engenders, even though many of the projects are so disparate in nature. I believe that everyone I've had contact with has helped me along in my scientific development. In the Raines Lab, I've had expert advice from elder grad students and postdocs who have moved on: Drs. Rasomoy Biswas, Ben Caes, Sayani Chattopadhyay, Ho-Hsuan Chou, Amit Choudary, Greg Ellis, Katrina Jensen, Mike Levine, Langdon Martin, Nick McGrath, Brett VanVeller, and Rex Watkins. Thanks specifically to Dr. Mike Palte for his sage advice for my doctorate and my career. I've been privileged to work more recently alongside Kristen Anderson, Matt Aronoff, Wen Chyan, Jesus Dones Monroig, Aubrey Ellison, Emily Garnett, Dr. Brian Gold, Brian Graham, Trish Hoang, Leland Hyman, Kalie Mix, Robert Newberry, Robert Presler, Thom Smith, Val Tripp, Kaylee Underkofler, Jim Vasta, and Ian Windsor. I've had an excellent opportunity for nerdy discussions with Dr. Çağlar Tanrıkulu. I want to specifically thank Chelcie Eller and Joelle Lomax for many late-night discussions concerning science and everything else.

I want to express my deepest gratitude to my girlfriend, Abby Panozzo, for her love and everlasting support. Even from far away, I can always count on her for a phone call to lift my spirits.

Last and very importantly, I am eternally indebted to my family. My parents, David and Cathy Johnston, and brother, Matt Johnston, have given me the unconditional love, support, and encouragement to believe that anything is possible.

Contents

List of Figures

List of Tables

Abbreviations

Akt/PKB	**Ak** mouse-**t**hymoma / **P**rotein **K**inase **B**
AMP	**A**denosine **M**ono**P**hosphate
APC/C	**A**naphase **P**romoting **C**omplex/**C**yclosome
ASD	**A**utism **S**pectrum **D**isorder
AUC	**A**rea **U**nder **C**urve
ANOVA	**AN**alysis **O**f **VA**riance
BLOSUM	**BLO**cks **SU**bstitution **M**atrix
BRRS	**B**annayan-**R**iley-**R**uvalcaba **S**yndrome
CENP-C	**CEN**tromere **P**rotein Antigen **C**
CK2	**C**asein **K**inase **2**
CREB	**C**yclic-AMP **R**esponse **E**lement **B**inding Protein
COSMIC	**C**atalogue **O**f **S**omatic **M**utations **I**n **C**ancer
CS	**C**owden **S**yndrome
DNA	**D**eoxyribo**N**ucleic **A**cid
DSB	**D**ouble **S**trand **B**reak
DSF	**D**ifferential **S**canning **F**luorimetry
DTBA	**D**i**T**hio**B**utyl**A**mine
DTT	**D**i**T**hio**T**hreitol
DUSP	**DU**al **S**pecificity Protein **P**hosphatase
EC	**E**nzyme **C**omission
EDTA	**E**thylene**D**iamine**T**etraacetic **A**cid

EGF	**E**pidermal **G**rowth **F**actor
FAK	**F**ocal **A**dhesion-**K**inase
HGMD	**H**uman **G**ene **M**utation **D**atabase
HIV	**H**uman **I**mmunodeficiency **V**irus
HEPES	4-(2-**H**ydroxy**E**thyl)-1-**P**iperazine**E**thane**S**ulfonic acid
MESG	7-**ME**thyl-6-**thioG**uanosine
mRNA	**m**essenger **R**ibo**N**ucleic **A**cid
NASP	**N**ull **A**utism **S**omatic **P**HTS
OD	**O**ptical **D**ensity
PBS	**P**hosphate-**B**uffered **S**aline
PCA	**P**rinciple **C**omponent **A**nalysis
PCR	**P**olymerase **C**hain **R**eaction
PDB	**P**rotein **D**ata **B**ank
PDK1	**P**hosphoinositide-**D**ependent **K**inase **1**
PHTS	**P**TEN **H**amartoma **T**umor **S**yndrome
PI	**P**hosphatidyl**I**nositol
PI3K	**P**hosphatidyl**I**nositol-**3**-**K**inase
PIP_2	**P**hosphatidyl**I**nositol-4,5-**bisP**hosphate
PIP_3	**P**hosphatidyl**I**nositol-3,4,5-**trisP**hosphate
PI(3,5)P_2	**P**hosphatidyl**I**nositol-**3,5-bisP**hosphate
PI(5)P_2	**P**hosphatidyl**I**nositol-**5**-**P**hosphate
PI(4)P_2	**P**hosphatidyl**I**nositol-**4**-**P**hosphate
PI(4,5)P_2	**P**hosphatidyl**I**nositol-**4,5-bisP**hosphate
PLC1	**P**hospho**l**ipase **C1**
PNPase	**P**urine **N**ucleotide **P**hosphorylase
PS	**P**roteus **S**yndrome
PTEN	**P**hosphatase and **TEN**sin homolog deleted from chromosome **TEN**
RBF	**R**adial **B**asis **F**unction
ROC	**R**eceiver **O**perating **C**haracteristic

RTK	**R**eceptor **T**yrosine **K**inase
SDS-PAGE	**S**odium **D**odecyl **S**ulphate–**P**oly**A**crylimide **G**el **E**lectrophoresis
SE	**S**tandard **E**rror
SNP	**S**ingle **N**ucleotide **P**olymorphism
SVM	**S**upport **V**ector **M**achine
TAT	**T**rans**A**ctivator of **T**ranscription
TB	**T**errific **B**roth
US	**U**nited **S**tates
UV–Vis	**U**ltra**V**iolet–**Vis**ual

This work is dedicated to my girlfriend, Abby,
and my parents, Cathy and Dave

Chapter 1

Introduction: PTEN Tumor Suppressor in Cancer

1.1 Cancer

In the United States in 2010, cancer accounted for 23.3% of all deaths, totaling close to 580,000 and just behind heart disease as the leading cause of death in the US (Heron, 2013). Worldwide in 2012, that number is 8.2 million, with 14.1 million new cases diagnosed (Torre *et al.*, 2015). Experts believe that these numbers will continue to grow as the overall population gets older.

These numbers are a radical change from relatively recently in our history (Jones *et al.*, 2012). The study of human disease has been able to cut down greatly on the numbers of deaths in general in the United States (by about 45% per capita since 1910). Diseases

like polio that foretold a short lifetime confined to a wheelchair were eradicated with vaccines, greatly improving quality of life. Bacterial infections, once the harbinger of an early death, are frequently eliminated by courses of antibiotics. Most of the incredible decline in death numbers, however, was led by achievements in the study of infectious diseases (Jones *et al.*, 2012). Similar intense research has not been able to find any similar magic bullet for the multifaceted disease that is cancer, which has increased 290% per capita since 1910 (Jones *et al.*, 2012).

Cancer is characterized by masses of cells called tumors that have bypassed normal growth checkpoints and grow without bound. These tumors usually begin in one kind of tissue, like the breast or colon, and sometimes gain the ability to travel to and grow in other parts of the body (Chaffer and Weinberg, 2011). The main mechanism for the bypass of growth checkpoints is by DNA/genome damage, mutation, deletion, and rearrangement. Current treatments include surgical removal of the tissue or organ in which the tumor started, radiation therapy, and drugs that are toxic to rapidly dividing cells. Efforts to develop treatments and cures for cancer have been hampered by the vast heterogeneity of tumors: no two tumors are exactly alike, and treatments that are effective in one case are often ineffective in other cases.

1.1.1 Hallmarks of Cancer

The variety of types of cancer has led researchers to posit "hallmarks" that correspond to capabilities that normal cells acquire that allow them to morph into cancer cells

(Figure 1.1; Hanahan and Weinberg, 2011; Hanahan and Weinberg, 2000). These hallmarks include sustaining proliferative signaling, evading growth suppressors, resisting cell death, enabling replicative immortality, inducing angiogenesis, and activating invasion and metastasis. The more recent review gave a few additional emerging hallmarks and enabling characteristics: deregulating cellular energetics, avoiding immune destruction, genome instability and mutation, and tumor-promoting inflammation. A given cancerous tissue may go through phases in which a few of these hallmarks are more influential than others. As cancers progress, they can acquire additional mutations that allow them to take advantage of new hallmarks. Cancers with additional mutations can adapt to treatments by switching their reliance on hallmarks. These organizing principles allow researchers to make sense of the complex disease.

1.1.2 When Cell Signaling Pathways Become Cancerous

A cell signaling pathway is a means by which signals outside of a cell are transmitted inside the cell and cause a change in the cell state or expression of genes within the cell (N. A. Campbell and Reece, 2004). Pathways exist for many different functions, including development and metabolism. When organisms are developing, they require activation of pathways that allow cells to quickly differentiate and proliferate. This activation results in the normal growth and differentiation of tissues and organs.

For example, a growth factor protein like epidermal growth factor (EGF) binds to a receptor protein on the outside of a cell in order to cause the cell to grow (Figure 1.2). In the case of EGF, this receptor protein is a receptor tyrosine kinase (RTK). The

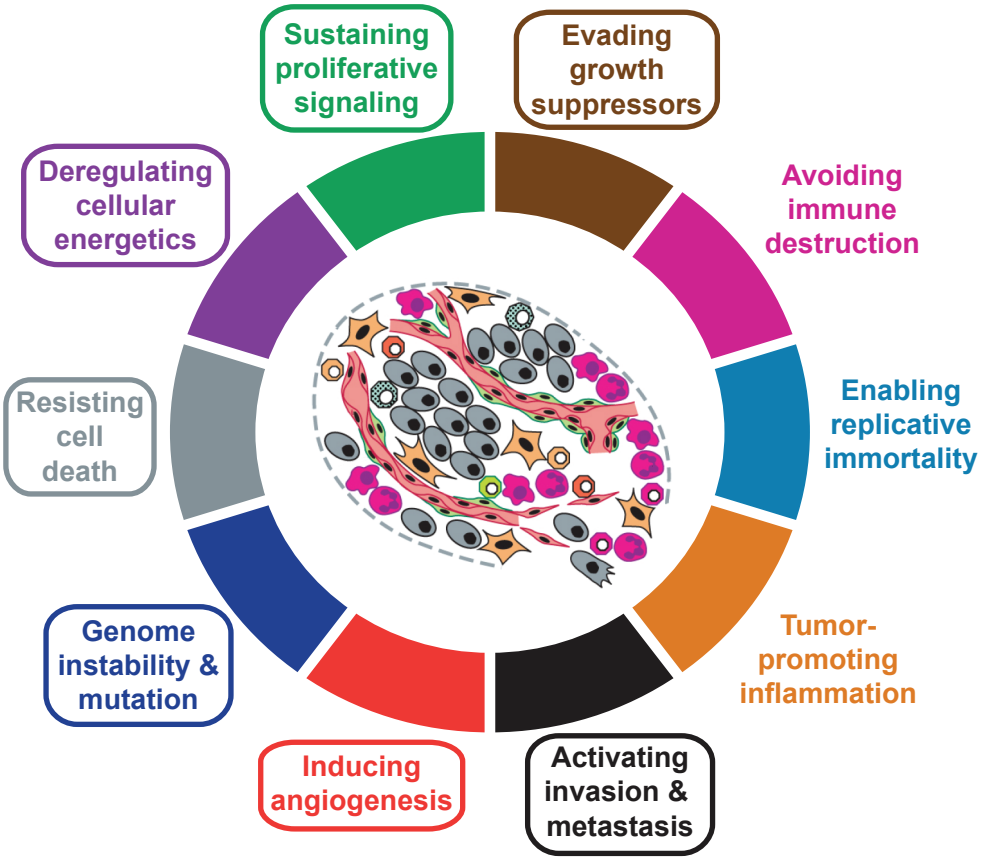

FIGURE 1.1: **Considering PTEN and the hallmarks of cancer.** The hallmarks of cancer as laid out in Hanahan and Weinberg (2011). These include the emerging hallmarks of cancer (deregulating cellular energetics; avoiding immune destruction) and enabling characteristics (genome instability and mutation; tumor-promoting inflammation). Inactivation of PTEN has been shown to lead to each of the hallmarks and characteristics surrounded by rounded rectangles.

RTK transmits the signal to the inner cell membrane with a conformational change, activating its kinase function (Cantley, 2002; Nelson and Cox, 2008). The signal is passed to a phosphatidylinositol-3-kinase (PI3K) by phosphorylation, and then PI3K transfers a phosphate group onto the inner cell membrane lipid phosphatidylinositol-4,5-bisphosphate (PIP_2). The product of this reaction is phosphatidylinositol-3,4,5-trisphosphate (PIP_3). PIP_3 serves as a binding site for the Akt kinase/protein kinase B

(Akt/PKB) and the kinase that activates Akt/PKB, phosphoinositide-dependent kinase 1 (PDK1). Once Akt/PKB is phosphorylated, it then activates several more proteins that drive gene expression and inhibits others that are important for apoptosis, resulting in cell proliferation and survival (Cantley, 2002; Fayard *et al.*, 2010).

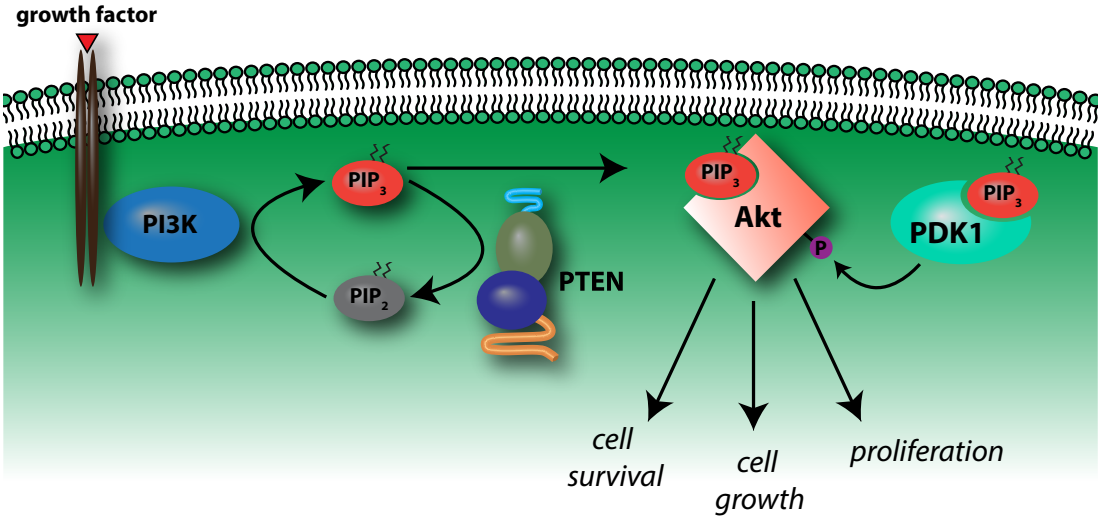

FIGURE 1.2: **PI3K/Akt/PKB pathway and PTEN.** Upon growth factor binding, this signal is transmitted through the membrane by the RTK. PI3K is activated and adds a phosphate residue to PIP_2, forming PIP_3. PIP_3 serves as a binding site for Akt/PKB and the kinase PDK1. PDK1 phosphorylates Akt/PKB, which activates the kinase, starting off many pathways supporting cell proliferation and survival.

Cancers can become malignantly growing masses of cells in a variety of ways. The Akt/PKB pathway described above is a proliferative signaling pathway and is kept under strict regulation so that sustained activation is not possible. If this regulation is bypassed, cancer could develop and would be attributed to the hallmark, "sustaining proliferative signaling." This pathway could be sustained by mutations that cause some proteins like PI3K or Akt/PKB to become overactive, or mutations that inactivate

proteins that antagonize the pathway. One very important antagonist of the Akt/PKB pathway is the phosphatase and tensin homolog deleted from chromosome ten (PTEN).

1.1.2.1 Tumor Suppressors

PTEN is an example of a tumor suppressor. Other tumor suppressors include p53, the gene product of the *TP53* gene.

1.2 PTEN

PTEN, or the **p**hosphatase and **ten**sin homologue deleted from chromosome **ten**, is a haploinsufficient tumor suppressor that functions in numerous cellular pathways that control cellular growth (Salmena *et al.*, 2008; Song *et al.*, 2012). The *PTEN* gene is now known to be mutated in 50–80% of sporadic tumors (including glioblastoma and prostate cancer) and 30–50% of breast, colon, and lung cancers (Salmena *et al.*, 2008). Striking recent investigations using mouse models with gradual decreases in PTEN levels have revealed that small changes in PTEN protein can have enormous effects on tumor development and lifespan (Alimonti *et al.*, 2010).

1.2.1 Discovery of PTEN

During study of chromosomal changes in gliomas, tumors often lost a copy chromosome ten more than other chromosomes (Bigner *et al.*, 1984). Finally corroborating this

finding in 1997, mutations were localized to the 10q23 locus, and PTEN was discovered by three groups independently (Steck *et al.*, 1997; J. Li *et al.*, 1997; D. M. Li and Sun, 1997). This was an important discovery, as it started off a series of important findings expanding knowledge of PTEN, including its physiological substrates (Maehama and Dixon, 1998; Tamura *et al.*, 1998), role in cell survival (Stambolic *et al.*, 1998), structure (J.-O. Lee *et al.*, 1999), nuclear localization (Perren *et al.*, 2000; Whiteman *et al.*, 2002), autoregulation (Vazquez *et al.*, 2001; R. B. Campbell *et al.*, 2003), role in chromosomal stability (Shen *et al.*, 2007), and role in cell cycle progression (Song *et al.*, 2011).

1.2.2 PTEN Dephosphorylates PIP_3 and Protein Substrates in the Cytosol

The primary sequence of PTEN contains the protein tyrosine phosphatase (PTP) and dual-specificity protein phosphatase (DUSP) motif HCxxGxxRS(T) (Denu and Dixon, 1995; Denu *et al.*, 1996). With this in mind, it was interesting that the protein seemed to be most active against the lipid supstrate PIP_3 (Maehama and Dixon, 1998). Therfore, the canonical and perhaps most important role of PTEN is to antagonize the PI3K/Akt/PKB pathway discussed previously (Figure 1.2). PTEN removes the phosphate at the 3-position of PIP_3 and converts it back into PIP_2 (Maehama and Dixon, 1998). PIP_2 does not bind to Akt/PKB and does not activate the Akt/PKB pathway. Loss of PTEN, therefore, allows the PI3K/Akt/PKB pathway to become overactive, leading to "sustained proliferative signaling."

In vitro, PTEN reveals itself to indeed also be a DUSP, dephosphorylating serine, threonine, and tyrosine substrates (Myers *et al.*, 1997). Its physiological protein substrates include focal adhesion kinase (FAK; Tamura *et al.*, 1998) and the cyclic-AMP response element binding protein (CREB; Gu *et al.*, 2011).

PTEN activity *in vitro* has been consistently studied using discontinuous assays based on radioactive phosphate or malachite green (Maehama and Dixon, 1998; Maehama *et al.*, 2000; Redfern *et al.*, 2010). These assays are simple and accurate, but detailed analyses of fast enzyme kinetics are often aided by a continuous assay. They can also generate a lot of information in a shorter amount of time. I develop a continuous assay and use it to explore an interesting facet of PTEN activity in Chapter 2.

1.2.3 PTEN Structure

The crystal structure of PTEN reveals two main globular domains, an N-terminal phosphatase domain with a protein tyrosine phosphatase motif and homology to tensin and a C2 domain (protein kinase C domain 2; Figure 1.3; J.-O. Lee *et al.*, 1999). Two additional domains at the N and C termini were not crystallized, comprising 14 residues at the N terminus and 50 residues at the C terminus. The phosphatase domain, which is mostly made up of α-helices, is stabilized by the C2 domain, which is mostly β-sheet, through several interdomain contacts (J.-O. Lee *et al.*, 1999). Both globular domains participate in the binding of membranes in order for PTEN to be active on its physiological substrate (Das *et al.*, 2003).

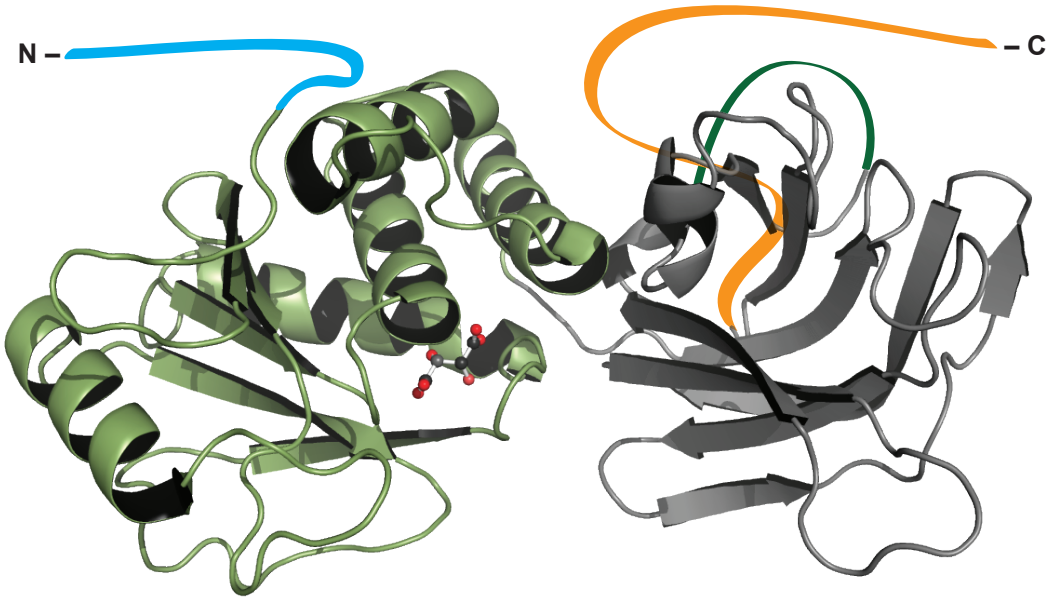

FIGURE 1.3: **Ribbon diagram of the three-dimensional structure of human PTEN** The enzyme has a phosphatase domain (light green) and C2 domain (gray). The enzymic active site contains an L-(+)-tartrate ion, which is rendered in ball-and-stick format. The structure lacks 7 and 49 residues at the N (light blue) and C termini (orange), respectively, and a 24-residue internal loop (dark green). The image was created with the program PyMOL from Schrödinger (New York, NY) and PDB entry 1d5r (J.-O. Lee *et al.*, 1999).

1.2.4 Nuclear PTEN

PTEN was initially found to be localized in the nucleus by histological staining (Perren *et al.*, 2000; Whiteman *et al.*, 2002). Variants of PTEN in some cancers either lacked nuclear staining or were localized to the cell membrane. Notably, PTEN was found to colocalize and directly associate with the centromere protein antigen C (CENP-C) while in metaphase (Shen *et al.*, 2007). Absence of PTEN in centromeres resulted in centromere fragments and Robertsonian fusions, indicative of widespread chromosomal

instability. In the same study, after noting that PTEN absence increases the likelihood of double strand breaks (DSBs) in chromosomal DNA, PTEN was also found to directly associate with the promoter and regulate transcription of Rad51 (Shen *et al.*, 2007). Rad51 is vitally important for homologous recombination-directed repair of DSBs (Pierce *et al.*, 2001). Absence of PTEN therefore also promotes the cancer-enabling characteristic "genome instability and mutation."

PTEN was also found to associate and activate the anaphase promoting complex/cyclosome (APC/C), a nuclear E3 ubiquitin ligase whose substrates are important for chromosomal stability and cell cycle progression (Song *et al.*, 2011).

1.2.5 Post-translational regulation of PTEN

The importance of nuclear localization of PTEN led researchers to speculate about how the protein translocates to the nucleus. Patients with tumors containing a mutation of conserved lysine 289 to glutamate demonstrated widespread nuclear exclusion of PTEN, and another conserved lysine, K13, was also shown to be important for nuclear translocation (Trotman *et al.*, 2007). In the study, the researchers showed that monoubiquitination at these two residues was crucial for nuclear transport and tumor suppressive ability. After monoubiquitination, PTEN can also be further ubiquitinated and marked for proteasomal degradation.

Proteins with an activated cysteine nucleophile are often sensitive to oxidation under oxidative stress, and PTEN is no exception. PTEN is readily oxidized by hydrogen

peroxide *in vitro* and *in vivo*, but is also oxidized when cells are treated with various growth factors (J. Kwon *et al.*, 2004). By using particular cysteine-to-alanine mutations, researchers showed that under oxidative stress, PTEN creates one reversible disulfide bond between the catalytic cysteine 124 and cysteine 71 (Figure 1.4; S.-R. Lee *et al.*, 2002).

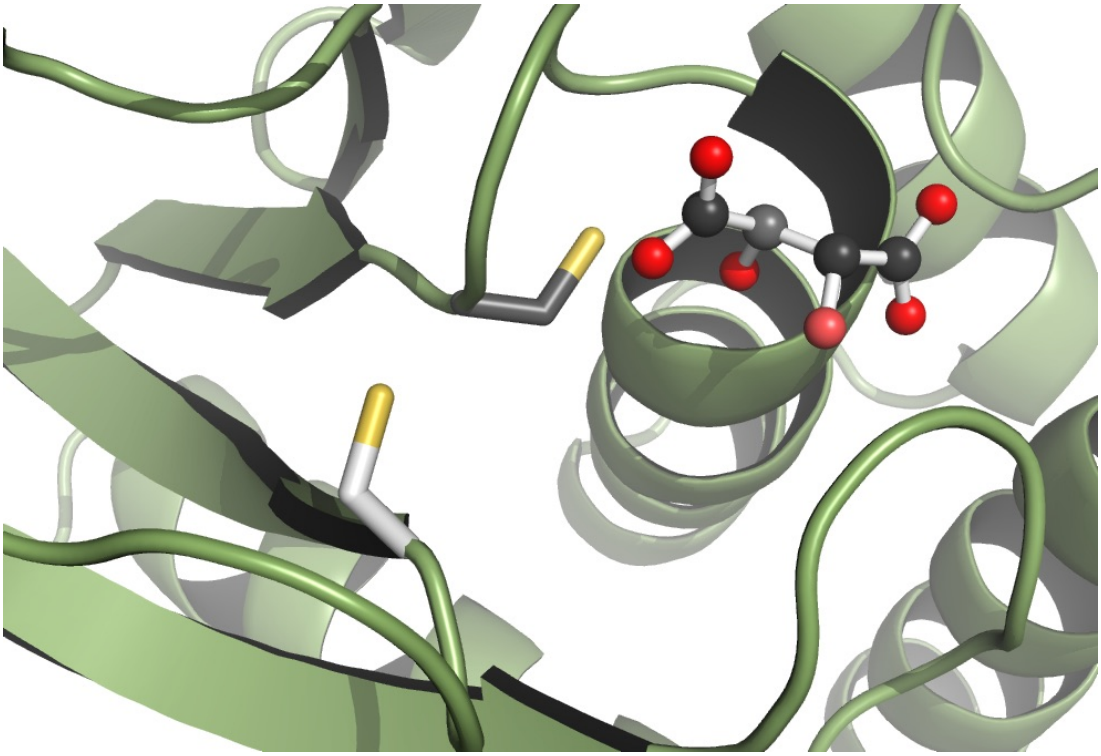

FIGURE 1.4: **Cysteine proximity in the active site of PTEN.** In the active cite of PTEN, Cys71 (shown with white carbons) is proximal to the important catalytic residue Cys124 (shown with black carbons). The distance between backbone C^{α} carbons is 5.1 Å. The enzymic active site contains an L(+)-tartrate ion, which is rendered in ball-and-stick format. The image was created with the program PyMOL from Schrödinger (New York, NY) and PDB entry 1d5r (J.-O. Lee *et al.*, 1999).

The C-terminal tail domain of PTEN has several serine and threonine residues that can be phosphorylated by casein kinase 2 (CK2). Phosphorylation is believed to cause the

tail domain to behave in an autoregulatory manner (Vazquez *et al.*, 2001) and may have effects on cell motility (Raftopoulou *et al.*, 2004).

PTEN catalysis has been observed to be cooperative. PIP_2 activation is apparent in assays using soluble lipidic or liposomal substrates (Maehama *et al.*, 2000; McConnachie *et al.*, 2003; Taylor and Dixon, 2003). PIP_2 activation is abrogated when a PIP_2 binding motif is mutated (R. B. Campbell *et al.*, 2003). Other phosphotidylinositide phosphatases appear to exhibit a similar product-activating phenotype. For example, product activation has appeared in assays of myotubularins (PI(3,5)P_2 →PI(5)P) (Schaletzky *et al.*, 2003), an insect-derived salivary inositol phosphatase (PI(4,5)P_2 →PI(4)P) (Andersen and Ribeiro, 2006), and eukaryotic Sac1 (PI(4)P→PI) (Zhong *et al.*, 2012). It has been proposed that association and binding to these products increases enzymatic activity by increasing association with the membrane (McConnachie *et al.*, 2003), but product activation is noted even when enzyme substrates are monodisperse in solution (R. B. Campbell *et al.*, 2003). It is also possible that binding to the product PIP_2 is accompanied by an increase in structure at the N terminus (Redfern *et al.*, 2008). In Chapter 2, I explore an interesting salt-dependence on the activation of PTEN by its product and present a compelling model to explain this phenomenon.

1.2.6 PTEN in Cell Motility and Polarity

Loss of PTEN has been associated with increased cell migration and cell motility in cancer cells (Tamura *et al.*, 1998; Liliental *et al.*, 2000; Raftopoulou *et al.*, 2004). This ability to control cell migration was initially thought to be attributed to regulation of

FAK (Tamura *et al.*, 1998). However, PTEN loss did not change phosphorylation levels of FAK and rather increased expression of Rac1 and Cdc42 through activation of the Akt/PKB pathway (Liliental *et al.*, 2000). Interestingly, completely inactivated C124S variants of PTEN with the C-terminal threonine mutated to alanine (T389A) were also able to control cell migration.

PIP_3 and PIP_2 are associated with cell polarity, with this role of PTEN conserved even in the slime mold *Dictyostelium discoideum* (Funamoto *et al.*, 2002). High concentrations of PIP_2 on the membrane recruit proteins that help form the normal apical surface of epithelial cells (Martin-Belmonte *et al.*, 2007). Loss of PTEN can therefore inhibit normal cell polarity, a characteristic important to epithelial cells.

1.2.7 PTEN-L (and PTENα)

Based on careful analysis of immunoblots and mRNA transcripts, two groups determined that a slightly larger (~70 kDa) protein band was due to alternative translation initiation at an upstream CUG codon (Hopkins *et al.*, 2013; Liang *et al.*, 2014). Termed "PTEN-L" (Pulido *et al.*, 2014), this isoform has an additional 173 residues on its N terminus and is 64.9 kDa. These residues contain an apparent signal sequence as well as a conserved stretch of six arginine amino acids. The signal sequence allows the protein to be secreted, and it was able to shrink PTEN-null tumors in mice when injected. This tumor suppressive activity was dependent on the poly-arginine stretch (Hopkins *et al.*, 2013). These residues were hypothesized to play a role similar to the HIV-TAT peptide in cell membrane transduction (Schwarze *et al.*, 1999).

This same transcript was studied in a different context, and the gene product was studied in the cytosol and called PTENα. These researchers found that PTENα was localized to the mitochondria, induces cytochrome-C activity, and is important for electron transport chain function. It is possible that both roles are physiological: the signal sequence noted in Hopkins *et al.*, 2013 is predicted to be a true signal sequence only by an older, particular version of the SignalP server: the hidden Markov model in version 2.0 (Nielsen *et al.*, 1997; Nielsen and Krogh, 1998). The current version, SignalP 4.0 (Petersen *et al.*, 2011), does not predict a signal sequence (Johnston, 2015, unpublished observations).

In Chapter 2, I find that PTEN-L does not exhibit the same dependence on salt as normal PTEN, indicating that PTEN-L may not be activated by the phosphatase product PIP_2. In Chapter 3, I find that PTEN-L is significantly more thermodynamically stable than normal PTEN.

1.2.8 PTEN and the Hallmarks of Cancer

It is clear that the PTEN tumor suppressor is one of the most important proteins in cancer (Figure 1.1). To illustrate this, here are the hallmarks of cancer PTEN is able to counteract:

- **Sustaining proliferative signaling:** PTEN's enzymatic role antagonizes an important proliferative signaling pathway, PI3K/Akt/PKB
- **Evading growth suppressors:** PTEN is itself a growth repressor
- **Resisting cell death:** PI3K/Akt/PKB pathway enables resistance to apoptosis (Manning and Cantley, 2007)
- **Inducing angiogenesis:** PI3K/Akt/PKB pathway increases angiogenesis (Manning and Cantley, 2007)

- **Activating invasion and metastasis:** Absence of PTEN leads to increased migration in cancer cells (Tamura *et al.*, 1998)
- **Deregulating cellular energetics:** PI3K/Akt/PKB pathway has a central role in regulation of glucose uptake and metabolism (Song *et al.*, 2012)
- **Genome instability and mutation:** PTEN has several important roles in the nucleus protecting chromosomal stability and double strand break repair (Section 1.2.4)

Simple inactivation of PTEN by mutation, epigenetic silencing, or oxidation allows a cancer cell gain numerous important advantages.

1.2.9 More Roles for PTEN?

Since its discovery in 1997, new findings that establish additional roles for PTEN in tumor suppression have been almost a yearly occurrence. The recent discovery of PTEN-L has indicated that there may be more facets to this protein that are yet to be discovered. What portions of the N-terminus of PTEN-L are important for tumor suppressive activity? Is the active version of PTEN-L a monomer or a higher order oligomer? Which form of PTEN performs tumor suppressive actions in the nucleus? How do normal cells and cancer cell lines respond to expression of PTEN-L without normal PTEN? I explore these questions and present additional data in Chapter 5.

1.3 PTEN Hamartoma Tumor Syndromes

The PTEN Hamartoma Tumor Syndromes (PHTSs) are a relatively recent grouping of what seem to be phenotypically diverse syndromes. Germline mutations in *PTEN*

are often components of Cowden, Bannayan-Riley-Ruvalcaba, and Proteus syndromes. PHTSs are defined as the subset of patients with these syndromes that have mutations in the *PTEN* gene (Ngeow and Eng, 2014).

Cowden Syndrome (CS) is characterized by a series of strict diagnostic criteria, most of which include appearance of sporadic tumors in a variety of tissues along with macrocephaly (Eng, 2003). When using the strict diagnostic criteria, 80% of patients with CS have mutations in the *PTEN* gene. Bannayan-Riley-Ruvalcaba Syndrome (BRRS; also Bannayan-Zonana Syndrome) is a rare pediatric disease characterized by macrocephaly, lipomatosis, and speckled penis. Germline mutations of *PTEN* have been found in 60% of patients with this syndrome. Proteus Syndrome (PS) is a disorder characterized by overgrowth of multiple tissues (Biesecker *et al.*, 1999). Patients that both meet and almost meet clinical qualifications for PS have been found to have mutations in the *PTEN* gene. Correlations from genotype to phenotype have been hampered by the fact that many mutations in *PTEN* overlap between syndromes: for example, a missense mutation found in a patient with BRRS is often also found in patients with CS, two clinically distinct syndromes.

1.4 Autism Spectrum Disorders

Autism and a related condition, Asperger's Syndrome were independently formulated by Leo Kanner and Hans Asperger in 1943 and 1944, respectively (Kanner, 1943; Asperger, 1944). Since then, there have been many different formulations for the condition that

is characterized by inhibited social reciprocity, repetitive movements, sensory overstimulation, and impaired communication skills (Caronna *et al.*, 2008). Autism spectrum disorders (ASDs) is the umbrella term that encompasses autism, Asperger's Syndrome and other related syndromes. ASD diagnoses are certainly increasing, but much of this increase in prevalence is likely due to the expanded definition and increased awareness of autism and related disorders (Gernsbacher *et al.*, 2005). Despite the presence of a large degree of heritability and extensive research, the etiology of all ASDs has not been narrowed down to a single gene or set of genes (Newschaffer *et al.*, 2007), although a small percentage of patients do seem to possess causal mutations (Willsey and State, 2015). ASDs with causal mutations are generally 'syndromic,' or present in the context of another known monogenic syndrome. Current research efforts focused on the segment of ASDs without causal mutations use systems biology approaches to contextualize differences in brain development (Willsey and State, 2015).

1.4.1 Autism and PTEN

The connection of PTEN to ASDs was made when several CS and BRRS probands' children exhibited behavior on the autism spectrum (Zori *et al.*, 1998; Goffin *et al.*, 2001; Parisi *et al.*, 2001; Delatycki *et al.*, 2003). Further studies that examined autistic patients with macrocephaly (not necessarily related to PHTSs) found 3 of 18 had mutations in the *PTEN* gene (Butler *et al.*, 2005). Later studies recommend testing for patients with ASDs with macrocephaly (Buxbaum *et al.*, 2007; Hobert *et al.*, 2014). Deletion of *PTEN* in the central nervous system in mice resulted in abnormal social behavior and

sensitivity to sensory stimuli, two characteristics common in human ASDs (C. H. Kwon *et al.*, 2006). It seems likely that the role of PTEN in the PI3K/Akt/PKB pathway may help explain the ASD phenotype: other proteins linked ASDs are present in the pathway (Willsey and State, 2015).

Studies of PTEN missense variants linked to ASDs have been challenging. There are not many examples, and some variants have phenotypic overlap: variants linked to ASDs are sometimes also linked to PHTSs. In general, a few principles have emerged. Variants of PTEN found in ASDs are more likely to have some degree of catalytic activity than those in PHTSs (Rodríguez-Escudero *et al.*, 2011). One variant was found to have a defect in product binding and activation (Redfern *et al.*, 2010). They are also often quickly degraded in cells (Spinelli *et al.*, 2015). I wanted to investigate whether this fast degradation was related to a reduction in thermal stability. As a method of measuring *in vitro* thermal stability had not yet been developed, I established one. I examine three variants of PTEN from both ASDs and PHTSs in Chapter 3.

1.5 Single Nucleotide Polymorphisms

Single nucleotide polymorphisms, or SNPs, are variations in the DNA of an organism that consists of a single base change. SNPs can occur in genes (either coding or non-coding regions) or in intergenic regions. Mutations in coding regions do occur, but they are selected against if the mutation badly affects an organism's fitness. In humans, there can be close to 4 million SNPs between two random individuals (Roach *et al.*,

2010). SNPs can be associated with medical risks and disease outcomes, geneaology, and phenotypes. Genetic testing services usually test for known SNPs (Imai *et al.*, 2011). Services exist on the web to that automate searching and collection of SNPs (Cariaso and Lennon, 2012).

Most SNPs in non-coding regions and intergenic spaces of DNA do not affect organisms, although there are many exceptions to this as we find more roles for the 95% of DNA in humans that does not code for proteins (Shabalina *et al.*, 2001). SNPs in coding regions of DNA can either be synonymous mutations or non-synonymous mutations. Synonymous mutations do not change the identity of the encoded amino acid, and do not normally affect the encoded protein. Some synonymous mutations have been found to affect protein abundance/activity, but this seemed to be mostly due to changes in splicing effector regions (Supek *et al.*, 2014). Conversely, non-synonymous SNPs that change the identity of an amino acid residue can have fundamental effects on protein activity. Experimentally testing the effect of every non-synonymous SNP would be a heroic effort, which is why many groups have developed computational protein impact predictors that attempt to solve this problem (Katsonis *et al.*, 2014).

1.5.1 Protein Impact Predictors

Computational methods that predict the outcome of a non-synonymous SNP generally fall into two categories: those based on protein/amino acid structure, and evolutionary methods based on sequence alignments (Katsonis *et al.*, 2014). Some computational predictors combine these two methods.

Structure-based non-synonymous SNP computational prediction methods generally assume that an amino acid mutation will change the overall stability of the protein (Topham *et al.*, 1997). They seek to calculate the change in folding energy due to the amino acid variation. They frequently require a protein structure in order to make predictions, but to avoid the computational expense of running molecular dynamics simulations, they use energy functions to calculate folding energy changes (Reumers *et al.*, 2005). Advantages to these methods include the possibility of exploring the local three-dimensional environment of an amino acid change (Capriotti and Altman, 2011). Residues that are distant in the amino acid sequence may be closer in three dimensional space, and changes to residues in the core of a protein may have more effects on stability than residues on the protein exterior. However, these methods are likely to miss residues that are important for protein-protein interactions, as these residues are generally on the exterior. Also, although there are many protein structures deposited in the Protein Data Bank every year (Berman *et al.*, 2013), only a small fraction of known proteins have structures, which are usually required to practice these methods.

Homology-based non-synonymous SNP prediction methods incorporate sequence alignments and substitution matrices to predict the consequences of amino acid changes (Cargill *et al.*, 1999). Sequences from homologous proteins that are either from the same organism or from different organisms are compared and are scored in various ways. Some of the first methods used BLOSUM62 matrices originally used for aligning divergent protein sequences (S. Henikoff and J. G. Henikoff, 1992). These methods assume that in protein sequences, amino acids at positions that are invariant, or conserved

positions, are less tolerant to changes than those that have many substitutions (Ng and S. Henikoff, 2003). They also take into account variations in character of an amino acid: if a sequence alignment shows that only arginine and lysine are allowed at a position, the method assumes that this position must have positive character. Logically, however, these methods require well-curated protein sequences with substantial variation in order to make the best predictions (Stone and Sidow, 2005). These sequences must additionally be for proteins that have similar or the same function.

Many SNP prediction methods combine structural information with homology-based information and substitution matrices. These methods are often implemented using machine learning methods (Katsonis *et al.*, 2014).

1.5.2 Machine Learning Support Vector Machines for Protein Impact Prediction

Machine learning is an umbrella term that refers to the construction of algorithms that are capable of learning from input data and making predictions (Bishop, 2006). One group of machine learning algorithms are called a support vector machines (SVMs). In a classification SVM, an algorithm is given a set of training data. This training data consists of many examples of the classes to predict, and each example contains a list of scores (a support vector) and the class that belongs to that list (Figure 1.5). Each individual score is called a feature, and every feature is present in each of the support vectors. Once trained, the SVM is prepared to predict the class of an unknown support vector.

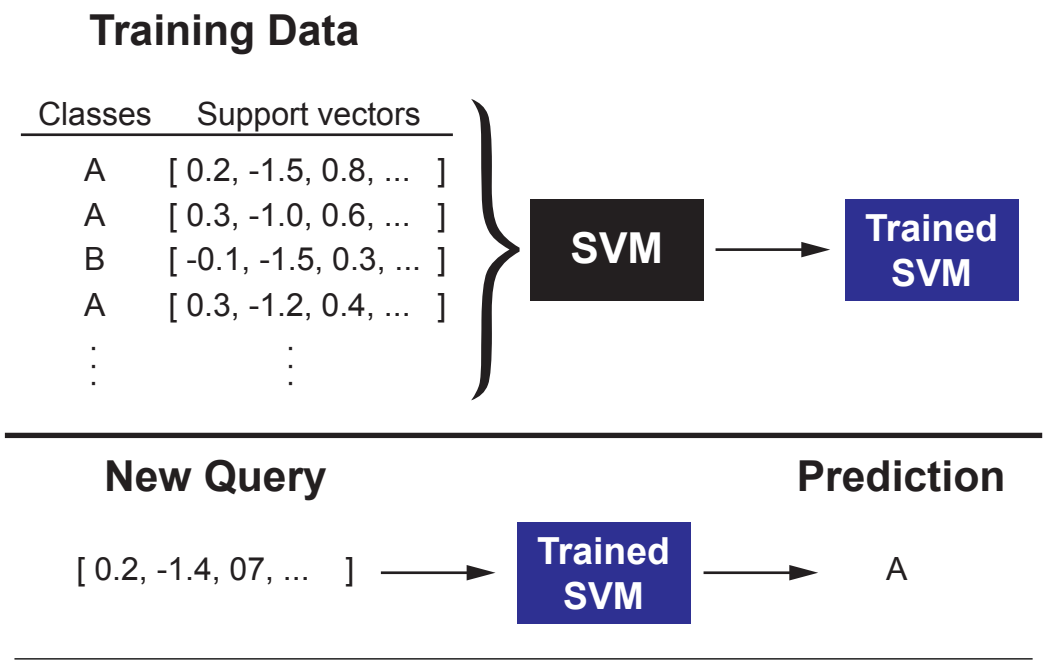

FIGURE 1.5: **Workflow for a support vector machine classifier.** The support vector machine is presented with a number of support vectors that are each associated with a specified class, A or B in this case. The trained SVM is then able to predict the class of an entirely new queried support vector.

SVMs are therefore useful for predicting the impact of a mutation because they can combine data derived from structural information as well as homology information. Features are also relatively easy to add as long as they can be calculated for mutations in the training data and new mutations.

1.5.2.1 Designer Impact Predictors

Most impact predictors are intended to be used throughout the proteome. However, some proteins are extremely important to the etiology, initiation, and progression of important diseases. PTEN is one of those proteins, and as I have shown, the importance of PTEN on cancer cannot be understated. It would be useful, therefore, to have an

protein impact predictor that is designed specifically for use on PTEN mutations. I have developed such a predictor and we discuss its development in Chapter 4.

1.6 Summary

As the human population ages, the scientific community is racing to further understand the factors by which cancer develops and tumors grow and metastasize. PTEN, as a part of a central cell signaling pathway, is poised to antagonize cell growth and proliferation. The importance of PTEN has been confirmed by the existence of many cancers containing *PTEN* mutations as well as PHTSs with germline mutations in the *PTEN* gene. PTEN has roles in the cell that go beyond its lipid phosphatase activity in the nucleus. For this and other reasons, an in-depth analysis of the biochemical mechanisms of PTEN activity is warranted. In the following thesis, I develop assays and and computer algorithms to understand mechanisms of PTEN activity and dysfunction.

Chapter 2

Catalysis by the Tumor Suppressor Enzymes PTEN and PTEN-L

2.1 Abstract

Phosphatase and tensin homologue deleted from chromosome ten (PTEN) is a lipid phosphatase tumor suppressor that is lost or inactivated in most human tumors. The enzyme catalyzes the hydrolysis of phosphatidylinositol-(3,4,5)-trisphosphate (PIP_3) to form phosphatidylinositol-(4,5)-bisphosphate (PIP_2) and inorganic phosphate. Here, we report on the first continuous assay for the catalytic activity of PTEN. Using this assay, we demonstrate that human PTEN is activated by the reaction product PIP_2, as well as

in solutions of low salt concentration. This activation is abrogated in the K13A variant, which has a disruption in a putative binding site for PIP_2. We also demonstrate that PTEN-L, which derives from alternative translation of the PTEN mRNA, is activated constitutively. These findings have implications for catalysis by PTEN in physiological environments and could expedite the development of PTEN-based chemotherapeutic agents.

2.2 Introduction

The PTEN gene located at human chromosome 10q23 encodes the tumor suppressor enzyme PTEN (EC 3.1.3.67) (Eng, 2003; Pulido *et al.*, 2014; Worby and Dixon, 2014). PTEN is thought to be mutated in 50–80% of sporadic human cancers (Salmena *et al.*, 2008). In the 15 years since the discovery of its canonical substrate, phosphatidylinositol-(3,4,5)-trisphosphate (PIP_3) (Maehama and Dixon, 1998), PTEN has entered center-stage for cancer biologists. By catalyzing the dephosphorylation of PIP_3 (Figure 2.1A), PTEN antagonizes the phosphatidylinositol-3-kinase (PI3K) Akt pathway, mediating cell proliferation and apoptosis. In addition to its phosphatase activity on PIP_3, PTEN dephosphorylates protein substrates in the cytosol (Tamura *et al.*, 1999). PTEN has roles elsewhere in the cell, specifically in the nucleus (Baker, 2007), where it is thought to have effects on gene expression, genomic stability, and cell-cycle regulation (Song *et al.*, 2012).

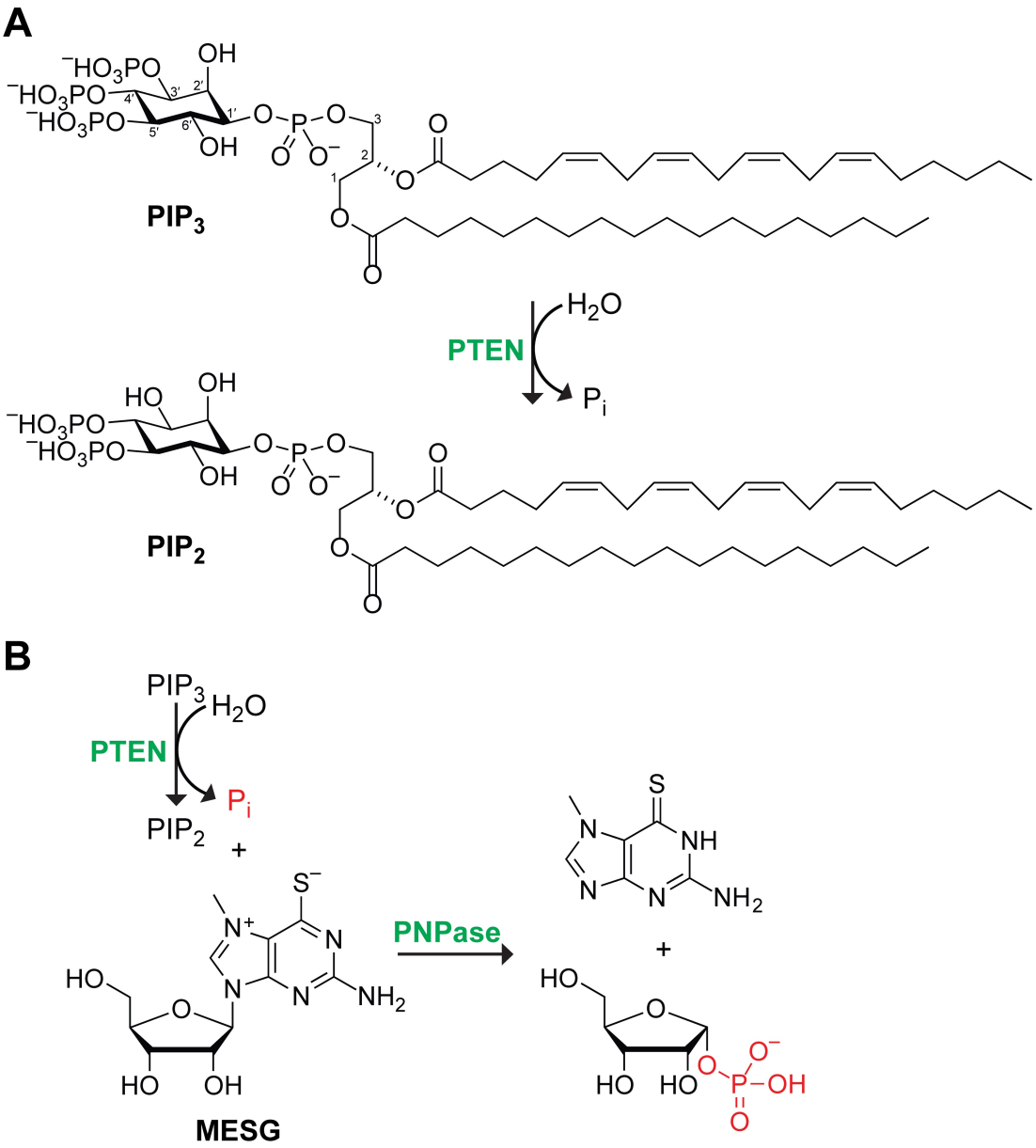

FIGURE 2.1: **Scheme of assay for catalysis by PTEN.** (A) PTEN catalyzes the hydrolysis of phosphatidylinositol-3,4,5-trisphosphate (PIP_3) to form inorganic phosphate and phosphatidylinositol-4,5-bisphosphate (PIP_2). Canonically, the fatty acids are arachidonic acid (20:4) and stearic acid (18:0). (B) In the coupled enzyme assay, purine nucleoside phosphorylase (PNPase) catalyzes the reaction of the inorganic phosphate produced by PTEN with 7-methyl-6-thioguanosine (MESG). Upon release, 7-methyl-6-thioguanine undergoes tautomerization, leading to a marked increase in absorbance at 360 nm.

Human PTEN has 403 amino-acid residues (47.2 kDa). The enzyme consists of two globular domains: a phosphatase domain with homology to dual specificity phosphatases and a C2 domain with homology to phospholipase C1 (PLC1; J.-O. Lee *et al.*, 1999). The phosphatase domain contains a canonical protein tyrosine phosphatase motif, HCXXGXXR (Denu *et al.*, 1996).

Hypomorphic mouse models have revealed that subtle reductions in the level of PTEN and thus its enzymatic activity can lead to large cancer-related phenotypes (Alimonti *et al.*, 2010). Extant assays to measure the catalytic activity of PTEN are, however, imprecise and tedious. Catalytic activity with canonical phosphatase substrates, such as *p*-nitrophenylphosphate, is too low to be useful . Instead, the activity of PTEN is most often measured with a discontinuous assay based on the formation of complex between the organic dye malachite green and inorganic phosphate (Hess and Derr, 1975) produced from a soluble lipidic (Maehama *et al.*, 2000; Taylor and Dixon, 2003) or liposomal (McConnachie *et al.*, 2003) PIP_3 substrate. The assay has a limited range, which ends at ~20 μm phosphate in a 10-mm cuvette. Still, in assays using soluble lipidic and liposomal substrates, the malachite green-based assay has revealed that PTEN is activated by its PIP_2 product, which binds near the N terminus.

In 2013, Parsons and coworkers reported on a form of PTEN called PTEN-L (64.9 kDa), which is translated from a conserved CUG codon (Hopkins *et al.*, 2013). The alternative form has 173 additional N-terminal amino-acid residues, including a secretion signal sequence and an Arg_6 motif that enables extracellular protein to enter the cytosol. When injected into mice lacking PTEN, PTEN-L caused tumors to regress completely.

PTEN-α, which is an intracellular version of PTEN-L, is translated from the same CUG codon (Liang *et al.*, 2014). PTEN-L has enzymatic activity, but its catalysis is even less well characterized than that of wild-type PTEN.

We are aware that PTEN is a lipid phosphatase—its catalytic activity *in cellulo* is manifested on the inner leaflet of the plasma membrane (Eng, 2003; Pulido *et al.*, 2014; Worby and Dixon, 2014). In an attempt to model catalysis *in cellulo*, assays of PTEN have employed a PIP_3 substrate embedded on the outer leaflet of a synthetic liposome (McConnachie *et al.*, 2003). These complex assays cannot be used to dissect fundamental aspects of catalysis by PTEN. For example, the multivalency that arises from binding to the PIP_2 product that is generated on the surface of a liposome enhances the affinity of PTEN for a PIP_3 substrate on that liposome. Hence, the degree to which PTEN is activated by individual molecules of PIP_2 is not apparent from data derived from liposome-based assays.

The enzyme purine nucleoside phosphorylase (PNPase; EC 2.4.2.1) catalyzes the reaction of inorganic phosphate with purine nucleosides to displace a purine nucleobase. Tautomerism within the nonnatural purine nucleobase 7-methyl-6-thioguanine leads to a large increase in its absorbance as a nucleobase rather than a nucleoside, and can serve as the basis for a sensitive, continuous assay for inorganic phosphate (Webb, 1992), like that produced by PTEN.

Here, we present the first continuous assay for the catalytic activity of PTEN. Our assay couples inorganic phosphate production by PTEN to catalysis by PNPase (Figure

2.1B). Using this assay, we find that the catalytic activity of human PTEN is much greater than reported previously, and that the activity of PTEN-L is comparable to that of PTEN. Finally, using a PTEN variant that lacks the binding motif for the phosphatidylinositol-(4,5)-bisphosphate (PIP_2) product (R. B. Campbell *et al.*, 2003), we delineate dramatic allosterism in catalysis by the wild-type enzyme. These findings underpin an understanding of the biology and pharmacology of PTEN.

2.3 Results

2.3.1 Production and Purification of PTEN

Wild-type PTEN, K13A PTEN, and PTEN-L were produced in *Escherichia coli* by recombinant DNA technology. Each protein had a C-terminal His_6-tag and was purified by Ni-affinity and gel-filtration chromatography, along with either anion exchange chromatography (wild-type PTEN and its K13A variant) or heparin-affinity chromatography (PTEN-L). Enzyme purity was assessed with SDS–PAGE (Figure 2.2A), and typical isolated yields of wild-type PTEN, K13A PTEN, and PTEN-L were 5, 5, and 1 mg per L of *E. coli* culture, respectively.

Earlier this year, Pandolfi and coworkers reported qualitative data suggesting that the overproduction of PTEN can lead to its dimerization *in cellulo* (Papa *et al.*, 2014). Yet, a quantitative analysis of the proteome of U2OS osteosarcoma cells growing in log phase detected <500 molecules of PTEN per cell, equivalent to a concentration of <0.2 nM (Beck *et al.*, 2011). At this low concentration, even with a nanomolar value of K_d, only

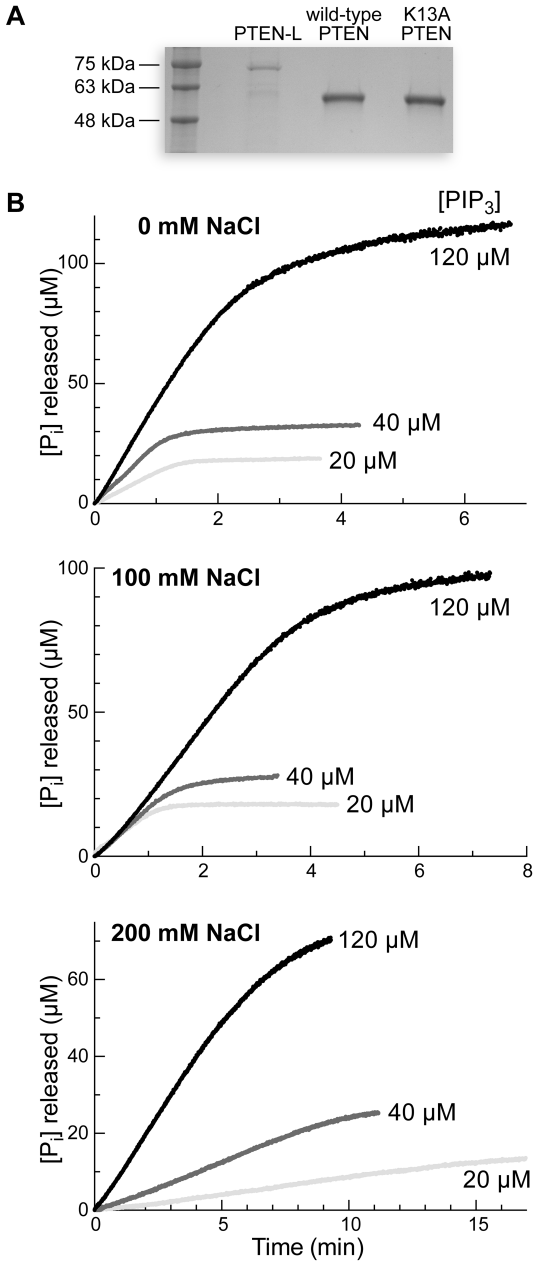

FIGURE 2.2: **Initial characterization of PTEN.** (A) Analysis of PTEN-L, wild-type PTEN, and K13A PTEN on a Coomassie R-250–stained polyacrylamide (12% w/v) gel containing sodium dodecylsulfate (0.1% w/v). (B) Representative progress curves for the turnover of PIP_3 (10, 15, or 40 um) by wild-type PTEN. Reactions were performed in 50 mM Tris–HCl buffer, pH 7.6, containing EDTA (2.0 mM), MESG (0.20 mM), DTBA (40 mM), and NaCl (0, 100, or 200 mM), and were initiated with the addition of PTEN to 20 nM. Absorbance at 360 nM was converted to concentration by using $\Delta\epsilon = 11\ \mathrm{mM^{-1}cm^{-1}}$.

a small fraction of PTEN would exist in a dimeric form. When we purify PTEN by gel-filtration chromatography at 100 mM NaCl, we observe only one peak corresponding to monomeric PTEN. (Concentrations of PTEN in these purifications approach 50 μM.) As our assays are performed at enzyme concentrations of $\leq$250 nM, we believe that our data report on catalysis by monomeric PTEN, replicating the state *in cellulo*.

2.3.2 Catalysis by PTEN in the Absence of Salt Exhibits Michaelis–Menten Kinetics

Representative time courses revealed that rates measured with our coupled assay were dependent on the concentration of the PIP_3 substrate (Figure 2.2B). We observed 85–95% conversion of PIP_3 to PIP_2 in all assays. In a proper coupled assay, the observed reaction velocity must be for the target enzyme and its substrate rather than the coupling enzyme and its substrate (Tipton, 2002). We found that doubling the concentration of PNPase or MESG had no effect on observed rates (data not shown), validating our assay.

Using our continuous assay, we discovered that salt concentration has a marked influence on catalysis by PTEN (Figure 2.3). When we refrained from adding salt to our assay solution, we were surprised to discover that PTEN exhibits Michaelis–Menten kinetics. This finding is in marked contrast to results from assays done in the presence of salt (R. B. Campbell *et al.*, 2003; McConnachie *et al.*, 2003), and the results are especially disparate at low substrate concentrations ($<$10 μM PIP_3). By using non-linear regression

to fit the initial velocity data to the Michaelis–Menten equation (Equation 2.1):

$$v_o = \frac{k_{\mathrm{cat}}\,[E]\,[S]}{K_{\mathrm{M}} + [S]} \tag{2.1}$$

we found that $k_{\mathrm{cat}}/K_{\mathrm{M}} = (174 \pm 40)\ \mu\mathrm{M}^{-1}\mathrm{min}^{-1} = (2.8 \pm 0.6) \times 10^6\ \mathrm{M}^{-1}\mathrm{s}^{-1}$, which is 101- to 102-fold larger than values obtained previously (R. B. Campbell *et al.*, 2003; Hopkins *et al.*, 2013; J.-O. Lee *et al.*, 1999; Taylor and Dixon, 2003).

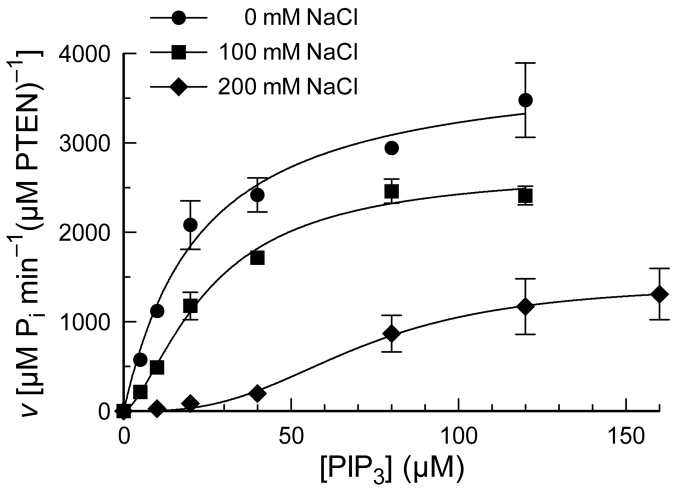

FIGURE 2.3: **Turnover of PIP_3 by wild-type PTEN in solutions of various salt concentrations.** Reactions were performed in 50 mM Tris–HCl buffer, pH 7.6, containing NaCl (0, 100, or 200 mM), EDTA (2.0 mM), MESG (0.20 mM), and DTBA (40 mM), and were initiated with the addition of PTEN to 20 nM. Values are for maximum reaction velocity (± SE) at <10% turnover of substrate in reactions performed in triplicate or more. The resulting kinetic parameters are listed in Table 2.1.

2.3.3 Catalysis by PTEN Exhibits Salt-dependent Cooperativity

Previous assays of the enzymatic activity of PTEN and other phosphoinositide phosphatases have been performed in the presence of added salt (Andersen and Ribeiro,

Enzyme	[NaCl] (mM)	k_{cat}/K_M ($\mu M^{-1}min^{-1}$)[a]	k_{cat} (min^{-1})	K_M (μM)	h[b]
Wild-type PTEN	0	174 ± 40	4000 ± 300	23 ± 5	1.00 ± 0.14
	100	108 ± 14[b]	2720 ± 130[b]	25 ± 3	1.54 ± 0.16
	200	20 ± 4[b]	1430 ± 200[b]	70 ± 11	2.93 ± 0.92
K13A PTEN	0	1.4 ± 0.4	91 ± 9	64 ± 16	1.25 ± 0.33
	100	1.0 ± 0.3	101 ± 12	100 ± 25	1.36 ± 0.35
	200	0.39 ± 0.13	139 ± 24	359 ± 96	1.35 ± 0.21
PTEN-L	0	100 ± 25	477 ± 28	4.8 ± 1.1	0.84 ± 0.30
	100	42 ± 8	515 ± 30	12 ± 2	1.23 ± 0.31
	200	10 ± 2	477 ± 40	47 ± 8	1.19 ± 0.17

TABLE 2.1: **Kinetic parameters for catalysis by wild-type PTEN, K13A PTEN, and PTEN-L.** Reactions were performed in 50 mM Tris–HCl buffer, pH 7.6, containing NaCl (0, 100, or 200 mM), EDTA (2.0 mM), MESG (0.20 mM), and DTBA (40 mM), and were initiated with the addition of PTEN to 20 nM.

2006; R. B. Campbell *et al.*, 2003; Schaletzky *et al.*, 2003; Zhong *et al.*, 2012). We found that, in the presence of salt at physiological concentrations, PTEN exhibits cooperative activity, which can be described by the Hill equation, adapted for enzymatic catalysis:

$$v_o = \frac{k_{cat}\,[E]\,[S]^h}{K_{0.5}^h + [S]^h} \tag{2.2}$$

where h is the Hill coefficient (Cornish-Bowden, 2014). When we performed our coupled assay in the presence of 100 mM and 200 mM NaCl, we saw a drop in enzymatic activity at all substrate concentrations, but a striking drop in activity at low concentrations of substrate (Figure 2.3). When fitted with the Hill equation, the data indicated Hill coefficients at 100 and 200 mM NaCl that differed significantly from unity (Table 2.1). In contrast, we found the Hill coefficient for reactions without salt to be $h = 1.03 \pm 0.33$.

[a]Values (± SE) were derived by fitting initial velocity data to Equation 2.1, unless noted otherwise.
[b]Values (± SE) were derived by fitting initial velocity data to eq 2, and include $k_{cat}/K_{0.5}$ and $K_{0.5}$ rather than k_{cat}/K_M and K_M.

These data indicate that the extent of cooperativity of catalysis by PTEN is correlated strongly with salt concentration. Although NaCl is the salt used in most assay solutions for PTEN activity, we found that other salts (e.g., KCl, $NaNO_3$, and NH_3Cl) elicit similar effects (data not shown).

2.3.4 Catalytic Activity of PTEN is Diminished by Disruption of the PIP_2-Binding Motif

Next, we explored whether the salt-dependent cooperativity that we observed with PTEN is due to the purported PIP_2-binding motif of its N terminus (Figure 2.4) (Martin, 1998). Previous studies suggested that disruption of this motif could disrupt activation and lower overall activity (R. B. Campbell *et al.*, 2003). Accordingly, we made a K13A substitution to disrupt this motif.

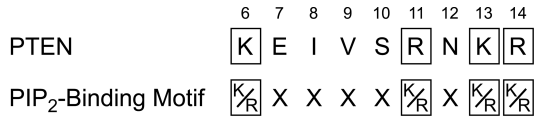

FIGURE 2.4: **Residues Lys-6 to Arg-14 of PTEN and the canonical PIP_2-binding motif.** Each conserved residue in this motif is altered in cancer according to the COSMIC database.

In the absence of salt, K13A PTEN displays much less catalytic activity than does the wild-type enzyme (Figure 2.5). Fitting the data to equation 2.1 gives a value of k_{cat}/K_M = (1.4 ± 0.4) $\mu M^{-1}min^{-1}$, which is ~1% that of wild-type PTEN (Table 2.1). At low concentrations of substrate (10 and 20 μM), the velocity of catalysis by K13A PTEN in the absence of salt resembles that of wild-type PTEN in the presence of 200 mM NaCl.

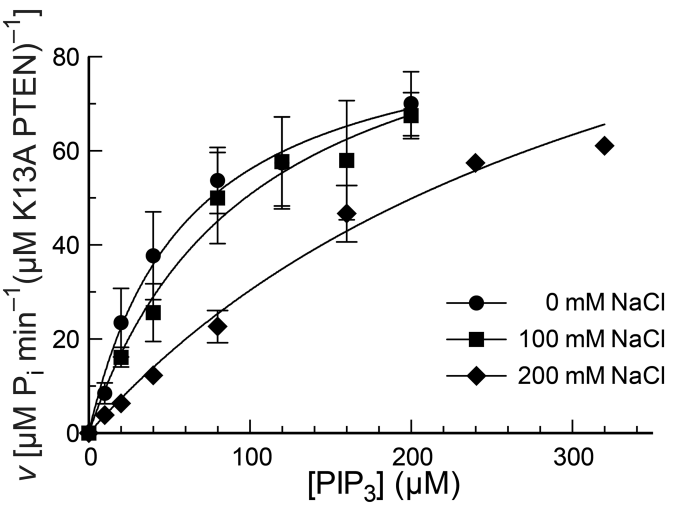

FIGURE 2.5: **Turnover of PIP_3 by K13A PTEN in solutions of various salt concentrations.** Reactions were performed in 50 mM Tris–HCl buffer, pH 7.6, containing NaCl (0, 100, or 200 mM), EDTA (2.0 mM), MESG (0.20 mM), and DTBA (40 mM), and were initiated with the addition of K13A PTEN to 20 nM. Values are for maximum reaction velocity (± SE) at <10% turnover of substrate in reactions performed in triplicate or more. The resulting kinetic parameters are listed in Table 2.1.

Upon addition of salt, the catalytic activity of K13A PTEN is diminished still further (Figure 2.5). All curves, including those in the absence of salt, are slightly sigmoidal, perhaps showing marginal product activation at high substrate concentrations. Fitting to the Hill equation (Equation 2.2) gives Hill coefficients that might differ significantly from unity (Table 2.1).

2.3.5 Catalytic Activity of PTEN-L is Constitutive

A form of PTEN is produced from an alternative translation-initiation codon (CUG) upstream on the canonical PTEN mRNA (Hopkins *et al.*, 2013). Alternative translation-initiation adds 173 amino-acid residues to the N terminus of the protein. Due to the

location of the additional residues on the N terminus, we hypothesized that the added domain could affect the activating effect of PIP_2.

Indeed, our data indicate that PTEN-L is 5-fold more effective at binding to its substrate than is wild-type PTEN (Figure 2.6) with $K_M = (4.8 \pm 1.1)$. Fitting the data to the Michaelis–Menten equation (Equation 2.1) gives $k_{cat}/K_M = (100 \pm 25)\ \mu M^{-1}min^{-1} = (1.7 \pm 0.4) \times 10^6\ M^{-1}s^{-1}$. Supplementation of salt to physiological levels did not seem to introduce allosterism, evident by the absence of sigmoidal kinetics (Figure 2.6). Fitting to the Hill equation (Equation 2.2) gives Hill coefficients that do not differ significantly from unity (Table 2.1). These data are consistent with the N terminus of PTEN-L replicating the activating effect of PIP_2 and maintaining an activated state of PTEN.

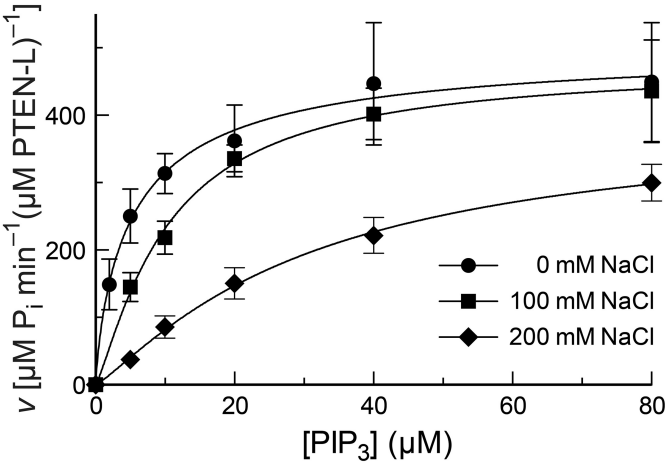

FIGURE 2.6: **Turnover of PIP_3 by PTEN-L in solutions of various salt concentrations.** Reactions were performed in 50 mM Tris–HCl buffer, pH 7.6, containing NaCl (0, 100, or 200 mM), EDTA (2.0 mM), MESG (0.20 mM), and DTBA (40 mM), and were initiated with the addition of PTEN-L to 20 nM. Values are for maximum reaction velocity (± SE) at <10% turnover of substrate in reactions performed in triplicate or more. The resulting kinetic parameters are listed in Table 2.1.

2.4 Discussion

PTEN is an important phosphatase tumor suppressor with many roles in the cell (Song *et al.*, 2012). Loss of PTEN, whether by mutation or by posttranslational inactivation, is causative in 50–80% of sporadic cancers (Salmena *et al.*, 2008). PTEN-L is a recently discovered secreted and membrane-permeable translational variant of PTEN (Hopkins *et al.*, 2013). Although many assays of the phosphatase activity of PTEN have been established, none has been continuous. In this work, we establish a continuous assay for PTEN hydrolysis of its endogenous substrate, PIP_3, reveal new aspects of activation by the product, PIP_2, confirm the location of the PIP_2-binding site, and demonstrate that PTEN-L does not require PIP_2 to retain an activated conformation. Other assays of PTEN activity have employed solutions of diverse salt concentration (Maehama *et al.*, 2000; Schaletzky *et al.*, 2003), a parameter that we find to have large effects on PTEN activity. In addition, we measure values of $k_{\mathrm{cat}}/K_{\mathrm{M}}$ that are more than an order-of-magnitude larger than those derived from other assays, indicating that PTEN and PTEN-L are much better catalysts than appreciated previously. Although the high values of $k_{\mathrm{cat}}/K_{\mathrm{M}}$ are due to the absence of salt, we also employ a highly purified enzyme (Figure 2.2A) with a minimal tag (His_6) and a superior reducing agent (DTBA; Lukesh *et al.*, 2012) to maintain the active-site cysteine residue in its reduced state. This residue is extremely sensitive to oxidation.

In previous work, we studied the effect of salt concentration on the ability of an enzyme to turnover its phosphorylated substrate (Park and Raines, 2001). In general, we found

high salt concentrations to lower the value of k_{cat}/K_M, but not affect that of k_{cat}. Salt counterions are associated with the enzyme and substrate prior to binding, and the dissociation of those ions during binding and consequent gain of entropy is determinant in raising the value of K_M. Here, we observe analogous effect on the value of K_M for PTEN, which increase with increasing salt concentration (Table 2.1). In contrast, we also observe analogous effects on the value of h for the wild-type enzyme, which likewise increases with increasing salt concentration. These data indicate that the binding of both PIP_3 to the active site and PIP_2 to the PIP_2-binding site are mediated by favorable Coulombic interactions. Moreover, the latter interaction appears to be especially strong at low salt concentration, where the value of $h = 1.03$ suggests that wild-type PTEN is readily saturable by PIP_2.

We are aware of another physicochemical explanation for a decrease in enzymatic activity at high salt concentration. Specifically, the addition of salt could entice a protein to aggregate via the hydrophobic effect, a process known as "salting out" (Baldwin, 1996; Melander and Horvath, 1977). We note, however, that the effect of salt concentration on the catalytic activity of PTEN is not constant but depends on the concentration of PIP_3, with the largest impact occurring at low PIP_3 concentrations (Figure 2.3). These data, along with the absence of turbidity in our assay solutions, indicate that PTEN aggregation is not responsible for the decrease in its catalytic activity at high salt concentration.

Catalysis by PTEN has notable elements of cooperativity. In the absence of salt, this cooperativity disappears, PTEN is activated fully, and kinetic data become amenable

to Michaelis–Menten analysis. In its cellular environment, however, catalysis by PTEN is cooperative. Activation by PIP_2 has been noted in assays using soluble lipidic or liposomal substrates (Maehama *et al.*, 2000; McConnachie *et al.*, 2003; Taylor and Dixon, 2003). Other phosphotidylinositide phosphatases appear to exhibit a similar product-activating phenotype. For example, product activation has appeared in assays of myotubularins ($PI(3,5)P_2 \rightarrow PI(5)P$; Schaletzky *et al.*, 2003), an insect-derived salivary inositol phosphatase ($PI(4,5)P_2 \rightarrow PI(4)P$; Andersen and Ribeiro, 2006), and eukaryotic Sac1 ($PI(4)P \rightarrow PI$; Zhong *et al.*, 2012). Limitations in extant assays have prevented detailed analysis of this kinetic behavior. Aside from phosphatidylinositol phosphatases, product activation like that of PTEN is a rare phenomenon. There are, however, other monomeric enzymes that display cooperativity, due mostly to large conformational changes (Porter and B. G. Miller, 2012).

Disrupting the PIP_2-binding motif (Figure 2.4) reduces the catalytic activity of PTEN severely (Figure 2.5). In addition, this disruption also abrogates the sigmoidal nature of substrate–velocity curves. These data are consistent with a mechanism of cooperativity that involves the product, PIP_2, binding to its N-terminal motif and activating the enzyme for catalysis of PIP_3 hydrolysis (R. B. Campbell *et al.*, 2003). This kinetic mechanism ensures that PTEN is most active at membranes, which present both the PIP_3 substrate and PIP_2 product. In addition, this kinetic mechanism could enable catalysis by phospholipase C (PLC) to diminish PTEN activity (and thus encourage cell proliferation) by decreasing the concentration of PIP_2. This mechanism could, for

example, increase the invasiveness of prostate cancer cells having high levels of PLCγ (Turner *et al.*, 1997).

Our continuous assay also enabled a detailed analysis of catalysis by PTEN-L. In addition to the striking 2.2 fold increase in $k_{\mathrm{cat}}/K_{\mathrm{M}}$ over wild-type PTEN at 0 mM NaCl, we find that PTEN-L does not respond to increased salt concentration in the same manner as does the wild-type enzyme. Salt concentration affects the value of K_{M} but does not introduce cooperativity. To summarize our findings, we put forth a model for catalysis by PTEN that is based on the canonical "tense" and "relaxed" states of hemoglobin (Monod *et al.*, 1965). In our model, PTEN can exist in "T" (low activity) and "R" (high activity) conformations (Figure 2.7). The association of PIP_2 with the N-terminal PIP_2-binding site makes the R state more favorable. By removing the PIP_2-binding site, we constrain K13A PTEN to the T state (Figure 2.7A). In the T state, both k_{cat} and K_{M} have low values (Figure 2.7B). For wild-type PTEN, the T state is retained until PIP_2 is bound. At low salt concentration, the equilibrium constant for PIP_2 association with the PIP_2-binding site becomes high, and association is favorable, even at low concentrations of PIP_2. Thus, the R state is more prevalent at low salt concentration and low substrate concentration. At high salt concentration, the binding of PIP_2 is less favored because counterion-release provides less entropic gain, and the T state is prevalent at low substrate concentrations. As the reaction proceeds and the concentration of PIP_2 increases, more PIP_2 is bound by PTEN and more of the enzyme is present in the R state. Interestingly, our data indicate that PTEN-L is constrained to the R state and that increased concentrations of PIP_2 do not effect any additional activation

(Figure 2.7C). Perhaps some of the additional N-terminal residues on PTEN-L bind to the PIP_2 motif and mimic the binding of PIP_2.

PTEN activity is eminently relevant to cancer (Salmena *et al.*, 2008). Small changes in cellular PTEN activity are known to have large effects on tumor propagation (Alimonti *et al.*, 2010), and exogenous PTEN-L shrinks tumors in mice (Hopkins *et al.*, 2013). Accordingly, small molecules that increase PTEN activity could have utility as cancer chemotherapeutic agents. In particular, molecules that encourage the conversion of endogenous PTEN from its T state to its R state could underlie a new chemotherapeutic strategy. Our continuous, colorimetric assay facilitates structure–function analyses, which could expedite the rational design of molecules that modulate PTEN activity. Moreover, our assay could be useful in high-throughput screens of molecular libraries for PTEN agonists.

2.4.1 Conclusion

We have developed a continuous assay for catalysis by PTEN. Using that assay we affirm the presence of a product-binding site, uncover salt-dependence on that binding site, and assess activity by PTEN-L. In contrast to PTEN-L, which is always in a high activity state, wild-type PTEN toggles between a low activity and high activity state based on the concentration of salt and reaction product. These findings provide new information on catalysis by this highly important enzyme, and could empower workers seeking to develop PTEN-based chemotherapeutic agents.

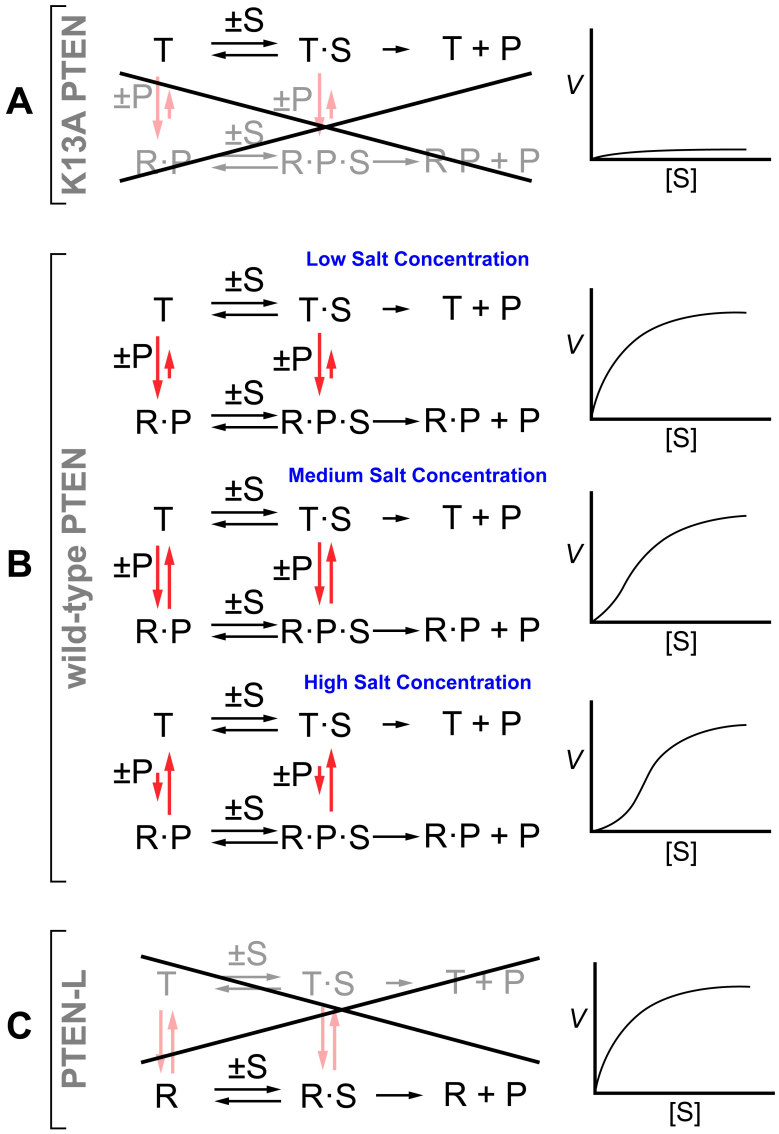

FIGURE 2.7: **Notional schemes and diagrams for catalysis by K13A PTEN, wild-type PTEN, and PTEN-L** (A) The binding motif for PIP2 (P) is absent in K13A PTEN. As a result, the K13A variant remains in its tense (T) state for all substrate concentrations at any salt concentration. (B) Wild-type PTEN has complex kinetic behavior. Low salt concentration favors the binding of PIP2. The wild-type enzyme is in its relaxed (R) state and exhibits Michaelis–Menten kinetics. Increasing salt concentration leads to decreasing affinity for PIP2 and a greater fraction of the enzyme being in the T state. As more PIP_3 (S) is hydrolyzed, the increasing concentration of P leads to a greater fraction of the enzyme being in the R state. (C) PTEN-L is in the R state at any salt concentration and is unaffected by P.

2.5 Materials and methods

2.5.1 Materials

E. coli BL21 (DE3) cells for protein purification were from Novagen (Madison, WI). Expression plasmid pET30B-PTEN was plasmid 20741 from Addgene (Cambridge, MA) and directs the expression of human PTEN with a C-terminal His_6 tag. Expression plasmid pET30B-PTEN-K13A was derived using a Quikchange site-directed mutagenesis system from Agilent (Santa Clara, CA), and expression plasmid pET30B-PTEN-Long-S was derived by Gibson assembly (Gibson *et al.*, 2009) using a gBlocks gene fragment from Integrated DNA Technologies (Coralville, IA). In pET30B-PTEN-L-S, the CTG codon encoding residue 1 was changed to ATG, the signal sequence (codons 2–21) was removed, the ATG codon at the translation start site for wild-type PTEN was replaced with ATA (codon 174), and other codons in the appended upstream region were optimized for expression in *E. coli* without affecting the encoded protein sequence.

Terrific broth (TB) medium contained tryptone (12 g), yeast extract (24 g), K_2HPO_4 (72 mM), KH_2PO_4 (17 mM), and glycerol (4 mL). Columns of HisTrap HP, HiTrap Q HP, HiTrap Heparin HP, and Superdex G200 resins for protein purification were from GE Biosciences (Piscataway, NJ).

diC_8-Phosphatidylinositol-3,4,5-trisphosphate (PIP_3) was from Avanti Polar Lipids (Alabaster, AL) and Echelon Biosciences (Salt Lake City, UT). Bacterial nucleoside phosphorylase (PNPase) was product N2415 from Sigma–Aldrich (St. Louis, MO), dissolved

in reaction buffer, and buffer-exchanged to remove residual phosphate. 7-Methyl-6-thioguanosine (MESG) was from Berry and Associates (Dexter, MI). Dithiobutylamine (DTBA (Lukesh *et al.*, 2012)) was product 774405 from Sigma–Aldrich. All other chemicals and reagents were of commercial reagent grade or better, and were used without further purification.

2.5.2 Production and Purification of PTEN

Methods for the expression and purification of PTEN were based on those of Ross and coworkers (R. B. Campbell *et al.*, 2003). Briefly, a PTEN expression plasmid was transformed into *E. coli* strain BL21(DE3), and grown in TB supplemented with kanamycin (30 μM). Expression was induced at OD = 0.5–0.6 at 600 nm by the addition of isopropyl β-D-1-thiogalactopyranoside to 0.10 mM, and cells were grown for 20–22 h at 21 °C to produce wild-type PTEN and its K13A variant, and 18 °C to produce PTEN-L. Cells were harvested by centrifugation and lysed in 20 mM sodium phosphate buffer, pH 7.4, containing NaCl (0.50 M), imidazole (20 mM), and β-mercaptoethanol (0.7% v/v) with a French pressure cell. Lysate was clarified by centrifugation at 20,000g, and the soluble fraction was applied to a HisTrap HP column. Protein was eluted with 0.50 M imidazole, and fractions containing PTEN were purified further by chromatography on a HiLoad 26/60 G200 Superdex gel-filtration column. As a final step, wild-type PTEN and its K13A variant were purified by chromatography on a HiTrap Q anion-exchange column at pH 7.4, and PTEN-L was purified by chromatography on a HiTrap Heparin HP affinity column using an ÄKTA system from Amersham–Pharmacia (Piscataway, NJ), and

the results were analyzed with the UNICORN Control System. Aliquots of protein were supplemented with DTT (10 mM), glycerol (25% v/v), and EDTA (2 mM), flash frozen in liquid nitrogen, and stored at –80 °C. Protein concentrations were measured with a Bradford assay (Bradford, 1976).

2.5.3 Continuous Assay for the Enzymatic Activity of PTEN

We sought to establish the first continuous assay for the catalytic activity of PTEN. Our assay is based on the utilization of inorganic phosphate (P_i) by PNPase, which catalyzes the reaction of P_i and 7 methyl-6-thioguanosine (MESG) to form ribose-1-phosphate and 7-methyl-6-thioguanine (Figure 2.2B) (Webb, 1992). This assay is continuous, taking advantage of the large absorbance difference of MESG and the free nucleobase, 7-methyl-6-thioguanine. The $\Delta\epsilon$ for this reaction is 11 $mM^{-1}cm^{-1}$ at 360 nm.

The putative assay must be sensitive enough to respond to small amounts of released P_i. Using the known value of $\Delta\epsilon$, we predicted that a release of 2 μM P_i would raise the absorbance in a 1-cm path-length cuvette by 0.022 OD. This absorbance increase can be measured readily with a typical spectrophotometer or plate reader. Also, PTEN requires a reducing environment for its catalytic activity as its active-site nucleophile is a cysteine thiolate. We found that PNPase is able to function in a highly reducing environment.

PNPase concentration was measured with a Bradford assay (Bradford, 1976) and added to a concentration of 57 μg/mL (2 μM) in reaction buffer, which was 50 mM Tris–HCl

buffer, pH 7.6, containing EDTA (2.0 mM), MESG (0.6 mM), and DTBA (40 mM). In our assays, we used the soluble diC_8 version of phosphatidylinositol-(3,4,5)-trisphosphate as the substrate, as others have used in discontinuous assays (R. B. Campbell *et al.*, 2003; J.-O. Lee *et al.*, 1999; Maehama *et al.*, 2000; McConnachie *et al.*, 2003; Taylor and Dixon, 2003). Known concentrations of substrate (0–320 μM) were added to the buffer, and reactions were initiated by the addition of PTEN or PTEN-L to 20 nM, or K13A PTEN to 250 nM. As specified, some reactions contained NaCl (0, 100, or 200 mM) or another salt. Unlike in discontinuous assays (R. B. Campbell *et al.*, 2003), we did not add PIP_2 product to the assay solution, so as to amplify any effects of PIP_2 generated *in situ* on the reaction kinetics. Measurements of absorbance at 360 nM were recorded at 25 °C with a Cary 60 UV–Vis spectrophotometer having a Varian Cary Single Cell Peltier temperature control accessory from Agilent Technologies (Santa Clara, CA). Data analysis was performed with Prism version 6 from Graphpad (San Diego, CA).

2.6 Acknowledgements

We are grateful to Dr. Alonzo Ross for supplying the PET30B-PTEN plasmid (Addgene plasmid #20741; Redfern *et al.*, 2008).

2.7 Copyright

Chapter 3

Conformational Stability and Catalytic Activity of PTEN Variants Linked to Cancers and Autism Spectrum Disorders

3.1 Abstract

Phosphoinositides are membrane components that play critical regulatory roles in mammalian cells. The enzyme PTEN, which catalyzes the dephosphorylation of the phosphoinositide PIP_3, is damaged in most sporadic tumors. Mutations in the *PTEN* gene

have also been linked to autism spectrum disorders and other forms of delayed development. Here, human PTEN is shown to be on the cusp of unfolding under physiological conditions. Variants of human PTEN linked to somatic cancers and disorders on the autism spectrum are shown to be impaired in their conformational stability, catalytic activity, or both. Those variants linked only to autism have higher activity than those linked to cancers. PTEN-L, which is a secreted *trans*-active isoform, has greater conformational stability than does the wild-type enzyme. These data indicate that PTEN is a fragile enzyme cast in a crucial role in cellular metabolism, and suggest that PTEN-L is a repository for a critical catalytic activity.

3.2 Introduction

Phosphatase and tensin homolog on chromosome 10 (PTEN; EC 3.1.3.67) catalyzes the hydrolysis of phosphatidylinositol-(3,4,5)-trisphosphate (PIP_3) to form phosphatidylinositol-(4,5)-bisphosphate (PIP_2; Maehama and Dixon, 1998). Its PIP_3 substrate activates the phosphatidylinositol-3-kinase (PI3K) Akt pathway that mediates cell proliferation. Hence, PTEN is a tumor suppressor whose recognized importance in human biology is increasing steadily (Eng, 2003; Song *et al.*, 2012; Worby and Dixon, 2014). In addition to lipid phosphatase activity on the plasma membrane, which could alone contribute significantly to tumor suppression, PTEN has important roles in nuclear processes that include the promotion of chromosomal stability, repair of DNA damage (Bassi *et al.*, 2013), and regulation of the cell cycle (Song *et al.*, 2011).

The *PTEN* gene is mutated in 50–80% of sporadic human cancers (Salmena *et al.*, 2008). Moreover, germline mutations in PTEN are associated with the molecularly defined PTEN hamartoma tumor syndromes (PHTSs). PHTSs include Cowden syndrome and Bannayan-Riley-Ruvalcaba syndrome, and are associated with increased cancer predisposition (Eng, 2003). *PTEN* mutations are also strongly associated with macrocephaly (Mester *et al.*, 2011).

Some patients on the autism spectrum have germline mutations in the *PTEN* gene (Varga *et al.*, 2009). Autism spectrum disorders (ASDs) are characterized by impaired social interactions, impaired verbal or nonverbal communication skills, and repetitive behaviors (Caronna *et al.*, 2008). ASDs are enigmatic: despite being heritable, defects in a single gene or set of genes do not seem to be present in all patients (Newschaffer *et al.*, 2007). The biochemical link between PTEN dysfunction and ASDs is not known, though loss of PTEN function in developing mouse brain cells leads to their overgrowth, and deletion of the *PTEN* gene in neurons has large effects on neuronal morphology and circuitry (Lv *et al.*, 2013; Kreis *et al.*, 2014).

Recently, alternative translation of the PTEN mRNA using an upstream CTG codon was discovered and found to result in the production of a secreted *trans*-active version of PTEN (Hopkins *et al.*, 2013). Termed "PTEN-L" (Pulido *et al.*, 2014), this isoform is able to shrink PTEN-null tumors in mice. The same isoform has also been observed in the cytosol of cells and controls cell death upon interaction with mitochondria (Liang *et al.*, 2014). Wild-type PTEN and PTEN-L have similar kinetic parameters for catalysis of PIP_3 hydrolysis (Johnston and Raines, 2015a).

Conformational stability is critical to the biological function of enzymes and other proteins (Knowles, 1987). Mutations that lead to unstable human proteins can be lead to disease. For example, p53, like PTEN, is a tumor suppressor protein that is altered in a large fraction of human cancers. Extensive analyses have demonstrated that many cancer-associated p53 variants have compromised thermostability (Brandt *et al.*, 2012; Bullock *et al.*, 1997). That compromise also afflicts angiogenin, a human ribonuclease that has neuroprotective activity but is damaged in some patients with amyotrophic lateral sclerosis (Crabtree *et al.*, 2007). To date, however, no data have been reported on the thermostability of PTEN or its disease-related variants.

In this work, we present a biochemical analysis of variants of PTEN that are linked to somatic cancer, PHTSs, and ASDs (Figure 3.1). First, we analyze the catalytic activity of these variants using a newly developed continuous assay (Johnston and Raines, 2015a). Then, we develop an assay to measure the conformational stability of PTEN and its variants, including PTEN L, under a variety of conditions. The ensuing data provide the necessary biochemical insight on the relationship between PTEN dysfunction and human disease.

3.3 Experimental Procedures

3.3.1 Materials

Escherichia coli BL21(DE3) cells for protein production were from Novagen (Madison, WI). Expression plasmid pET30B-PTEN was a gift from Alonzo Ross (plasmid 20741

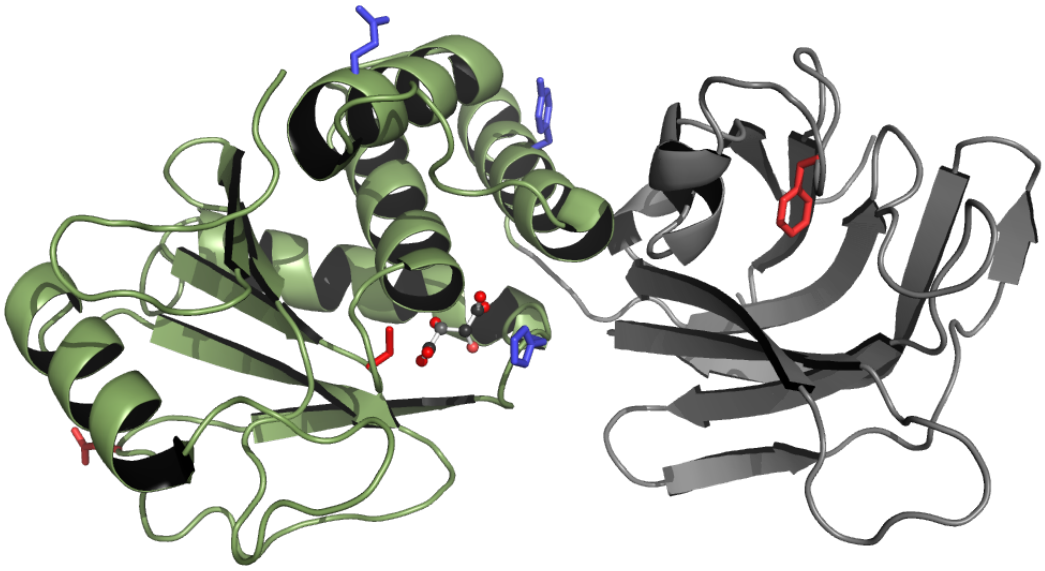

FIGURE 3.1: **Ribbon diagram of the three-dimensional structure of human PTEN.** The enzyme has a phosphatase domain (green) and C2 domain (gray). The side chains of amino-acid residues that are substituted in cancers (red) and autism spectrum disorders (blue) are shown explicitly. The enzymic active site contains an L(+)-tartrate ion, which is rendered in ball-and-stick format. The structure lacks 7 and 49 residues at the N and C termini, respectively, and a 24-residue internal loop. The image was created with the program PyMOL from Schrödinger (New York, NY) and PDB entry 1d5r (J.-O. Lee *et al.*, 1999).

from Addgene, Cambridge, MA) and directs the expression of human PTEN with a C-terminal His_6 tag (Johnston and Raines, 2015a). Plasmids that direct the production of PTEN variants were created with the QuikChange site-directed mutagenesis kit from Agilent (Santa Clara, CA). Expression plasmid pET30B-PTEN-L-S was derived by Gibson assembly (Gibson *et al.*, 2009) using a gBlocks® gene fragment from Integrated DNA Technologies (Coralville, IA). In pET30B-PTEN-L-S, the CTG encoding residue 1 was replaced with an ATG, the signal sequence (codons 2–21) was removed, the ATG at the translation start site for wild-type PTEN was replaced with ATA (codon 174), and other codon optimizations for *E. coli* expression were implemented that did not

affect the protein sequence in codons 2–173 (Hopkins *et al.*, 2013; Johnston and Raines, 2015a).

Terrific broth (TB) contained tryptone (12 g), yeast extract (24 g), K_2HPO_4 (72 mM), KH_2PO_4 (17 mM), and glycerol (4 mL). Columns of HisTrap HP, HiTrap Q HP, HiTrap Heparin HP, and Superdex G200 resins for protein purification were from GE Biosciences (Piscataway, NJ).

diC_8-Phosphatidylinositol-3,4,5-trisphosphate (PIP_3) was from Avanti Polar Lipids (Alabaster, AL) and Echelon Biosciences (Salt Lake City, UT). Bacterial nucleoside phosphorylase (PNPase) was product N2415 from Sigma-Aldrich (St. Louis, MO), dissolved in reaction buffer, and buffer-exchanged to remove residual phosphate. 7-Methyl-6-thioguanosine (MESG) was from Berry and Associates (Dexter, MI). Dithiobutylamine (DTBA Lukesh *et al.*, 2012) was product 774405 from Sigma-Aldrich. A 5000× solution of SYPRO® Orange Protein Gel Stain was from Life Technologies (Grand Island, NY). Ficoll® PM 70 was product 257529A from Santa Cruz Biotechnology (Dallas, TX) and had a molecular mass of 70 kDa. Phosphate-buffered saline (PBS) contained NaCl (137 mM), KCl (2.7 mM), Na_2HPO_4 (10 mM), and KH_2PO_4 (1.8 mM) at pH 7.4. All other chemicals and reagents were of commercial reagent grade or better, and were used without further purification.

3.3.2 Production and Purification of PTEN

Methods for the expression and purification of PTEN were based on those of Ross and coworkers (R. B. Campbell *et al.*, 2003). PTEN expression plasmids were transformed into *E. coli* strain BL21(DE3), and grown in TB supplemented with kanamycin (30 μM). Expression was induced at OD = 0.5–0.6 at 600 nm by the addition of isopropyl β-D-1-thiogalactopyranoside to 0.10 mM, and cells were grown for 20–22 h at 18 °C. Cells were harvested by centrifugation and lysed in 20 mM sodium phosphate buffer, pH 7.4, containing NaCl (0.50 M), imidazole (20 mM), and β-mercaptoethanol (0.7% v/v) with a French pressure cell. Lysate was clarified by centrifugation at 20,000g, and the soluble fraction was applied to a HisTrap HP column. Protein was eluted with 0.50 M imidazole, and fractions containing PTEN were purified further by chromatography on a HiLoad 26/60 G200 Superdex gel-filtration column. As a final step, wild-type PTEN and variants were purified by chromatography on a HiTrap Q anion-exchange column at pH 7.4, and PTEN-L was purified by chromatography on a HiTrap Heparin HP affinity column using an ÄKTA system from Amersham-Pharmacia (Piscataway, NJ), and the results were analyzed with the UNICORN Control System. Aliquots of protein were supplemented with dithiothreitol (10 mM), glycerol (25% v/v), and ethylenediaminetetraacetic acid (EDTA; 2 mM); flash frozen in liquid nitrogen; and stored at –80 °C. Protein concentrations were measured with a Bradford assay (Bradford, 1976).

3.3.3 Assays of Conformational Stability

The conformational stability of wild-type PTEN and its variants were assessed with differential scanning fluorimetry (DSF; Niesen *et al.*, 2007). This technique relies on the increase in fluorescence of the dye SYPRO® Orange upon its binding to hydrophobic residues of a protein that are exposed during thermal denaturation. Wild-type PTEN or a variant was dissolved at a concentration of 0.1 μg/μL in 100 mM 4-(2-hydroxyethyl)-1-piperazineethanesulfonic acid–(HEPES)–NaOH buffer, pH 7.4, containing NaCl (100 mM) and DTBA (10 mM). SYPRO® Orange, which is supplied at a concentration of 5000×, was added to a concentration of 15×. In experiments to probe molecular crowding, Ficoll® PM 70 or sucrose was present at a concentration of 50, 100, 150, 200, 250, or 300 mg/mL. Assay solutions were exposed to a temperature gradient from 10–95 °C with an increase of 1.0 °C per min. Upon heating, the fluorescence of solutions was monitored by using an excitation at (580 ± 10) nm and emission at (623 ± 14) nm. Heating and fluorescence-monitoring were performed with a ViiA™ 7 Real-Time PCR System from Life Technologies (Grand Island, NY). Assays were also performed in PBS rather than HEPES buffer, in the presence of calcium ions (added from 0.1 μM–1.2 mM), or with a heating rate of 0.2 °C per min rather than 1.0 °C per min.

Thermal denaturation data were prepared for analysis with ViiA™ 7 version 1.0 software, and analyzed with Protein Thermal Shift™ version 1.2 software, both from Life Technologies (Grand Island, NY). Subsequent data analysis and plotting was performed with Prism version 6 software from Graphpad (San Diego, CA). The value of T_{m} was

the temperature at the midpoint of the thermal transition between the low fluorescence of folded protein and the high fluorescence of unfolded protein after fitting to the Boltzmann equation (Niesen *et al.*, 2007).

3.3.4 Assays of Enzymatic Activity

Assays of the catalytic activity of wild-type PTEN and its variants were performed by using the continuous assay described previously (Johnston and Raines, 2015a). Briefly, PNPase concentration was measured with a Bradford assay (Bradford, 1976) and added to a concentration of 57 μg/mL (2 μM) in reaction buffer, which was 50 mM Tris–HCl buffer, pH 7.6, containing EDTA (2.0 mM), MESG (0.40–0.60 mM), and DTBA (40 mM). Known concentrations of PIP_3 substrate (0–320 μM) were added to the buffer, and reactions were initiated by the addition of PTEN. Wild-type PTEN was used at a concentration of 10 nM, PTEN-L at 20 nM, and PTEN variants at 100–300 nM. Measurements of absorbance at 360 nM were recorded at 25 °C with a Cary 60 UV–Vis spectrophotometer having a Varian Cary Single Cell Peltier temperature control accessory from Agilent Technologies (Santa Clara, CA). Data were analyzed with Prism version 6 software from Graphpad.

3.4 Results

3.4.1 Thermostability of Wild-type PTEN

We attempted to measure the conformational stability of wild-type PTEN with several methods, including thermal denaturation or chemical denaturation as monitored by ultraviolet spectroscopy or circular dichroism spectroscopy. In our hands, only DSF (Niesen *et al.*, 2007) provided a precise measure of conformational stability (Figures 3.5; 3.6; 3.7). With this assay, we found that wild-type PTEN has a T_m of (40.3 ± 0.1) °C (Table 3.1). This value was not affected by the presence of calcium ions at intracellular (0.1–0.4 μM) or extracellular (1.2 mM) concentrations (data not shown).

Enzyme	T_m (°C)[a]	k_{cat}/K_M ($\mu M^{-1}min^{-1}$)[b]	k_{cat} (min^{-1})[b]	K_M (μM)[b]
Wild-type PTEN	40.3 ± 0.1	174 ± 40[c]	4000 ± 300[c]	23 ± 5[c]
C124S	40.8 ± 0.1	<0.03	ND[d]	ND[d]
N82T	39.2 ± 0.3	27 ± 6	1300 ± 200	48 ± 18
F337S	32.2 ± 0.2	16 ± 5	700 ± 140	48 ± 18
H93R	38.7 ± 0.3	4.5 ± 0.4	171 ± 9	37 ± 5
Y176C	39.0 ± 0.4	55 ± 10	1800 ± 180	32 ± 9
E157G	38.4 ± 0.5	49 ± 11	1400 ± 150	28 ± 9
PTEN-L	46.7 ± 0.2	100 ± 25[c]	477 ± 28[c]	4.8 ± 1.1[c]

TABLE 3.1: **Parameters of wild-type PTEN and dysfunctional variants.**

[a]Values (± SE) were determined by DSF in 100 mM HEPES–NaOH buffer, pH 7.4, containing NaCl (100 mM), DTBA (10 mM), and SYPRO® Orange Protein Gel Stain (15×) with heating at 1 °C/min. Data are shown in Figures 3.2, 3.5, 3.6, and 3.7.

[b]Values (± SE) are for the turnover of diC_8-phosphatidylinositol-3,4,5-trisphosphate in 50 mM Tris–HCl buffer, pH 7.6, containing NaCl (0, 100, or 200 mM), EDTA (2.0 mM), MESG (0.20 mM), and DTBA (40 mM), as initiated by the addition of PTEN to 20 nM. Values (± SE) were derived by fitting initial velocity data to the Michaelis-Menten equation (eq 2.1).

[c]Values are from Johnston and Raines (2015a).

[d]ND, not determined.

3.4.2 Thermostability of PTEN-L

We assessed the conformational stability of PTEN-L, the "long" isoform of PTEN, with DSF. Strikingly, we found that PTEN-L, which has 173 additional residues on its N-terminus, has a T_{m} of (46.7 ± 0.2) °C (Figure 3.2). This value is 6.4 °C greater than that of wild-type PTEN.

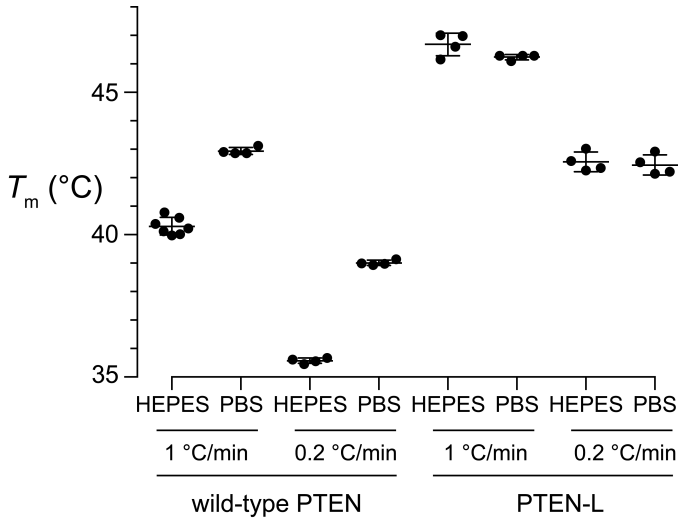

FIGURE 3.2: **Thermostability of human PTEN and PTEN-L.** Values of T_{m} were determined with DSF (ΔT = 1 °C/min or 0.2 °C/min) in 100 mM HEPES–NaOH buffer, pH 7.4, containing NaCl (100 mM), DTBA (10 mM), and SYPRO® Orange Protein Gel Stain (15×), or in PBS. Each data point is for an individual experiment.

3.4.3 Effect of Inorganic Phosphate and Heating Rate on the Value of T_{m}

Ligands have long been known to increase the conformational stability of proteins(O'Sullivan and Tompson, 1890; Schellman, 1975; Molina Martinez *et al.*, 2013) along with their resistance to proteolysis (Park and Marqusee, 2005). As PTEN is a phosphatase, we

assessed its thermostability in PBS, a buffer that is isotonic with human cells and contains 11.8 mM inorganic phosphate. We found that the T_m value of wild-type PTEN is (42.9 ± 0.1) °C in PBS (Figure 3.2), an increase of 2.6 °C compared to that in HEPES buffer. In contrast, the T_m value of PTEN-L is (46.2 ± 0.1) °C in PBS, which is actually a slight decrease compared to that in HEPES buffer. These data suggest that wild-type PTEN has greater affinity for inorganic phosphate than does PTEN-L.

Like the binding of ligands, the rate of sample heating is also known to affect the measured value of T_m (Rüegg *et al.*, 1977). Slower rates enable the folded and unfolded states of a protein to equilibrate more extensively and can give rise to lower T_m values. Instead of the typical heating rate of 1 °C/min for a DSF experiment (Niesen *et al.*, 2007), we used a rate of 0.2 °C/min. We found that the measured T_m values for wild-type PTEN and PTEN-L in HEPES buffer decrease to (35.6 ± 0.1) and (41.6 ± 0.2) °C, respectively, with the slower heating rate (Figure 3.2). Likewise, the T_m values in PBS decrease upon slow heating to (39.0 ± 0.1) and (42.4 ± 0.2) °C. Again, PTEN-L is much less affected by inorganic phosphate than is wild-type PTEN. Indeed, the ΔT_m = 6 °C in HEPES buffer and ΔT_m = 3 °C in PBS are independent of heating rate. We performed all subsequent measurements of thermostability in the absence of inorganic phosphate to avoid confounding ligand-binding with conformational stability.

3.4.4 Effect of Molecular Crowding on the Value of T_m

The concentration of molecules in the cytosol approaches 300 mg/mL (Ellis, 2001), and is even greater in the nucleus (Dhar *et al.*, 2011). The conformational stability

of proteins can be increased by the ensuing molecular crowding (Elcock, 2010; Ellis, 2001; H.-X. Zhou *et al.*, 2008). To determine whether molecular crowding affects the conformational stability of PTEN, we determined the value of T_m for wild-type PTEN in the presence of a molecular crowding agent, Ficoll® PM 70 (0–300 mg/mL), which is a high molecular-weight, highly branched polymer of sucrose. We found that the T_m value increases with the concentration of Ficoll® PM 70 (Figure 3.3). At 300 mg/mL Ficoll® PM 70, which mimics the concentration of macromolecules in the cytosol (Ellis, 2001), the T_m value is increased by 2 °C. To control for specific interactions with the sucrose units, we also determined the value of T_m for wild-type PTEN in the presence of sucrose itself (0–300 mg/mL). We found that the T_m value has an even greater dependence on the concentration of sucrose than on that of Ficoll® PM 70. At 300 mg/mL sucrose, the T_m value of PTEN is increased by 4 °C.

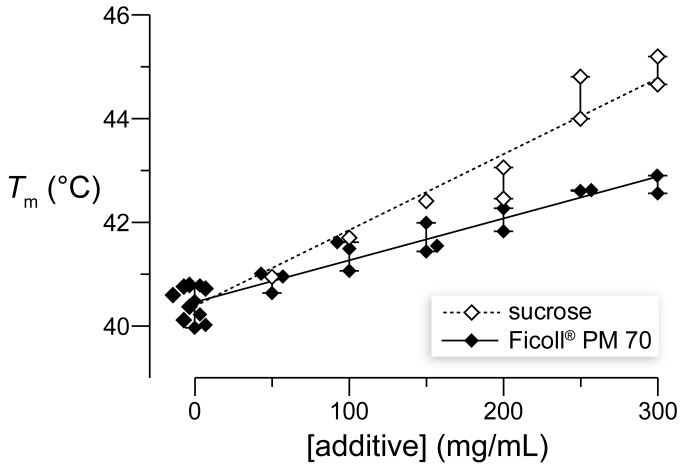

FIGURE 3.3: **Effect of molecular crowding on the thermostability of human PTEN.** Values of T_m were determined with DSF ($\Delta T = 1$ °C/min) in 100 mM HEPES–NaOH buffer, pH 7.4, containing NaCl (100 mM), DTBA (10 mM), SYPRO® Orange Protein Gel Stain (15×), and Ficoll® PM 70 or sucrose. Each data point is for an individual experiment. Data in the absence of additive are from Figure 3.2.

3.4.5 Cancer-linked Variants of PTEN

We produced and purified three variants of PTEN that have been found in somatic tumors as well as in the germline of patients with PHTSs (Figure 3.1). We began with an active-site variant. Catalysis by PTEN entails nucleophilic attack by the sulfur of Cys124 on the C-3 phosphoryl group of PIP_3. The substitution of Cys124 with a serine residue is found in some somatic tumors (Forbes *et al.*, 2015). The C124S substitution leads to a variant with undetectable catalytic activity (Table 3.1). We did, however, find that this variant has a T_m of (40.8 ± 0.1) °C, indicative of thermostability comparable to that of wild-type PTEN (Figure 3.4). Thus, the C124S substitution devastates catalysis by PTEN, but has little effect on conformational stability.

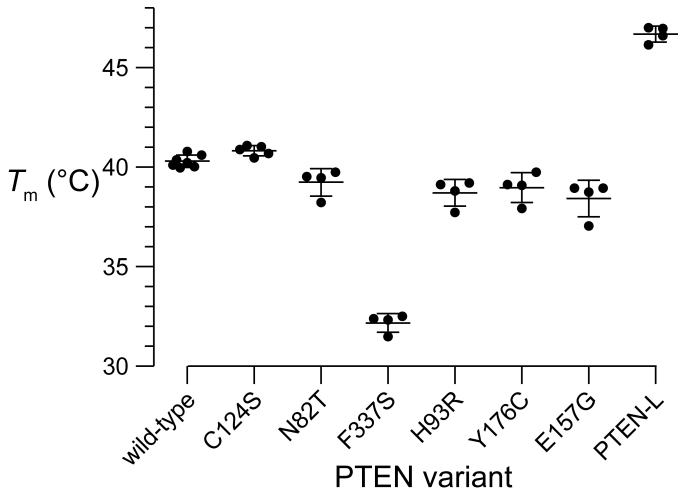

FIGURE 3.4: **Thermostability of human PTEN and its variants.** Values of T_m were determined with DSF ($\Delta T = 1$ °C/min) in 100 mM HEPES–NaOH buffer, pH 7.4, containing NaCl (100 mM), DTBA (10 mM), and SYPRO® Orange Protein Gel Stain (15×). Each data point is for an individual experiment. Data for wild-type PTEN and PTEN-L are from Figure 3.2. Raw data are shown in Figures 3.5–3.7. Values of T_m are listed in Table 3.1.

In a patient with early onset breast cancer, the codon for Asn82 in PTEN is replaced with one for a threonine residue (Figer *et al.*, 2002). Residue 82 is on the surface of the phosphatase domain of the protein (Figure 3.1). We found that N82T PTEN has a k_{cat}/K_M value of (27 ± 6) $\mu M^{-1}min^{-1}$ (Table 3.1; Figure 3.4), which is 15% that of the wild-type enzyme. This decrease in activity arises from both a reduction in the value of k_{cat} and an increase in the value of K_M. Themostability was compromised as well to give a T_m of (39.2 ± 0.3) °C. We conclude that the N82T substitution is detrimental to both catalysis and conformational stability.

In some patients with Cowden syndrome, which is a PHTS, Phe337 is replaced with a serine residue (Lachlan *et al.*, 2007). Residue 337 is located in the interior of the C2 domain of PTEN. We found that the F337S variant has a k_{cat}/K_M value of (16 ± 5) $\mu M^{-1}min^{-1}$ (Table 3.1; Figure 3.4), which is 9% that of wild-type PTEN. The F337S variant has a T_m of (32.2 ± 0.2) °C (Figure 3.1), which is the lowest observed herein and nearly 10 °C less than that of wild-type PTEN (though still well above 25 °C, which was the temperature in assays of catalytic activity). Thus, the F337S substitution is highly detrimental to catalysis by PTEN and to its conformational stability.

3.4.6 Autism-linked Variants of PTEN

We also produced and purified three variants of PTEN that have been found in patients on the autism spectrum. Among these variants was one in which His93 is replaced with an arginine residue. As had been shown previously (Redfern *et al.*, 2010), the catalytic activity of H93R PTEN is affected severely by this substitution, which is located close to

the interface between the phosphatase and C2 globular domains of PTEN (Figure 3.1). We found that H93R PTEN has a k_{cat}/K_M value of (4.5 ± 0.4) $\mu M^{-1}min^{-1}$ (Table 3.1; Figure 3.4), which is 3% that of the wild-type enzyme. Previous work indicated that the H93R substitution causes the protein to bind less strongly to liposomes containing the PIP_2 product (Redfern *et al.*, 2010). The binding of PIP_2 causes PTEN to shift into a relaxed state, resulting in higher activity (R. B. Campbell *et al.*, 2003; Johnston and Raines, 2015a). Accordingly, an inability to bind to PIP_2 should lead to low levels of activity, as observed herein. H93R PTEN had a low T_m of (38.1 ± 0.3) °C, which is close to physiological temperature in humans.

The tyrosine residue at position 176 of PTEN is replaced with cysteine in an autistic boy (Orrico *et al.*, 2009). At 9 years old, this boy suffered from delayed speech and inhibited social interactions. Like His93, Tyr176 is located in the interface between the two globular domains (Figure 3.1). Y176C PTEN has the highest catalytic activity of all variants tested herein, with a k_{cat}/K_M value of (55 ± 10) $\mu M^{-1}min^{-1}$, which is 32% that of wild-type PTEN (Table 3.1; Figure 3.4). The Y176C variant has a slightly diminished value of T_m of (39.0 ± 0.4) °C. Thus, Y176C PTEN suffers from only a modest decrease in catalytic efficacy and conformational stability.

In a pair of twins, one exhibiting a partial developmental delay and another on the autism spectrum (Varga *et al.*, 2009), Glu157 was replaced with a glycine residue.11 This residue is located on the surface of the phosphatase domain. Like the Y176C variant, E157G PTEN has relatively high activity, with a k_{cat}/K_M value of (49 ± 11) $\mu M^{-1}min^{-1}$ (Table 3.1, Figure 3.4). Moreover, this variant also has a T_m of (38.4 ±

0.5) °C (Figure 3.1), which is only 2 °C less than that of the wild-type enzyme. Thus, E157G PTEN is similar to Y176C PTEN in its catalytic activity and conformational stability. These two variants, which are active but only marginally stable, might be able to act in some cellular environments but be impaired in others.

3.5 Discussion

3.5.1 PTEN has a Fragile Conformation

Human PTEN has an elongated structure composed of two distinct domains (Figure 3.1). The conformational stability of this structure had not been assessed previously. The raw data from thermal denaturation experiments were indicative of a transition between two states, not three (Figures 3.5; 3.6; 3.7). Apparently, the two domains of PTEN unfold cooperatively rather than independently. This single unfolding transition gave rise to a T_{m} value that is close to the physiological temperature of humans (Figure 3.2).

We found that the T_{m} value of PTEN correlates with the concentration of Ficoll® PM 70 (Figure 3.3), a sucrose polymer that can mimic molecular crowding *in cellulo* (Ellis, 2001). We also found, however, that much of this added stability arises from specific interactions between the sucrose units and PTEN, as a sucrose molecule confers approximately twice the increase in T_{m} value as does a sucrose unit within the Ficoll® PM 70 polymer. We conclude that molecular crowding does not lead to a substantial increase in the thermostability of PTEN. Hence, PTEN is poised on the edge of instability

and a point mutation that leads to a small decrease in PTEN thermostability can have detrimental consequences *in cellulo*.

The fragility of PTEN is in marked contrast to that of another important tumor suppressor, p53. Recently, Veprintsev, Fersht, and coworkers used DSF to show that human p53 has a T_m value of 46 °C (Brandt *et al.*, 2012), which is well above that of human PTEN under any condition used herein (Figures 3.2; 3.3; 3.4). These data suggest that PTEN is more vulnerable than is p53 to inactivation *in cellulo* by an amino-acid substitution.

Unlike human PTEN, human PTEN-L is not a fragile protein. Its T_m value is 10 °C above physiological temperature. Previously, the 173 appended residues were shown to enable secretion of PTEN-L and uptake by other cells (Hopkins *et al.*, 2013). Our data indicate that these residues also serve to endow PTEN with greater conformational stability. That attribute befits a protein that must survive in the extracellular matrix, and provides humans with a reservoir of PTEN activity that is less vulnerable to inactivation. The three-dimensional structure of PTEN-L is unknown. Like wild-type PTEN, PTEN-L unfolds with a single transition (Figures 3.5; 3.6; 3.7). This cooperative unfolding, along with the conformational stability conferred by the appended residues, is consistent with the 173 N terminal residues of PTEN-L adopting a defined three-dimensional structure that interacts intimately with one or both of its globular domains. Kinetic data suggest that the N-terminal residues of PTEN-L interacts with the PIP_2-binding motif (residues 6–14 of wild-type PTEN; Johnston and Raines, 2015a).These experimental data conflict with a bioinformatics analysis predictive of a disordered N terminus in PTEN-L (Malaney *et al.*, 2013).

3.5.2 Cancer-linked Variants of PTEN

The importance of PTEN to cancer progression and many other cellular functions and malfunctions cannot be understated (Song *et al.*, 2012). We characterized three variants of PTEN that are linked to cancers. We found that two of these three variants are deficient in either conformational stability or catalytic activity. C124S PTEN lacked detectable catalytic activity; F337S PTEN has a T_{m} that is nearly 10 °C lower than that of wild-type PTEN, and would be unfolded *in cellulo*. In contrast, N82T PTEN is less compromised than the other two variants. This finding is consistent with the in vivo data of Newschaffer and coworkers, who reconstituted a humanized PI3K/PTEN system in Saccharomyces cerevisiae cells (Rodríguez-Escudero *et al.*, 2011). The N82T substitution is linked with early-onset breast cancer. We note that Asn82 is located on the surface of the protein and could play a role in PTEN-protein interactions (Hopkins *et al.*, 2014). Moreover, the installation of a threonine residue at position 82 converts this segment of the protein into a putative substrate for the cellular kinases STE, STE7, and MAP2K2 (Xue *et al.*, 2011). Phosphorylation there could be detrimental to PTEN activity *in cellulo*.

3.5.3 Autism-linked Variants of PTEN

All three of the variants of PTEN tested herein exhibited T_{m} values between 38 and 39 °C. Two of these variants (E157G and Y176C) were still efficacious catalysts with $k_{\mathrm{cat}}/K_{\mathrm{M}}$ values near 50 $\mu\mathrm{M}^{-1}\mathrm{s}^{-1}$, which is 1/3 that of the wild-type enzyme. These

data are again consistent with observations in S. cerevisiae cells (Rodríguez-Escudero *et al.*, 2011). Another variant (H93R) is found in patients with PHTS as well as in somatic cancer (Hobert *et al.*, 2014; Forbes *et al.*, 2015). This variant had been analyzed previously(Redfern *et al.*, 2010) and found to be defective in binding to the product PIP_2, an event that is important for the manifestation of the catalytic activity of PTEN (Johnston and Raines, 2015a). We too found that the H93R PTEN has low catalytic activity.

3.6 Conclusions

We have reported the first measurements of the thermostability of human PTEN. We find that PTEN is a quasi-stable protein at physiological temperature, even in the presence of a ligand (inorganic phosphate) or a molecular crowding agent. PTEN dysfunction leads to the overgrowth, excessive proliferation, and accelerated differentiation of human cells (Lv *et al.*, 2013; Song *et al.*, 2012). Accordingly, we have also reported a biochemical analysis of six PTEN variants that are implicated in somatic cancers and diseases on the autism spectrum. We find that those variants linked to cancers are more damaged than those linked to autism. This conclusion, which is based on biochemical data (Table 3.1), is consistent with observed effects of allelic mutations *in cellulo* (Spinelli *et al.*, 2015). Notably, the PTEN-L isoform is more stable than wild-type PTEN. As both PTEN and PTEN-L are encoded by the same gene, the uptake of PTEN-L could provide a cell with some relief from a deleterious mutation. In addition to underpinning an understanding

of the biology and pharmacology of PTEN, these findings encourage the development of small-molecule ligands that stabilize disease-related variants of PTEN and thus enhance their enzymatic activity *in cellulo*.

3.7 Acknowledgements

We are grateful to Dr. D. J. Aceti (University of Wisconsin–Madison) for help with DSF experiments, and Dr. Alonzo Ross for supplying the PET30B-PTEN plasmid (Addgene plasmid #20741; Redfern *et al.*, 2008).

3.7.1 Funding

This work was supported by Grant R01 GM044783 (NIH). S.B.J. was supported by a Dennis Weatherstone Predoctoral Fellowship from Autism Speaks and by Molecular Biosciences Training Grant T32 GM007215 (NIH). The ViiA^{TM} 7 Real-Time PCR System for DSF was obtained with support from Grant U01 GM094622 (NIH).

3.8 Copyright

3.9 Supporting Information

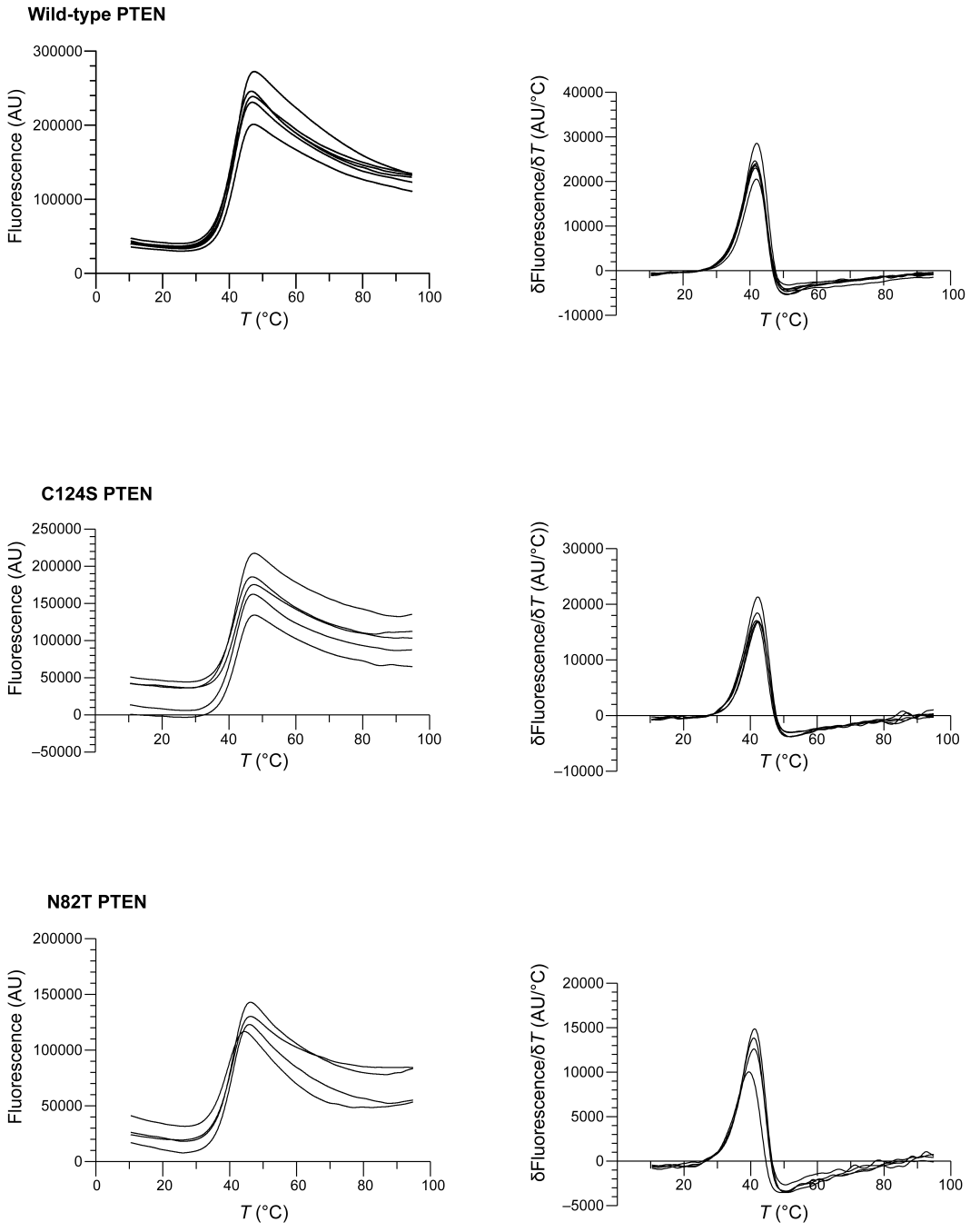

FIGURE 3.5: **Raw melt data for wild-type, C124S, and N82T PTEN.** Raw data for differential scanning fluorimetry experiments of human PTEN and its variants in 100 mM HEPES–NaOH buffer, pH 7.4, containing NaCl (100 mM), DTBA (10 mM), and SYPRO® Orange Protein Gel Stain (15×). Samples were heated at 1.0 °C per min.

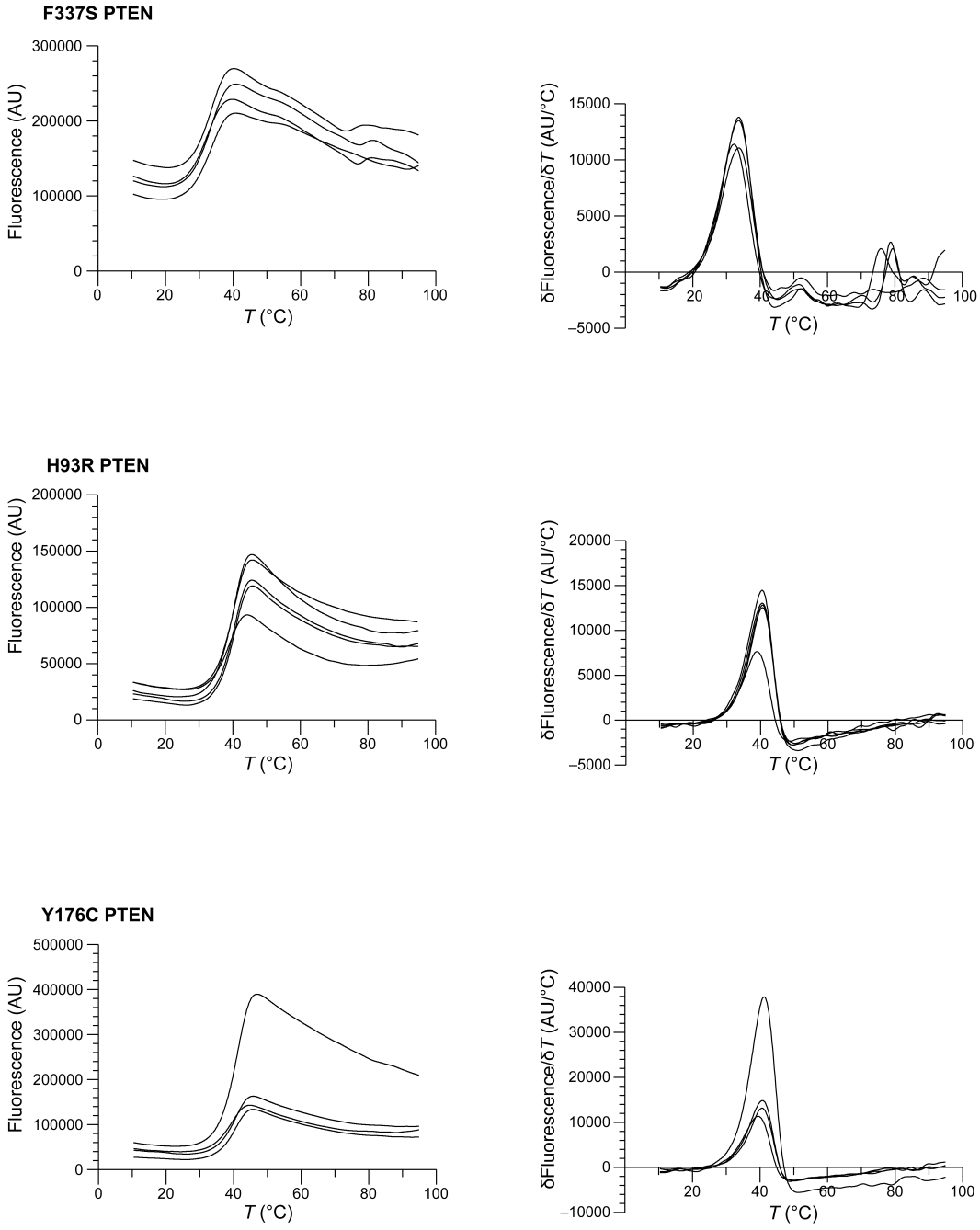

FIGURE 3.6: **Raw melt data for F337S, H93R, and Y176C PTEN.** Raw data for differential scanning fluorimetry experiments of human PTEN and its variants in 100 mM HEPES–NaOH buffer, pH 7.4, containing NaCl (100 mM), DTBA (10 mM), and SYPRO® Orange Protein Gel Stain (15×). Samples were heated at 1.0 °C per min.

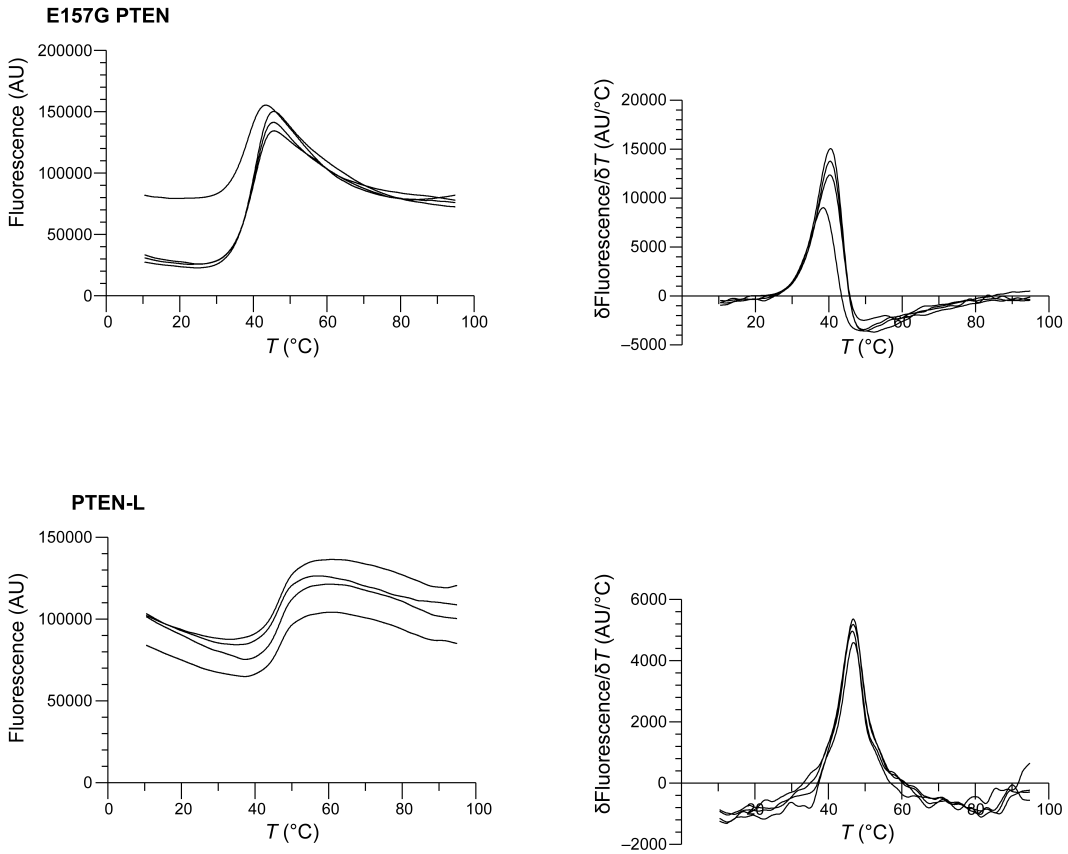

FIGURE 3.7: **Raw melt data for E157G PTEN and PTEN-L.** Raw data for differential scanning fluorimetry experiments of human PTEN and its variants in 100 mM HEPES–NaOH buffer, pH 7.4, containing NaCl (100 mM), DTBA (10 mM), and SYPRO® Orange Protein Gel Stain (15×). Samples were heated at 1.0 °C per min.

Chapter 4

PTENpred: A Designer Protein Impact Predictor

4.1 Abstract

Making connections between genotype and phenotype has become more important than ever in recent years. Whole exome sequencing will be even more inexpensive as more and better techniques are developed, but in cancer, many of the genes responsible for transformation of normal cells are known. Current software for measuring the impact of non-synonymous single nucleotide polymorphisms is designed for analysis of all proteins. We present a protein impact predictor, PTENpred, that is trained on and meant to predict phenotypes related to a single important protein, PTEN. PTEN is implicated in most cancers and is also connected to germline disorders including Cowden

syndrome and autism. PTENpred prediction output is accompanied by an interactive three-dimensional display of the crystal structure. Our predictor is designed for use by biologists, clinicians, and laymen interested in interpreting the possible effect of a novel PTEN mutation.

4.2 Introduction

PTEN, or the phosphatase and tensin homolog deleted from chromosome ten, is a tumor suppressor that functions in a number of important cellular pathways as a lipid and protein phosphatase (J. Li *et al.*, 1997; Maehama and Dixon, 1998; Tamura *et al.*, 1999). The PTEN gene is now known to be mutated in 50–80% of sporadic tumors (including glioblastoma and prostate cancer) and 30–50% of breast, colon, and lung cancers (J. Li *et al.*, 1997; Salmena *et al.*, 2008). In cancer cell lines lacking PTEN, overexpression of PTEN leads to restoration of a non-cancerous phenotype (Stambolic *et al.*, 1998). PTEN germline mutations give rise to an array of syndromes generally characterized by extreme growth (Silva *et al.*, 2008). Interestingly, different missense mutations result in dysfunctional PTEN that is implicated in cancer syndromes as well as syndromes as diverse as autism. It is not clear why different mutations cause different syndromes.

A variety of computational and structural machine-learning methods have been used in efforts to probe the effects of non-synonymous single nucleotide polymorphisms (SNPs, Chan *et al.*, 2007; P. J. Miller *et al.*, 2011; Thompson *et al.*, 2012). These changes result in a variation in the amino-acid sequence of a protein. Current methods include some

that only use multiple protein alignments, some that only use structural information, and some that combine these two methods (Katsonis *et al.*, 2014). In some cases, as in those related to mismatch repair gene missense substitutions, predictive approaches have been developed that are recommended for use in a clinical setting (Thompson *et al.*, 2012). The *in silico* methods are quick, non-invasive ways to diagnose issues in mismatch repair genes.

Structure-based non-synonymous SNP computational prediction methods generally calculate the stability change of the protein with the amino-acid change (Topham *et al.*, 1997). These methods can explore the local three-dimensional environment of an amino-acid change (Capriotti and Altman, 2011). Residues that are distal in the amino-acid sequence can be proximal in three dimensional space, and changes to residues in the core of a protein can have more effects on conformational stability than do residues on the protein exterior (Cordes *et al.*, 1996). Still, these methods are likely to miss residues that are important for protein–protein interactions, as these residues are generally on the exterior. Also, although there are many protein structures deposited in the Protein Data Bank every year (Berman *et al.*, 2013), only a small fraction of proteins have known structures as is usually required by these methods. Homology-based non-synonymous SNP prediction methods incorporate sequence alignments and substitution matrices to predict the consequences of amino-acid change (Cargill *et al.*, 1999). Sequences from homologous proteins that are from either the same organism or different organisms are compared and are scored in various ways.

Support vector machines (SVMs) are machine learning algorithms that are able to take input data, called vectors, that are associated with a category (Bishop, 2006). Each vector can have many pieces of data, called features, that are from a variety of sources. Each feature allows the SVM to consider an additional set of data, like accessible surface area, by adding an extra column of input information. After taking in a number of vectors and their associated classes as training data, they can then predict the class of an unknown vector (Figure 1.5).

SNP computational prediction methods have mostly been trained on data from non-synonymous SNPs from a variety of proteins. We believed that, as the importance of PTEN in cancer and other syndromes becomes more and more clear, a specific predictor for PTEN mutations was necessary. Here, we present a designer protein impact predictor called PTENpred. The classifier is trained on a curated set of PTEN mutation data with the phenotypes that are associated with the specific PTEN mutation. We believe that PTENpred will have broad utility.

4.3 Methods

4.3.1 The PTENpred Algorithm

PTENpred takes input from many different analyses and combines them using a support vector machine (SVM) algorithm (Bishop, 2006). Each feature is a score that has been calculated from the structure in the PDB (for accessible surface area or secondary

structure scores) or a score that is the result of a predictor designed to predict the results of an amino-acid change in any given protein. Secondary structure and accessible surface area scores were derived from the PDB entry 1d5r where possible (Frishman and Argos, 1995; Eisenhaber and Argos, 1993) and were otherwise predicted by SPIDER2 (Heffernan *et al.*, 2015), an evolution of the SPINE-X algorithm (Faraggi *et al.*, 2012).

The selected predictors are based either completely on homology (SIFT; Ng and S. Henikoff, 2001, MAPP Stone and Sidow, 2005, and Provean Choi *et al.*, 2012) or on both homology and structural information (Polyphen-2: Ramensky *et al.*, 2002; Adzhubei *et al.*, 2010; SuSPect: Yates *et al.*, 2014; and VarMod: Pappalardo and Wass, 2014). VarMod also incorporates protein interaction data from Interactome3D (Mosca *et al.*, 2013).

4.3.2 Variation Data and Categories

The input data on PTEN amino acid variations were derived from many different sources (Appendix A). The total number of variations (676) were sorted into four categories: null (70), autism-related (16), somatic cancer associated (502), and germline PHTS associated (88). Null variants were derived from dbSNP (Sherry *et al.*, 2001), the Human Gene Mutation Database (HGMD; Stenson *et al.*, 2014), and variants found to be active in a yeast PI3K/PTEN system (Rodríguez-Escudero *et al.*, 2011). Autism-related variants and variants related to PHTS were derived from the HGMD and other individual publications. Somatic cancer variants were from the Catalogue of Somatic Mutations in Cancer (COSMIC; Forbes *et al.*, 2015).

As expected, we found significant overlap between mutations associated with somatic cancer and those associated with germline PHTS. Two variables for somatic mutations were taken into account to resolve these overlaps: the number of times this particular mutation has been found in somatic cancer overall and the average number of total PTEN mutations found in each sample. For example, the variant Y155C occurs 10 times in tumor samples found in the COSMIC database. Of those 10 times, the average number of total PTEN mutations is 1.3. From these numbers, we can hypothesize that Y155C is a relatively common PTEN variation in somatic cancer and that this variation might indeed inactivate PTEN fully. The Y155C variant is also found in a patient with Cowden Syndrome (CS; Gicquel *et al.*, 2003), indicating that germline variation can result in inactivation of PTEN. Most mutations found in both PHTS and the COSMIC database are categorized as PHTS variations.

4.3.3 Dataset Grouping

The contents of several categories were small compared to the total number of variations. Accordingly, we thought it would be helpful to group categories in five different ways. For easy comparison to already-established predictors, we grouped categories into two classes: "null and pathogenic" (where null is the null category and pathogenic is a group of the autism-related, somatic cancer-related, and PHTS-related categories, hereby designated N/ASP) and "null-autism and pathogenic" (where null-autism contains both autism and null categories, and pathogenic contains somatic cancer and PHTS categories, hereby designated NA/SP). We also established groups of three categories:

"null, autism, and pathogenic" (where pathogenic is somatic cancer and PHTS categories, hereby designated N/A/SP) and "null, mild affecting, and PHTS" (where mild affecting is somatic cancer and autism categories, hereby designated N/AS/P). The last grouping has each category alone (designated N/A/S/P). A separate SVM classifier was trained on each of the five groupings.

4.3.4 SVM Classifier Training

The SVM classifiers were trained using Python version 2.7.9 (Downey *et al.*, 2002) and the scikit-learn project package version 0.15.2 (Pedregosa *et al.*, 2011), which is itself an implementation based on the LIBSVM package (Chang and Lin, 2011). The data set was scaled using the StandardScaler object in scikit-learn. Each classifier used the SVC method in scikit-learn with the Radial Basis Function (RBF) kernel. Class weights were adjusted to be inversely proportional to their frequencies (*i.e.,* classes with fewer members are weighted more). Multiclass classification for the 3- and 4-category datasets is implemented using the "one-against-one" approach (Knerr *et al.*, 1990).

Accuracy was analyzed using nested cross-validation. One fold from a randomized, stratified 6-fold division of the data was set aside for testing. Optimal hyperparameters (C and γ) were then chosen using grid search cross-validation with 8 stratified folds on the training set. Optimization of hyperparameters used the F1 score, the harmonic mean of precision and recall (Powers, 2011). This process was repeated 6 times with each of the folds being set aside for testing once. The reported accuracy is the average $\pm$ standard deviation of correctly predicted variations.

As the calculated accuracy was stable and did not vary widely for each of the 6 folds after iterative nested cross-validation, finalized classifiers were generated by the same method used on the training set: grid search cross-validation with 8 stratified folds on the entire data set.

4.3.5 Comparison to Provean and Polyphen-2

To compare PTENpred performance to Provean and PolyPhen-2 (Choi *et al.*, 2012; Capriotti and Altman, 2011), the test set of variations for each of the two-category classifiers was run on each service. Receiver operating characteristic (ROC) curves and area under the ROC curve (AUC-ROC) were generated using scikit-learn (Pedregosa *et al.*, 2011) and the matplotlib Python-based computer plotting package (Hunter, 2007).

4.3.6 Resources

The web application is implemented using Python version 2.7.6 on a server running Ubuntu 14.04.2 LTS server edition.

4.4 Results

4.4.1 PTENpred Accuracy

We measured the accuracy of PTENpred using nested 6-fold cross-validation for each of the category splits, measuring the average percentage of correctly predicted classes on

the test fold. The results are shown in Table 4.1. Nested cross-validation was iterated, and a one-way ANOVA test was performed to ensure that no statistical difference existed between iterated cross-validation scores (data not shown).

Category Split	Accuracy (%)
Null / Pathogenic	74 ± 5
Null Autism / Pathogenic	66 ± 3
Null / Autism / Pathogenic	78 ± 4
Null / Autism Somatic / Pathogenic	66 ± 5
Null / Autism / Somatic / Pathogenic	64 ± 3

TABLE 4.1: **Accuracy scores for PTENpred.** Values (± SD) were estimated by stratified 6-fold cross-validation. The classifier was trained on 5 folds of data and was used to predict the last fold.

4.4.2 Visualization of PTENpred Predictions

We performed principle component analysis on our data to decompose data down to a lower dimensional space, keeping only the most significant features. We then fitted our classifiers to this decomposed data. We found that only the category splits with two classes (N/ASP and NA/SP) produced classifiers that were consistent with classifiers trained on higher-dimensional data (consistency was tested with iterative nested cross-validation). These classifiers are trained on all of the data and were used to generate contour maps. We then plotted a randomized, stratified 20% of the data so as to visualize PTENpred predictions (Figure 4.1).

To visualize predictions further, we calculated and plotted receiver operating characteristic (ROC) curves (Figure 4.2). These curves were generated by averaging ROC data over 6 stratified cross-validation folds.

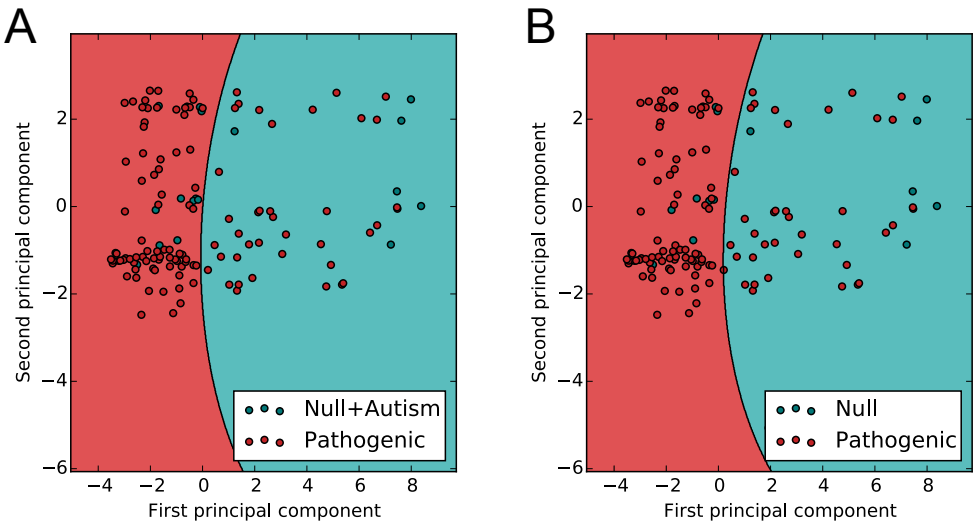

FIGURE 4.1: **Depiction of predictions of PTENpred projected on two principle components.** Using principle component analysis, 22 features from support vectors were projected onto two dimensions. The PTENpred classifier was trained on the entire two-dimensional data set and was used to create the contour areas. 20% of the available data was then graphed to visualize correctly predicted and incorrectly predicted residues. **A**, N/ASP classifier predictions, **B**, NA/SP classifier predictions.

4.4.3 PTENpred Performance Comparisons

To compare PTENpred performance to currently available protein impact predictors, we calculated ROC curves in the same way as in Figure 4.2. We present this comparison in Figure 4.3.

4.4.4 Web Application

We constructed an implementation of the PTENpred predictor on a local server in the Department of Biochemistry at the University of Wisconsin–Madison. Using the input field, a user can input a variant of PTEN in the form of "L70P", for example, to indicate a change at the 70th codon of PTEN from leucine to proline. A user can also select

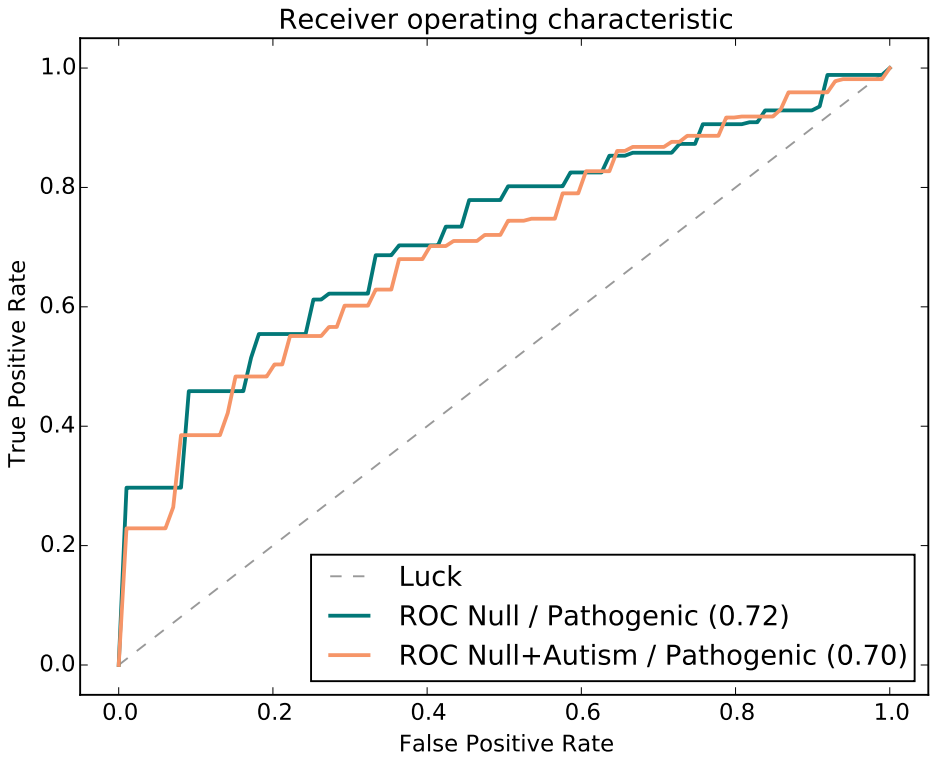

FIGURE 4.2: **Cross-validated ROC analysis on predictions of PTENpred for binary classifiers.** The two binary classifiers, N/ASP and NA/SP, were used to generate a receiver operating characteristic plot. The ideal point for the curve is to be at the upper left, where the True Positive Rate is 1.0 and the False Positive Rate is 0.0. Therefore, area under the curve (max = 1.0) is a measure of the success of the predictor. 6 stratified folds of the data were created, and the classifiers were trained on 5 folds and used to create an ROC curve. This procedure was performed 6 times with each fold of the data being used as the test set once. These ROC curves were averaged to create these mean ROC plots.

which of the five classifiers to use to classify the variant (N/ASP, NA/SP, N/A/SP, N/AS/P, or N/A/S/P). An in-production version of the classifier can be accessed at `http://128.104.116.121/predict.php`. For now, users are required to be connected to the internet via the BiochemNet_Secure wireless network or via ethernet in the University of Wisconsin–Madison Biochemistry buildings.

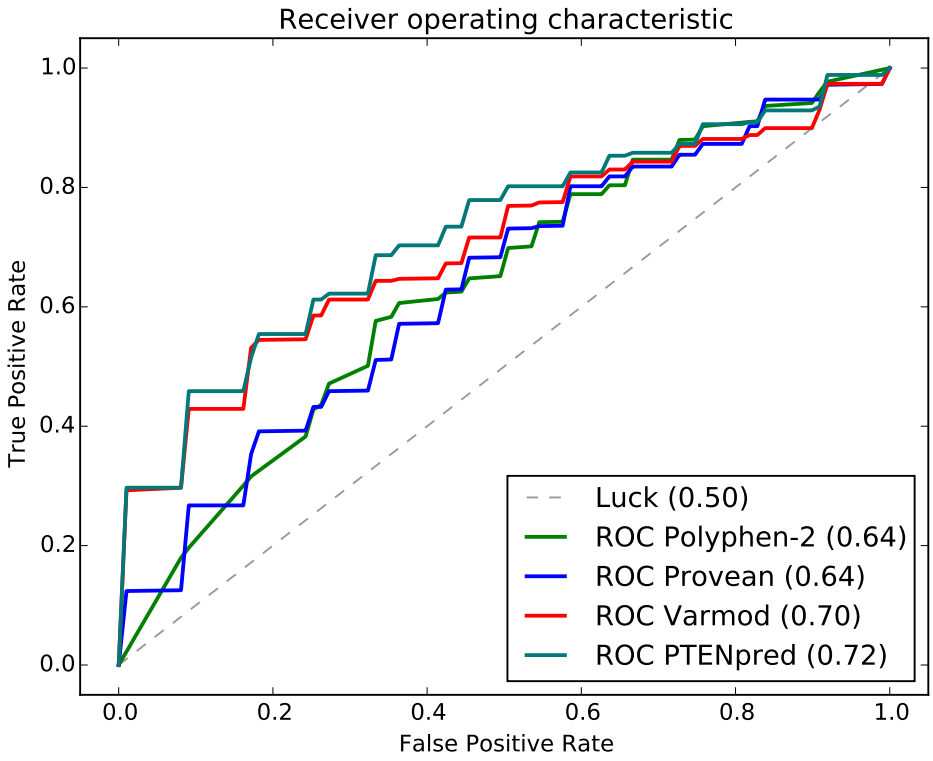

FIGURE 4.3: **Predictions of PTENpred binary classifier with three other leading impact predictors.** The binary classifier, N/ASP was used to generate a receiver operating characteristic plot as in Figure 4.2. ROC analysis was also performed for three other prediction methods: Polyphen-2 (Adzhubei *et al.*, 2010), Provean (Choi *et al.*, 2012), and VarMod (Pappalardo and Wass, 2014). For each method, ROC curves for each fold of the data were generated, and these curves were averaged.

As output, PTENpred gives the predicted class information, and also presents a JavaScript-implemented version of Jmol (JSmol; Hanson *et al.*, 2013) to display the location of the wild-type residue in the query.

4.5 Conclusions

We have presented the first designer protein impact predictor, PTENpred. This predictor is the first for non-synonymous SNPs that is focused on one particular protein, the tumor suppressor PTEN, which is altered in 50–80% of human cancer patients. PTENpred is comparable in accuracy to several other protein predictors (Figure 4.3). We believe that focusing on one protein allows for curation of mutations and possible correlation with specific disease states and phenotypes. The successful implementation of this sort of designer protein impact predictor relies on phenotypic knowledge of many different variations. PTENpred can be used by clinicians and biologists to elucidate the nature of any new PTEN variation discussed in the clinic or laboratory.

Chapter 5

Future Directions

5.1 Toward an Activator of PTEN Activity

PTEN, as discussed in Chapter 1, is an incredibly important protein to tumor formation and cancer development. As PTEN activity is sometimes impaired by post-translational modification (Song *et al.*, 2012), molecules that activate PTEN activity could be very useful in the treatment of cancer or germline PHTSs. I confirm in Chapter 2 previous findings that PTEN requires product activation to reach optimal activity (R. B. Campbell *et al.*, 2003). The product formed in our assay is diC_8-PIP_2, and activation is not apparent with diC_6-PIP_2 or diC_4-PIP_2 (data not shown; R. B. Campbell *et al.*, 2003). This indicates that activation is dependent on a sizable hydrophobic moiety. I confirm additionally in Chapter 2 that PTEN activation is dependent on the presence of a canonical PIP_2 binding motif located on the N-terminus of PTEN. For these reasons,

I believe that PTEN could use an alternative amphipathic molecule for activation of activity.

The continuous assay developed in Chapter 2 for activity of PTEN requires a few relatively inexpensive reagents and would be amenable to scale up in a high-throughput manner (Lavery *et al.*, 2001). Molecules that activate PTEN activity in a similar way to PIP_2 could be found by measuring for PTEN activity on an alternative substrate $PI(3,4)P_2$ whose product does not demonstrably activate PTEN (R. B. Campbell *et al.*, 2003). In this fashion, molecules that activate PTEN activity could be discovered and used as a therapeutic for cancer and possibly germline PTEN disorders. It may be important to explore molecules that are sufficient for the activation of PTEN that do not competitively inhibit the protein.

5.2 Toward an Stabilizer of PTEN

5.2.1 Rationale

PTEN is also a relatively unstable molecule *in vivo*, as I discuss in Chapter 3. In addition, I show that variants of PTEN implicated in autism and cancer are additionally destabilized. For these reasons, molecules that stabilize PTEN may also have use as therapeutics in cancer and germline PTEN disorders. We note in Chapter 3 that use of a phosphate buffer instead of a HEPES buffer seems to stabilize PTEN.

5.2.2 Preliminary Results and Discussion

I have performed additional DSF experiments that indicate an interesting relationship with substrate and product molecules. In Figure 5.1, we see that a catalytically inactive version of PTEN is considerably stabilized by the presence of PIP_3, but is seemingly destabilized by the presence of PIP_2. This dichotomy does not seem to be due to the nature of the protein itself, as wild type PTEN is also destabilized upon addition of PIP_2 (Figure 5.1). We note that some of this problem may be caused by an additional interaction of PIP_2 with the some component of the analysis mixture, as DSF melting curves in the presence of PIP_2 have a modified profile (Figure 5.2). Last, we note that all of these reactions have been performed in HEPES buffer.

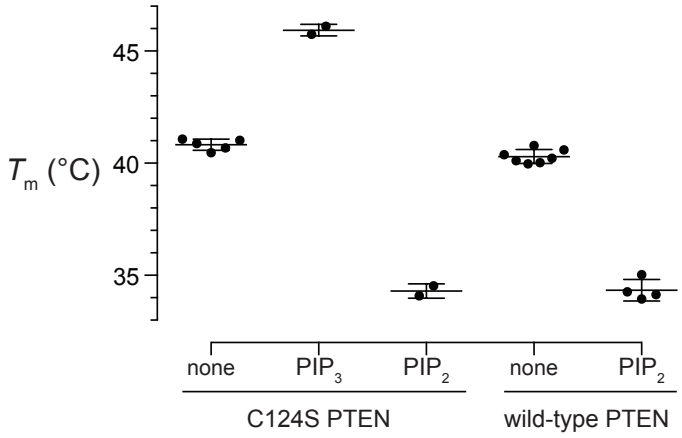

FIGURE 5.1: **Thermostability of human PTEN and catalytically inactive PTEN with substrate and product.** Values of T_m were determined with DSF (ΔT = 1 °C/min) in 100 mM HEPES–NaOH buffer, pH 7.4, containing NaCl (100 mM), DTBA (10 mM), and SYPRO® Orange Protein Gel Stain (15×). Points indicated with PIP_2 and PIP_3 had 20 μM diC_8 lipid added. Each data point is for an individual experiment. Data in the absence of additive are from Figure 3.2.

It is tempting to hypothesize a model for these results. In HEPES buffer, the removal of a single phosphate group (PIP_3 vs. PIP_2) has a huge impact on C124S protein

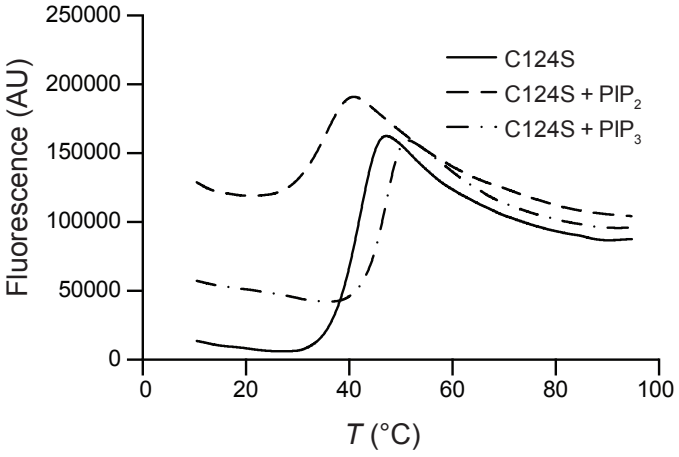

FIGURE 5.2: **Raw melt data for C124S PTEN in the presence of substrate and product.** Raw data for 3 representative differential scanning fluorimetry experiments of C124S PTEN in 100 mM HEPES–NaOH buffer, pH 7.4, containing NaCl (100 mM), DTBA (10 mM), SYPRO® Orange Protein Gel Stain (15×), and indicated samples had PIP_2 and PIP_3 (50 μM diC_8 lipid). Samples were heated at 1.0 °C per min.

stability (>10 °C in T_m), and it seems that PIP_2 has the same effect on wild-type PTEN (PIP_3 could not be tested as this is immediately converted into PIP_2). Perhaps PIP_2 destabilizes PTEN and in this manner activates the protein, as we see catalytic activation of PTEN by PIP_2 as well.

I sought to determine whether the stabilizing effect of PIP_3 and the destabilizing effect of PIP_2 was saturable. We performed these experiments in phosphate buffer, because I had seen previously that phosphate buffer brings with it its own marginal stabilization effects. As I reported in Chapter 3, changing to a phosphate-based buffer stabilizes wild-type PTEN (~5 °C), but strikingly, phosphate buffer stabilizes catalytically inactive C124S PTEN by almost 20 °C (Figure 5.3). In this case, I did finally see similarities in the effects of PIP_2 and PIP_3: a gradual destabilization that did not seem to be saturable.

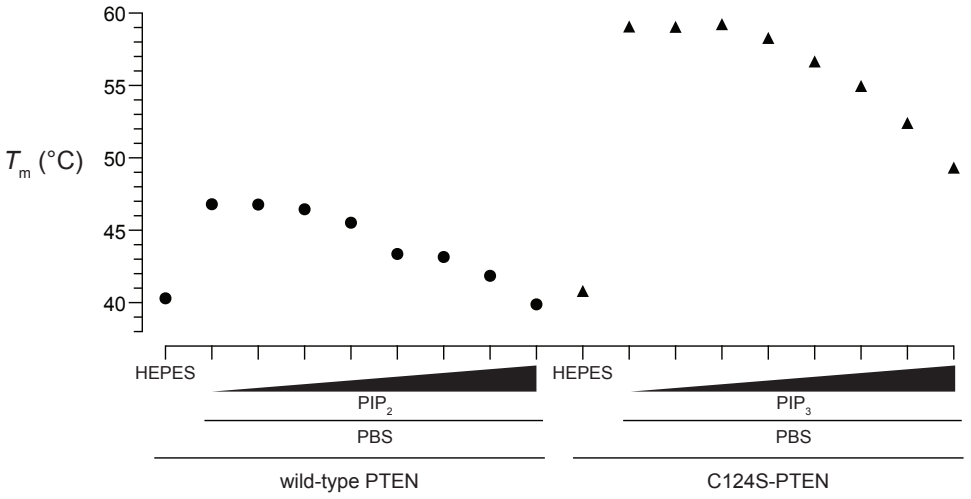

FIGURE 5.3: **Thermostability of human PTEN and catalytically inactive PTEN with substrate and product.** Values of T_m were determined with DSF (ΔT = 1 °C/min) in 100 mM HEPES–NaOH buffer, pH 7.4, containing NaCl (100 mM), DTBA (10 mM), and SYPRO® Orange Protein Gel Stain (15×), or in PBS. Points indicated with an increasing level of PIP_2 and PIP_3 are single experiments, and had 0, 1, 5, 10, 20, 30, 50, and 80 μM diC_8 lipid added. Data in HEPES buffer in the absence of additive are the average value from Figure 3.2

These results are consistent with the model where PIP_2 leads to a destabilization that then increases PTEN activity, but they indicate more questions than answers. For instance, why does PIP_3 stabilize C124S PTEN only in HEPES buffer? Why does phosphate buffer stabilize the catalytically inactive form of PTEN substantially more than wild-type?

5.2.3 Future Thoughts

It is apparent that PTEN stability is easily affected by different ligands, particularly those with negative charges. It is also possible, however, that PTEN could be stabilized or destabilized by many other kinds of ligands, and this could be readily and quickly

analyzed by DSF (Niesen *et al.*, 2007). David Aceti in the Markley group has developed several ligand screens for testing small molecule ligand effects on proteins, and more ligands that stabilize and destabilize PTEN could be found. These ligands could then be tested to see what effect they have on PTEN activity. This could shed light on what kinds of ligands (stabilizing, destabilizing, neutral) activate PTEN activity.

5.3 PTEN as a Protein Therapeutic

The Raines group has much experience in improving and detecting translocation of proteins from outside the cell into endosomes and cytosol (Fuchs *et al.*, 2007; Rutkoski and Raines, 2008; Levine *et al.*, 2013). As we have discussed previously, subtle changes in PTEN dosage have enormous consequences for survival in a mouse model (Alimonti *et al.*, 2010). Additionally, it seems that the expressed isoform of PTEN called PTEN-L is secreted from cells and may have a role in cancer prevention in humans (Hopkins *et al.*, 2013). Indeed, PTEN-L injected into a mouse model of cancer substantially reduced tumor size. In my experience, however, PTEN-L has proven extremely difficult to purify. Therefore, engineered versions of PTEN, a more accessible recombinant protein, capable of translocating cell membranes may prove to be an excellent cancer treatment.

Our group has shown that changes encoded by sequence can have great effects on protein translocation. Poly-arginine tags and arginine grafting are two methods that may endow PTEN with cell-penetrating abilities, and we have experience with both of these methods (Fuchs and Raines, 2005; Fuchs *et al.*, 2007; Fuchs and Raines, 2007). We are

also actively investigating other methods based on chemical modification of wild-type proteins that might deliver these proteins tracelessly into the cytosol in their native state.

5.4 Cysteine-71 as an Oxidation Protector

As discussed in Section 1.2.5 and depicted in Figure 1.4, the crystal structure of PTEN indicates that Cys71 is quite close in three-dimensional space to the active-site catalytic cysteine, Cys124. The only disulfide detected *in vivo* is that between Cys71 and Cys124 (S.-R. Lee *et al.*, 2002). At first glance, this might seem a defect—another cysteine so close in three-dimensional space. However, consider the alternative: thiols (Cys-SH) can be quickly oxidized to sulfenyl (Cys-SOH) groups, which can then be further oxidized irreversibly to sulfinyl (Cys-SO_2H) and sulfonyl (Cys-SO_3H) groups (Reddie *et al.*, 2008). PTEN has even been detected in a sulfenylated form (Paulsen *et al.*, 2012). The nearby cysteine 71 locks the catalytic cysteine 124 into the disulfide state, which is always reversible. This hypothesis could be relatively easily investigated by changing Cys71 to alanine or serine and testing this PTEN variant *in vitro* and *in cellulo*.

5.5 Nature of PTEN-L Oligomerization

We have reason to believe that PTEN-L may be an oligomer in solution. First, purification of the protein on gel filtration results in elution of active protein starting at the

void volume of the Superdex G200 column, indicating sizes anywhere between the actual size of PTEN-L (65 kDa) to 600 kDa.

Complicating these facts, PTEN-L is quite difficult to purify recombinantly from *E. coli*. It is large, runs relatively high for its size on an SDS–PAGE gel, and tends to co-purify with what seems to be an *E. coli* chaperone protein. PTEN-L runs very close to this protein on an SDS–PAGE gel (Figure 5.4A). We cut out each of the bands shown in the gel and tested them by mass spectrometry, and both bands were hits for both PTEN-L and *E. coli* Hsp70.

As Hsp70 is an ATP-dependent chaperone protein, we have also taken samples similar to that depicted in Figure 5.4A and subjected them to 13 mM ATP. After a 20-min incubation at 37 °C, a white solid formed. Both the precipitated protein (data not shown) and filtered supernatant (Figure 5.4B) contained PTEN-L according to immunoblot analysis.

We also subjected these samples to a mild trypsin treatment (0.7 mg/mL) for 20 min at 37 °C. This treatment decreased the presence of both bands, but also seemed to retain a small amount of PTEN-L (Figure 5.4B). After treatment with trypsin, this sample was subjected to chromatography on a gel-filtration column. The PTEN-L band eluted with the void volume, indicating a size of >600 kDa. Additional tests with mild trypsin treatment might allow purification of PTEN-L and could possibly indicate the oligomerization status of the protein.

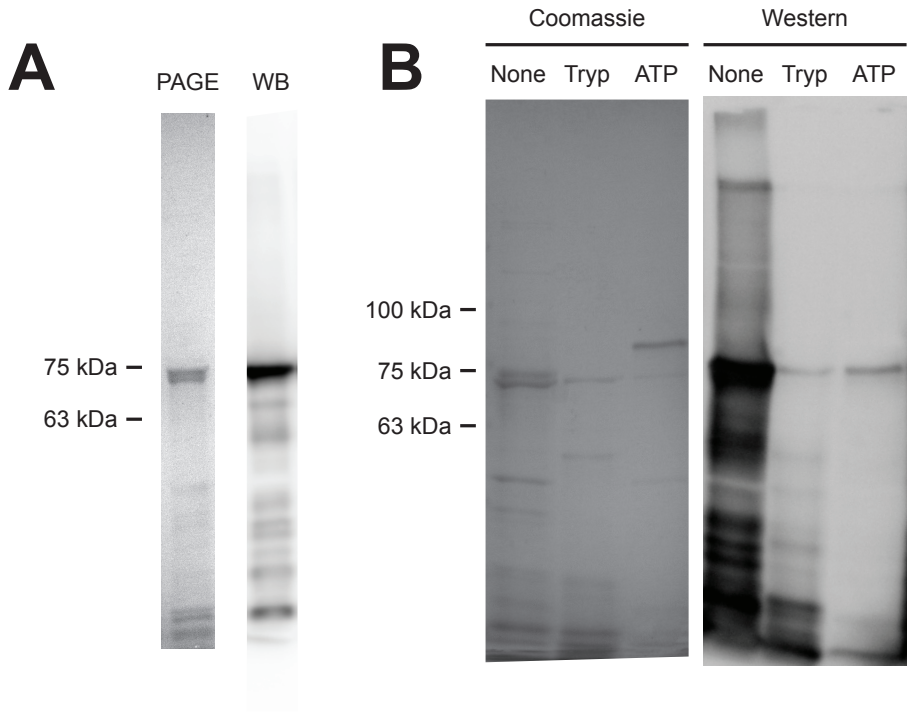

FIGURE 5.4: **Co-purification of PTEN-L with Hsp70 and treatment results.** **A**, The left lane labeled "PAGE" is a depiction of the double band on an SDS–PAGE gel stained with Coomassie R-250. The right lane is an immunoblot of the same lane input. The antibody used was PTEN (A2B1) from Santa Cruz Biotechnology (Dallas, TX). **B**, After combining and concentrating fractions similar to those in **A**, one third of the leftovers each were exposed to three treatments. None, no treatment. Tryp, exposed to mild trypsin treatment (0.7 mg/mL) for 20 min at 37 °C. ATP, exposed to 13 mM ATP and incubated for 20 min at 37 °C, then filtered.

5.6 N-terminus of PTEN-L

PTEN-L was discovered only recently (Hopkins *et al.*, 2013). It has been shown that a 6-arginine stretch is important for anti-tumor activity, but there are 173 additional amino acids in PTEN-L. We have shown that the additional amino acids are able to keep PTEN in a constitutively activated state (Chapter 2) and provide additional stabilization

(Chapter 3). It remains to be seen, however, which parts of the N-terminus of PTEN-L are important for these added features. Our group is poised to perform experiments gradually removing parts of the N-terminus and testing these variant proteins for activity and stability. These experiments could indicate important features that could be added to wild-type PTEN to create a stabilized, hyperactive version of the protein.

Appendix A

PTENpred Input Data

TABLE A.1: **Input mutations for PTENpred.** The below table contains all of the input mutations for the PTENpred mutation predictor. Codon is the position of the mutation in wild-type PTEN, WT is the amino acid in wild-type PTEN, Var is the variant amino acid, Count is the number of somatic tumors in the COSMIC database that contain this mutation, Average is the average number of mutations in PTEN for each somatic tumor sample, Type is the categorization for the specified mutation, and Source is the source of the mutation.

Codon	WT	Var	Count	Average	Type	Source
1	M	K	1	1.00	Somatic	Forbes *et al.*, 2015
1	M	T	4	2.50	Somatic	Forbes *et al.*, 2015
2	T	I	1	1.00	Somatic	Forbes *et al.*, 2015
3	A	S	1	2.00	Somatic	Forbes *et al.*, 2015
3	A	V	1	6.00	Somatic	Forbes *et al.*, 2015
3	A	D	2	1.00	Somatic	Forbes *et al.*, 2015
5	I	L	1	1.00	Somatic	Forbes *et al.*, 2015
5	I	V	1	2.00	Somatic	Forbes *et al.*, 2015
6	K	I	1	1.00	Somatic	Forbes *et al.*, 2015
6	K	N	2	2.00	Somatic	Forbes *et al.*, 2015
6	K	R	2	3.00	Somatic	Forbes *et al.*, 2015
6	K	E	1	3.00	Somatic	Forbes *et al.*, 2015
7	E	G	1	3.00	Somatic	Forbes *et al.*, 2015
8	I	T	1	1.00	Somatic	Forbes *et al.*, 2015
10	S	R	2	1.00	Somatic	Forbes *et al.*, 2015
10	S	I	1	4.00	Somatic	Forbes *et al.*, 2015
10	S	N	3	1.33	Somatic	Forbes *et al.*, 2015
10	S	G			Null	Sherry *et al.*, 2001
11	R	K	1	4.00	Somatic	Forbes *et al.*, 2015
13	K	E	2	1.50	Somatic	Forbes *et al.*, 2015
13	K	Q	1	1.00	Somatic	Forbes *et al.*, 2015
13	K	N	1	2.00	Somatic	Forbes *et al.*, 2015
14	R	M	1	2.00	Somatic	Forbes *et al.*, 2015
14	R	G	6	2.17	Somatic	Forbes *et al.*, 2015
14	R	S	1	1.00	Somatic	Forbes *et al.*, 2015
15	R	I	4	1.75	Somatic	Forbes *et al.*, 2015
15	R	G	2	4.00	Somatic	Forbes *et al.*, 2015
15	R	K	4	2.00	Somatic	Forbes *et al.*, 2015
15	R	S	3	1.00	PHTS	Nagy *et al.*, 2011
16	Y	C	2	1.50	Somatic	Forbes *et al.*, 2015
17	Q	P	1	1.00	Somatic	Forbes *et al.*, 2015
18	E	G	1	2.00	Somatic	Forbes *et al.*, 2015
19	D	G	1	4.00	Somatic	Forbes *et al.*, 2015
19	D	E	1	1.00	Null	Sherry *et al.*, 2001
19	D	N	1	1.00	Somatic	Forbes *et al.*, 2015

20	G	E	1	1.00	Somatic	Forbes *et al.*, 2015
20	G	R	1	1.00	Somatic	Forbes *et al.*, 2015
21	F	L	1	2.00	Somatic	Forbes *et al.*, 2015
21	F	S	2	2.00	Somatic	Forbes *et al.*, 2015
23	L	F	3	1.00	Somatic	Forbes *et al.*, 2015
23	L	V	1	1.00	Somatic	Forbes *et al.*, 2015
24	D	E	3	1.00	Somatic	Forbes *et al.*, 2015
24	D	N	3	1.00	Somatic	Forbes *et al.*, 2015
24	D	H	2	1.00	PHTS	M.-H. Tan *et al.*, 2011
24	D	Y	5	1.60	PHTS	Celebi *et al.*, 1999
24	D	G	6	1.67	PHTS	M.-H. Tan *et al.*, 2011
24	D	V	1	3.00	Somatic	Forbes *et al.*, 2015
25	L	S	1	1.00	Somatic	Forbes *et al.*, 2015
25	L	F	3	1.00	PHTS	M.-H. Tan *et al.*, 2011
26	T	A	1	2.00	Somatic	Forbes *et al.*, 2015
26	T	I	2	2.00	Somatic	Forbes *et al.*, 2015
26	T	P	2	1.50	PHTS	M.-H. Tan *et al.*, 2011
27	Y	D	4	1.50	Somatic	Forbes *et al.*, 2015
27	Y	S	1	1.00	Somatic	Forbes *et al.*, 2015
27	Y	H	1	2.00	Somatic	Forbes *et al.*, 2015
27	Y	N	3	1.00	Somatic	Forbes *et al.*, 2015
27	Y	C	5	2.00	Somatic	Forbes *et al.*, 2015
28	I	M	2	2.50	Somatic	Forbes *et al.*, 2015
28	I	S	1	1.00	Somatic	Forbes *et al.*, 2015
29	Y	S	1	1.00	Somatic	Forbes *et al.*, 2015
30	P	Q	1	2.00	Somatic	Forbes *et al.*, 2015
31	N	K	1	3.00	Somatic	Forbes *et al.*, 2015
31	N	H	1	2.00	Somatic	Forbes *et al.*, 2015
32	I	N			PHTS	M.-H. Tan *et al.*, 2011
33	I	S	2	1.50	Somatic	Forbes *et al.*, 2015
34	A	V	1	2.00	Somatic	Forbes *et al.*, 2015
34	A	D	1	2.00	PHTS	D. J. Marsh *et al.*, 1999
35	M	L	1	1.00	Somatic	Forbes *et al.*, 2015
35	M	I	3	1.00	Somatic	Forbes *et al.*, 2015
35	M	R	1	1.00	PHTS	Olschwang *et al.*, 1998
35	M	T	1	1.00	PHTS	X. Zhou *et al.*, 2001
35	M	V	4	1.00	PHTS	M.-H. Tan *et al.*, 2011
36	G	V	2	1.00	Somatic	Forbes *et al.*, 2015
36	G	E	5	1.40	Somatic	Forbes *et al.*, 2015
36	G	R	6	1.00	PHTS	Celebi *et al.*, 2000
37	F	L	1	2.00	Somatic	Forbes *et al.*, 2015
37	F	S	2	2.00	Somatic	Forbes *et al.*, 2015

38	P	R	1	2.00	Somatic	Forbes *et al.*, 2015
38	P	L	2	1.00	Somatic	Forbes *et al.*, 2015
38	P	S	12	1.08	Somatic	Forbes *et al.*, 2015
39	A	T	1	2.00	Somatic	Forbes *et al.*, 2015
39	A	P			PHTS	Tate *et al.*, 2008
39	A	V	1	4.00	Somatic	Forbes *et al.*, 2015
42	L	V	1	1.00	Somatic	Forbes *et al.*, 2015
42	L	P	1	1.00	Somatic	Forbes *et al.*, 2015
42	L	R	6	1.00	Somatic	Forbes *et al.*, 2015
43	E	K			PHTS	M.-H. Tan *et al.*, 2011
44	G	D	4	1.00	Autism	Varga *et al.*, 2009
45	V	I	1	3.00	Somatic	Forbes *et al.*, 2015
45	V	A	1	1.00	Somatic	Forbes *et al.*, 2015
46	Y	H	3	2.67	Somatic	Forbes *et al.*, 2015
46	Y	C	2	3.00	Somatic	Forbes *et al.*, 2015
46	Y	D	1	1.00	Somatic	Forbes *et al.*, 2015
47	R	M	3	2.33	Somatic	Forbes *et al.*, 2015
47	R	G	4	1.75	Somatic	Forbes *et al.*, 2015
48	N	I	2	1.50	Somatic	Forbes *et al.*, 2015
48	N	D	2	1.50	Somatic	Forbes *et al.*, 2015
48	N	K			PHTS	Vega *et al.*, 2003
49	N	I	1	1.00	Somatic	Forbes *et al.*, 2015
49	N	T	1	1.00	Somatic	Forbes *et al.*, 2015
52	D	G	2	3.00	PHTS	M.-H. Tan *et al.*, 2011
52	D	N	1	1.00	Somatic	Forbes *et al.*, 2015
53	V	G	1	1.00	Somatic	Forbes *et al.*, 2015
53	V	I	1	3.00	Somatic	Forbes *et al.*, 2015
53	V	A			Null	Rodríguez-Escudero *et al.*, 2014
54	V	L	1	1.00	Somatic	Forbes *et al.*, 2015
54	V	A	1	4.00	Somatic	Forbes *et al.*, 2015
54	V	E	1	5.00	Somatic	Forbes *et al.*, 2015
55	R	S	1	1.00	Somatic	Forbes *et al.*, 2015
55	R	M	1	4.00	Somatic	Forbes *et al.*, 2015
55	R	G	3	1.33	Somatic	Forbes *et al.*, 2015
56	F	C	1	2.00	Somatic	Forbes *et al.*, 2015
56	F	V			Null	Rodríguez-Escudero *et al.*, 2014
57	L	S	2	1.00	Somatic	Forbes *et al.*, 2015
57	L	W	3	1.00	Somatic	Forbes *et al.*, 2015
58	D	Y	1	1.00	Somatic	Forbes *et al.*, 2015
58	D	N	1	2.00	Somatic	Forbes *et al.*, 2015
59	S	P	1	1.00	Somatic	Forbes *et al.*, 2015
59	S	L	2	1.00	Somatic	Forbes *et al.*, 2015

60	K	T	1	1.00	Somatic	Forbes *et al.*, 2015
61	H	D			Autism	Reardon *et al.*, 2001
61	H	P	1	1.00	Somatic	Forbes *et al.*, 2015
61	H	Q	1	2.00	Somatic	Forbes *et al.*, 2015
61	H	L	1	1.00	Somatic	Forbes *et al.*, 2015
61	H	R	11	1.00	PHTS	M.-H. Tan *et al.*, 2011
61	H	Y	1	1.00	PHTS	M.-H. Tan *et al.*, 2011
62	K	N	1	1.00	Somatic	Forbes *et al.*, 2015
62	K	R	1	2.00	Somatic	Forbes *et al.*, 2015
62	K	I	1	1.00	Somatic	Forbes *et al.*, 2015
63	N	Y	1	1.00	Somatic	Forbes *et al.*, 2015
65	Y	D	1	1.00	Somatic	Forbes *et al.*, 2015
65	Y	N	1	1.00	Somatic	Forbes *et al.*, 2015
65	Y	C	1	2.00	Somatic	Forbes *et al.*, 2015
66	K	N	5	1.80	Somatic	Forbes *et al.*, 2015
66	K	Q	1	1.00	Somatic	Forbes *et al.*, 2015
66	K	E	2	2.00	Somatic	Forbes *et al.*, 2015
67	I	T	1	3.00	Somatic	Forbes *et al.*, 2015
67	I	R	1	1.00	PHTS	D. Marsh *et al.*, 1998
67	I	K	2	1.00	Somatic	Forbes *et al.*, 2015
68	Y	D			Autism	Loffeld *et al.*, 2006
68	Y	N	2	1.00	Somatic	Forbes *et al.*, 2015
68	Y	H	9	1.22	PHTS	D. Marsh *et al.*, 1998
68	Y	C	4	2.25	PHTS	Lobo *et al.*, 2009
70	L	V			Autism	Hobert *et al.*, 2012
70	L	H	1	1.00	Somatic	Forbes *et al.*, 2015
70	L	F	1	2.00	Somatic	Forbes *et al.*, 2015
70	L	I	1	4.00	Somatic	Forbes *et al.*, 2015
70	L	P	1	1.00	PHTS	Eng, 2003
71	C	Y	4	1.25	Somatic	Forbes *et al.*, 2015
71	C	W	2	1.50	Somatic	Forbes *et al.*, 2015
72	A	V	1	1.00	Somatic	Forbes *et al.*, 2015
73	E	V	1	2.00	Somatic	Forbes *et al.*, 2015
73	E	K	1	2.00	Somatic	Forbes *et al.*, 2015
74	R	T	1	1.00	Somatic	Forbes *et al.*, 2015
74	R	I	1	2.00	Somatic	Forbes *et al.*, 2015
75	H	N	1	2.00	Somatic	Forbes *et al.*, 2015
76	Y	C	1	2.00	Somatic	Forbes *et al.*, 2015
78	T	A	1	1.00	Somatic	Forbes *et al.*, 2015
79	A	N			Null	Sequence Alignment
79	A	T	3	2.00	PHTS	Figer *et al.*, 2002
80	K	E	1	1.00	Somatic	Forbes *et al.*, 2015

80	K	N	1	1.00	Somatic	Forbes *et al.*, 2015
81	F	C	3	1.33	Somatic	Forbes *et al.*, 2015
81	F	L	3	2.00	Somatic	Forbes *et al.*, 2015
82	N	T	2	1.00	Somatic	Forbes *et al.*, 2015
84	R	G	1	1.00	Somatic	Forbes *et al.*, 2015
85	V	F	1	1.00	Somatic	Forbes *et al.*, 2015
85	V	G	1	2.00	Somatic	Forbes *et al.*, 2015
85	V	A	5	1.40	Somatic	Forbes *et al.*, 2015
86	A	V	1	2.00	Somatic	Forbes *et al.*, 2015
86	A	P	2	1.00	Somatic	Forbes *et al.*, 2015
86	A	S	2	4.00	Somatic	Forbes *et al.*, 2015
87	Q	P	1	3.00	Somatic	Forbes *et al.*, 2015
87	Q	R	1	2.00	Somatic	Forbes *et al.*, 2015
88	Y	S	1	1.00	Somatic	Forbes *et al.*, 2015
88	Y	C	11	1.55	Somatic	Forbes *et al.*, 2015
88	Y	H	2	1.00	Somatic	Forbes *et al.*, 2015
88	Y	N	1	1.00	Somatic	Forbes *et al.*, 2015
89	P	A			Null	Rodríguez-Escudero *et al.*, 2014
90	F	S	2	1.50	Somatic	Forbes *et al.*, 2015
90	F	C	1	3.00	Somatic	Forbes *et al.*, 2015
90	F	L	2	1.00	Null	Rodríguez-Escudero *et al.*, 2014
90	F	A			Null	Rodríguez-Escudero *et al.*, 2014
91	E	G	2	2.00	Somatic	Forbes *et al.*, 2015
91	E	A	1	1.00	Null	Rodríguez-Escudero *et al.*, 2014
91	E	Q	2	1.00	Somatic	Forbes *et al.*, 2015
92	D	H	3	2.00	Somatic	Forbes *et al.*, 2015
92	D	A	1	1.00	Somatic	Forbes *et al.*, 2015
92	D	Y	1	2.00	Somatic	Forbes *et al.*, 2015
92	D	V	2	1.00	Somatic	Forbes *et al.*, 2015
92	D	G	8	2.38	Somatic	Forbes *et al.*, 2015
92	D	N			Null	Rodríguez-Escudero *et al.*, 2014
92	D	E	9	1.22	PHTS	Eng, 2003
93	H	R			Autism	Butler *et al.*, 2005
93	H	L	1	1.00	Somatic	Forbes *et al.*, 2015
93	H	Q	3	1.00	Somatic	Forbes *et al.*, 2015
93	H	D	1	1.00	Somatic	Forbes *et al.*, 2015
93	H	Y	6	1.00	PHTS	Kohno *et al.*, 1998
94	N	Y	1	1.00	Somatic	Forbes *et al.*, 2015
94	N	S	2	3.00	Somatic	Forbes *et al.*, 2015
94	N	A			Null	Rodríguez-Escudero *et al.*, 2014
94	N	I	1	2.00	Somatic	Forbes *et al.*, 2015
95	P	S	4	1.50	Somatic	Forbes *et al.*, 2015

95	P	A			Null	Rodríguez-Escudero *et al.*, 2014
95	P	L	6	1.33	PHTS	M.-H. Tan *et al.*, 2011
96	P	L	5	2.00	Somatic	Forbes *et al.*, 2015
96	P	T	1	2.00	Somatic	Forbes *et al.*, 2015
96	P	S	3	2.33	Somatic	Forbes *et al.*, 2015
96	P	A	1	12.00	Null	Rodríguez-Escudero *et al.*, 2014
96	P	Q	1	1.00	PHTS	Bussaglia *et al.*, 2002
96	P	R			PHTS	M.-H. Tan *et al.*, 2011
97	Q	A			Null	Rodríguez-Escudero *et al.*, 2014
98	L	A			Null	Rodríguez-Escudero *et al.*, 2014
99	E	K	1	4.00	Somatic	Forbes *et al.*, 2015
101	I	M	1	1.00	Somatic	Forbes *et al.*, 2015
101	I	T	8	1.00	PHTS	M.-H. Tan *et al.*, 2011
101	I	N	1	2.00	Somatic	Forbes *et al.*, 2015
103	P	S	2	1.50	Somatic	Forbes *et al.*, 2015
105	C	W	4	1.00	Somatic	Forbes *et al.*, 2015
105	C	S	3	2.00	Somatic	Forbes *et al.*, 2015
105	C	F	6	1.33	Somatic	Forbes *et al.*, 2015
105	C	G	2	1.00	Somatic	Forbes *et al.*, 2015
105	C	R	2	1.00	Somatic	Forbes *et al.*, 2015
105	C	Y	4	1.00	PHTS	D. J. Marsh *et al.*, 1999
107	D	N	2	1.00	Somatic	Forbes *et al.*, 2015
107	D	H	1	1.00	Somatic	Forbes *et al.*, 2015
107	D	A	1	1.00	Somatic	Forbes *et al.*, 2015
107	D	Y	5	1.00	Somatic	Forbes *et al.*, 2015
108	L	R	3	1.00	Somatic	Forbes *et al.*, 2015
108	L	P	4	2.75	PHTS	W.-H. Tan *et al.*, 2007
109	D	N	2	1.00	Somatic	Forbes *et al.*, 2015
110	Q	K	1	3.00	Somatic	Forbes *et al.*, 2015
110	Q	R	2	2.00	Somatic	Forbes *et al.*, 2015
111	W	L			Null	Sequence Alignment
111	W	R	3	1.67	PHTS	X. Zhou *et al.*, 2001
112	L	I	1	6.00	Somatic	Forbes *et al.*, 2015
112	L	Q	2	2.00	Somatic	Forbes *et al.*, 2015
112	L	V	5	1.20	PHTS	M.-H. Tan *et al.*, 2011
112	L	P	3	2.00	PHTS	Tsou *et al.*, 1998
113	S	R	1	1.00	Somatic	Forbes *et al.*, 2015
113	S	G	2	3.00	Somatic	Forbes *et al.*, 2015
114	E	G	5	2.60	Somatic	Forbes *et al.*, 2015
115	D	N	1	1.00	Somatic	Forbes *et al.*, 2015
116	D	G	7	2.00	Somatic	Forbes *et al.*, 2015
117	N	S	1	1.00	Somatic	Forbes *et al.*, 2015

118	H	P			Autism	Orrico *et al.*, 2009
118	H	R	2	1.00	Somatic	Forbes *et al.*, 2015
118	H	L	2	1.00	Somatic	Forbes *et al.*, 2015
119	V	F	2	1.00	Somatic	Forbes *et al.*, 2015
119	V	D	1	2.00	Somatic	Forbes *et al.*, 2015
119	V	I	3	2.00	Somatic	Forbes *et al.*, 2015
119	V	A	3	2.67	Somatic	Forbes *et al.*, 2015
119	V	L			PHTS	De Vivo *et al.*, 2000
120	A	T	2	1.00	Somatic	Forbes *et al.*, 2015
120	A	E			PHTS	M.-H. Tan *et al.*, 2011
121	A	P	3	1.00	Somatic	Forbes *et al.*, 2015
121	A	T	2	1.00	Somatic	Forbes *et al.*, 2015
121	A	V			Null	Rodríguez-Escudero *et al.*, 2014
121	A	E	2	2.00	Somatic	Forbes *et al.*, 2015
122	I	S	1	1.00	Somatic	Forbes *et al.*, 2015
122	I	N	1	3.00	Somatic	Forbes *et al.*, 2015
122	I	T	3	1.67	Somatic	Forbes *et al.*, 2015
122	I	V			Null	Rodríguez-Escudero *et al.*, 2014
123	H	Q			Autism	McBride *et al.*, 2010
123	H	L	1	1.00	Somatic	Forbes *et al.*, 2015
123	H	Y	7	1.29	Somatic	Forbes *et al.*, 2015
123	H	D	2	1.50	PHTS	Bussaglia *et al.*, 2002
123	H	R	2	4.00	PHTS	Nelen *et al.*, 1997
124	C	G	1	1.00	Somatic	Forbes *et al.*, 2015
124	C	Y	1	1.00	PHTS	Sawada *et al.*, 2004
124	C	S	8	1.38	PHTS	M.-H. Tan *et al.*, 2011
124	C	R	4	3.50	PHTS	Nelen *et al.*, 1997
124	C	W			PHTS	M.-H. Tan *et al.*, 2011
125	K	N	3	1.00	Somatic	Forbes *et al.*, 2015
125	K	T	1	3.00	Somatic	Forbes *et al.*, 2015
125	K	E	2	1.50	Somatic	Forbes *et al.*, 2015
125	K	R			Null	Rodríguez-Escudero *et al.*, 2014
126	A	D	4	1.00	Somatic	Forbes *et al.*, 2015
126	A	T	6	1.50	Somatic	Forbes *et al.*, 2015
126	A	S	3	2.00	Somatic	Forbes *et al.*, 2015
126	A	V	3	1.67	Somatic	Forbes *et al.*, 2015
126	A	P	2	1.50	PHTS	M.-H. Tan *et al.*, 2011
127	G	V	2	1.50	Somatic	Forbes *et al.*, 2015
127	G	R	5	4.20	Somatic	Forbes *et al.*, 2015
127	G	E	5	1.00	Somatic	Forbes *et al.*, 2015
128	K	N	9	1.11	Somatic	Forbes *et al.*, 2015
128	K	Q	2	2.00	Somatic	Forbes *et al.*, 2015

128	K	R	6	2.50	Somatic	Forbes *et al.*, 2015
128	K	E	1	2.00	PHTS	Ellison and Driscoll, 2010
129	G	R	7	1.29	Somatic	Forbes *et al.*, 2015
129	G	V	3	1.00	Somatic	Forbes *et al.*, 2015
129	G	A			Null	Rodríguez-Escudero *et al.*, 2014
129	G	E	3	1.33	PHTS	Liaw *et al.*, 1997
130	R	P	14	2.00	Somatic	Forbes *et al.*, 2015
130	R	G	116	1.50	PHTS	Lobo *et al.*, 2009
130	R	Q	97	1.71	PHTS	Kurose *et al.*, 1999
130	R	L	18	1.89	PHTS	D. Marsh *et al.*, 1998
131	T	N	1	1.00	Somatic	Forbes *et al.*, 2015
131	T	A	2	1.00	Somatic	Forbes *et al.*, 2015
131	T	S			Null	Rodríguez-Escudero *et al.*, 2014
131	T	I	1	1.00	Somatic	Forbes *et al.*, 2015
131	T	P	1	1.00	Somatic	Forbes *et al.*, 2015
132	G	S	3	1.33	Somatic	Forbes *et al.*, 2015
132	G	R	1	1.00	Somatic	Forbes *et al.*, 2015
132	G	C	2	1.50	Somatic	Forbes *et al.*, 2015
132	G	V	5	1.00	PHTS	Tekin *et al.*, 2006
132	G	D	8	1.25	PHTS	Derrey *et al.*, 2004
132	G	A			PHTS	W.-H. Tan *et al.*, 2007
133	V	I	2	1.00	Somatic	Forbes *et al.*, 2015
134	M	T	1	1.00	Autism	McBride *et al.*, 2010
134	M	I	3	2.67	Somatic	Forbes *et al.*, 2015
134	M	L	2	1.50	Somatic	Forbes *et al.*, 2015
134	M	V	1	6.00	Somatic	Forbes *et al.*, 2015
134	M	R	1	2.00	PHTS	Figer *et al.*, 2002
135	I	T	1	3.00	Somatic	Forbes *et al.*, 2015
135	I	M	2	2.00	Somatic	Forbes *et al.*, 2015
135	I	K	4	1.00	PHTS	M.-H. Tan *et al.*, 2011
135	I	V	2	1.50	PHTS	D. J. Marsh *et al.*, 1999
135	I	R			PHTS	Boccone *et al.*, 2006
136	C	F	6	2.00	Somatic	Forbes *et al.*, 2015
136	C	R	8	1.25	PHTS	Kubo *et al.*, 2000
136	C	Y	12	1.58	PHTS	Scala *et al.*, 1998
137	A	T	1	2.00	Somatic	Forbes *et al.*, 2015
137	A	V	1	1.00	Somatic	Forbes *et al.*, 2015
138	Y	C	2	2.00	Somatic	Forbes *et al.*, 2015
138	Y	D	2	2.00	Somatic	Forbes *et al.*, 2015
139	L	F	2	2.00	Somatic	Forbes *et al.*, 2015
139	L	V	1	3.00	Somatic	Forbes *et al.*, 2015
140	L	F	1	3.00	Somatic	Forbes *et al.*, 2015

140	L	S	1	10.00	Somatic	Forbes *et al.*, 2015
141	H	Y	1	1.00	Somatic	Forbes *et al.*, 2015
141	H	R	2	3.00	Somatic	Forbes *et al.*, 2015
141	H	N	2	3.50	Somatic	Forbes *et al.*, 2015
142	R	L	1	1.00	Somatic	Forbes *et al.*, 2015
142	R	W	10	1.60	Somatic	Forbes *et al.*, 2015
142	R	Q	5	1.60	Somatic	Forbes *et al.*, 2015
144	K	T	2	3.50	Somatic	Forbes *et al.*, 2015
144	K	Q	2	3.00	Somatic	Forbes *et al.*, 2015
144	K	I	1	1.00	Somatic	Forbes *et al.*, 2015
145	F	I	1	1.00	Somatic	Forbes *et al.*, 2015
146	L	V	1	2.00	Somatic	Forbes *et al.*, 2015
147	K	M	1	6.00	Somatic	Forbes *et al.*, 2015
147	K	T	1	10.00	Somatic	Forbes *et al.*, 2015
147	K	R	1	1.00	Somatic	Forbes *et al.*, 2015
148	A	T	2	1.00	Somatic	Forbes *et al.*, 2015
148	A	S	1	2.00	Somatic	Forbes *et al.*, 2015
148	A	E	1	1.00	Somatic	Forbes *et al.*, 2015
149	Q	R	1	2.00	Somatic	Forbes *et al.*, 2015
150	E	D	1	1.00	Somatic	Forbes *et al.*, 2015
150	E	A	1	1.00	Somatic	Forbes *et al.*, 2015
150	E	Q	1	1.00	Somatic	Forbes *et al.*, 2015
150	E	G	6	3.50	Somatic	Forbes *et al.*, 2015
151	A	T	5	1.00	Somatic	Forbes *et al.*, 2015
151	A	D	1	3.00	Somatic	Forbes *et al.*, 2015
152	L	V	1	1.00	Somatic	Forbes *et al.*, 2015
152	L	R	1	2.00	Somatic	Forbes *et al.*, 2015
152	L	I	1	5.00	Somatic	Forbes *et al.*, 2015
152	L	P	2	1.50	PHTS	M.-H. Tan *et al.*, 2011
153	D	E	1	2.00	Somatic	Forbes *et al.*, 2015
153	D	N	1	1.00	Somatic	Forbes *et al.*, 2015
153	D	Y	2	1.50	Somatic	Forbes *et al.*, 2015
153	D	H			Null	Rodríguez-Escudero *et al.*, 2014
154	F	C	1	3.00	Somatic	Forbes *et al.*, 2015
154	F	L	3	2.00	Somatic	Forbes *et al.*, 2015
154	F	V	1	1.00	Somatic	Forbes *et al.*, 2015
154	F	S	1	1.00	Somatic	Forbes *et al.*, 2015
155	Y	N	1	2.00	Somatic	Forbes *et al.*, 2015
155	Y	H	4	1.25	PHTS	M.-H. Tan *et al.*, 2011
155	Y	C	10	1.30	PHTS	Gicquel *et al.*, 2003
156	G	R	2	3.00	Somatic	Forbes *et al.*, 2015
157	E	G			Autism	Varga *et al.*, 2009

157	E	K	1	4.00	Somatic	Forbes *et al.*, 2015
158	V	L			PHTS	De Vivo *et al.*, 2000
159	R	S	8	1.38	Somatic	Forbes *et al.*, 2015
159	R	G			PHTS	M.-H. Tan *et al.*, 2011
159	R	T			PHTS	M.-H. Tan *et al.*, 2011
159	R	K	5	1.20	Somatic	Forbes *et al.*, 2015
160	T	S	1	2.00	Somatic	Forbes *et al.*, 2015
160	T	I	1	1.00	Somatic	Forbes *et al.*, 2015
160	T	A	1	2.00	Somatic	Forbes *et al.*, 2015
161	R	I	2	1.00	Somatic	Forbes *et al.*, 2015
161	R	K	2	1.00	Somatic	Forbes *et al.*, 2015
161	R	G	1	2.00	Null	Rodríguez-Escudero *et al.*, 2014
162	D	H	2	3.00	Somatic	Forbes *et al.*, 2015
162	D	G	3	1.00	Somatic	Forbes *et al.*, 2015
162	D	E			PHTS	M.-H. Tan *et al.*, 2011
162	D	V	3	2.00	Somatic	Forbes *et al.*, 2015
163	K	E	1	1.00	Somatic	Forbes *et al.*, 2015
163	K	A			Null	Rodríguez-Escudero *et al.*, 2014
164	K	N	1	4.00	Somatic	Forbes *et al.*, 2015
164	K	E	1	4.00	Somatic	Forbes *et al.*, 2015
164	K	R	3	2.67	Somatic	Forbes *et al.*, 2015
164	K	A			Null	Rodríguez-Escudero *et al.*, 2014
165	G	A			Null	Rodríguez-Escudero *et al.*, 2014
165	G	V	1	1.00	PHTS	D. Marsh *et al.*, 1998
165	G	E	7	1.14	PHTS	Nelen *et al.*, 1999
165	G	R	11	1.55	PHTS	Banneau *et al.*, 2010
166	V	L	1	1.00	Somatic	Forbes *et al.*, 2015
166	V	I	1	2.00	Null	Rodríguez-Escudero *et al.*, 2014
167	T	P	1	1.00	Somatic	Forbes *et al.*, 2015
167	T	S	1	1.00	Somatic	Forbes *et al.*, 2015
167	T	I	1	1.00	Somatic	Forbes *et al.*, 2015
167	T	A	7	1.14	Somatic	Forbes *et al.*, 2015
168	I	F	1	1.00	Null	Rodríguez-Escudero *et al.*, 2014
168	I	A			Null	Rodríguez-Escudero *et al.*, 2014
169	P	H	1	1.00	Null	Rodríguez-Escudero *et al.*, 2014
169	P	A			Null	Rodríguez-Escudero *et al.*, 2014
170	S	G	1	1.00	Somatic	Forbes *et al.*, 2015
170	S	N	8	1.13	Somatic	Forbes *et al.*, 2015
170	S	A			Null	Rodríguez-Escudero *et al.*, 2014
170	S	I	3	1.00	PHTS	M.-H. Tan *et al.*, 2011
170	S	R			PHTS	D. J. Marsh *et al.*, 1997
171	Q	H	1	1.00	Somatic	Forbes *et al.*, 2015

171	Q	E	2	1.00	Somatic	Forbes *et al.*, 2015
171	Q	P	2	1.00	Somatic	Forbes *et al.*, 2015
171	Q	K	1	1.00	Somatic	Forbes *et al.*, 2015
172	R	W	1	2.00	Somatic	Forbes *et al.*, 2015
172	R	G	1	4.00	Somatic	Forbes *et al.*, 2015
173	R	S	1	1.00	Somatic	Forbes *et al.*, 2015
173	R	H	29	1.38	PHTS	Lachlan *et al.*, 2007
173	R	C	48	1.79	PHTS	Lachlan *et al.*, 2007
173	R	P			PHTS	Kirches *et al.*, 2010
174	Y	N	1	1.00	Somatic	Forbes *et al.*, 2015
174	Y	D	3	1.33	Somatic	Forbes *et al.*, 2015
175	V	A	1	10.00	Somatic	Forbes *et al.*, 2015
175	V	L	1	1.00	Somatic	Forbes *et al.*, 2015
176	Y	C			Autism	Orrico *et al.*, 2009
177	Y	S	1	1.00	Somatic	Forbes *et al.*, 2015
177	Y	F	2	3.50	Somatic	Forbes *et al.*, 2015
177	Y	C	6	1.00	Somatic	Forbes *et al.*, 2015
177	Y	H	1	1.00	Somatic	Forbes *et al.*, 2015
178	Y	C	1	1.00	Somatic	Forbes *et al.*, 2015
178	Y	F	1	2.00	Somatic	Forbes *et al.*, 2015
179	S	I	1	1.00	Somatic	Forbes *et al.*, 2015
180	Y	N	1	3.00	Somatic	Forbes *et al.*, 2015
180	Y	C	1	4.00	Somatic	Forbes *et al.*, 2015
181	L	P			PHTS	Thiffault *et al.*, 2004
182	L	F	2	2.50	Somatic	Forbes *et al.*, 2015
182	L	S			PHTS	M.-H. Tan *et al.*, 2011
182	L	V	1	1.00	Somatic	Forbes *et al.*, 2015
183	K	N	1	2.00	Somatic	Forbes *et al.*, 2015
184	N	I	1	1.00	Somatic	Forbes *et al.*, 2015
185	H	D	1	1.00	Somatic	Forbes *et al.*, 2015
187	D	Y	1	1.00	Somatic	Forbes *et al.*, 2015
188	Y	H			PHTS	M.-H. Tan *et al.*, 2011
188	Y	S	1	1.00	Somatic	Forbes *et al.*, 2015
189	R	K	2	1.00	Somatic	Forbes *et al.*, 2015
190	P	L	1	3.00	Somatic	Forbes *et al.*, 2015
191	V	A			Null	Rodríguez-Escudero *et al.*, 2014
192	A	T	1	1.00	Somatic	Forbes *et al.*, 2015
193	L	P	1	1.00	Somatic	Forbes *et al.*, 2015
197	K	R	1	2.00	Somatic	Forbes *et al.*, 2015
198	M	K	2	1.00	Somatic	Forbes *et al.*, 2015
198	M	V	1	3.00	Somatic	Forbes *et al.*, 2015
202	T	I	1	2.00	Autism	Varga *et al.*, 2009

204	P	S	1	1.00	Somatic	Forbes *et al.*, 2015
204	P	Q	1	1.00	Somatic	Forbes *et al.*, 2015
204	P	L	3	1.00	Somatic	Forbes *et al.*, 2015
204	P	T	2	1.00	Somatic	Forbes *et al.*, 2015
205	M	I	2	3.00	Somatic	Forbes *et al.*, 2015
205	M	V			PHTS	M.-H. Tan *et al.*, 2011
211	C	Y	1	1.00	Somatic	Forbes *et al.*, 2015
213	P	H	2	1.50	Somatic	Forbes *et al.*, 2015
213	P	R	1	1.00	Somatic	Forbes *et al.*, 2015
213	P	S	1	1.00	Somatic	Forbes *et al.*, 2015
214	Q	R	1	1.00	Somatic	Forbes *et al.*, 2015
215	F	S	2	2.50	Somatic	Forbes *et al.*, 2015
216	V	A	1	2.00	Somatic	Forbes *et al.*, 2015
216	V	M	2	2.00	Somatic	Forbes *et al.*, 2015
217	V	A	1	2.00	Somatic	Forbes *et al.*, 2015
217	V	D	1	3.00	PHTS	Kim *et al.*, 2005
217	V	I	1	1.00	Somatic	Forbes *et al.*, 2015
218	C	F	1	1.00	Somatic	Forbes *et al.*, 2015
218	C	Y			Null	Sequence Alignment
219	Q	H	1	2.00	Somatic	Forbes *et al.*, 2015
222	V	M	1	1.00	Somatic	Forbes *et al.*, 2015
222	V	A	4	3.00	Somatic	Forbes *et al.*, 2015
225	Y	C	1	1.00	Somatic	Forbes *et al.*, 2015
226	S	F	1	1.00	Somatic	Forbes *et al.*, 2015
227	S	F	1	2.00	Somatic	Forbes *et al.*, 2015
227	S	P	2	3.00	Somatic	Forbes *et al.*, 2015
228	N	P			Null	Sequence Alignment
230	G	E	2	1.00	Somatic	Forbes *et al.*, 2015
230	G	R	2	1.50	Somatic	Forbes *et al.*, 2015
232	T	A	1	1.00	Somatic	Forbes *et al.*, 2015
232	T	S			Null	Sequence Alignment
234	R	L	1	4.00	Somatic	Forbes *et al.*, 2015
234	R	W	4	2.25	Somatic	Forbes *et al.*, 2015
234	R	Q	1	1.50	PHTS	Staal *et al.*, 2002
235	E	G	1	2.00	Somatic	Forbes *et al.*, 2015
238	F	S	1	2.00	Somatic	Forbes *et al.*, 2015
238	F	L	2	2.50	Somatic	Forbes *et al.*, 2015
238	F	Y			Null	Sequence Alignment
239	M	R	1	1.00	Somatic	Forbes *et al.*, 2015
239	M	V	1	1.00	Somatic	Forbes *et al.*, 2015
241	F	S	2	1.50	Autism	Butler *et al.*, 2005
241	F	L	4	4.00	Somatic	Forbes *et al.*, 2015

242	E	K	1	1.00	Somatic	Forbes *et al.*, 2015
242	E	G	1	1.00	Somatic	Forbes *et al.*, 2015
243	F	L	1	1.00	Somatic	Forbes *et al.*, 2015
243	F	S	1	1.00	Somatic	Forbes *et al.*, 2015
244	P	H	1	1.00	Somatic	Forbes *et al.*, 2015
244	P	S	1	1.00	Somatic	Forbes *et al.*, 2015
244	P	R	2	1.00	Somatic	Forbes *et al.*, 2015
246	P	L	12	1.58	PHTS	D. J. Marsh *et al.*, 1999
247	L	F	1	2.00	Somatic	Forbes *et al.*, 2015
248	P	L	1	2.00	Somatic	Forbes *et al.*, 2015
248	P	H	1	2.00	Somatic	Forbes *et al.*, 2015
249	V	E	1	1.00	Somatic	Forbes *et al.*, 2015
251	G	A	1	1.00	Somatic	Forbes *et al.*, 2015
251	G	C	4	1.00	Somatic	Forbes *et al.*, 2015
251	G	V	5	1.00	Somatic	Forbes *et al.*, 2015
251	G	S	1	10.00	Somatic	Forbes *et al.*, 2015
251	G	D	3	1.00	Somatic	Forbes *et al.*, 2015
252	D	G	3	1.00	Autism	Butler *et al.*, 2005
252	D	Y	6	1.33	Somatic	Forbes *et al.*, 2015
252	D	V	1	1.00	Somatic	Forbes *et al.*, 2015
253	I	T	2	2.00	Somatic	Forbes *et al.*, 2015
253	I	N	4	1.25	Somatic	Forbes *et al.*, 2015
254	K	E	2	2.00	Somatic	Forbes *et al.*, 2015
254	K	T			PHTS	M.-H. Tan *et al.*, 2011
255	V	G	1	3.00	Somatic	Forbes *et al.*, 2015
255	V	A	2	4.00	Somatic	Forbes *et al.*, 2015
256	E	K	2	1.50	Somatic	Forbes *et al.*, 2015
256	E	Q	1	2.00	Somatic	Forbes *et al.*, 2015
257	F	L	1	2.00	Somatic	Forbes *et al.*, 2015
257	F	S	1	3.00	Somatic	Forbes *et al.*, 2015
258	F	L	1	2.00	Somatic	Forbes *et al.*, 2015
258	F	Y	1	2.00	Somatic	Forbes *et al.*, 2015
260	K	A			Null	Rodríguez-Escudero *et al.*, 2014
261	Q	A			Null	Rodríguez-Escudero *et al.*, 2014
262	N	A			Null	Rodríguez-Escudero *et al.*, 2014
263	K	R	2	4.00	Somatic	Forbes *et al.*, 2015
263	K	A			Null	Rodríguez-Escudero *et al.*, 2014
264	M	A			Null	Rodríguez-Escudero *et al.*, 2014
264	M	R	1	1.00	Somatic	Forbes *et al.*, 2015
265	L	A			Null	Rodríguez-Escudero *et al.*, 2014
266	K	A			Null	Rodríguez-Escudero *et al.*, 2014
270	M	I	2	1.50	Somatic	Forbes *et al.*, 2015

270	M	T	1	3.00	Somatic	Forbes *et al.*, 2015
271	F	L	3	4.67	Somatic	Forbes *et al.*, 2015
271	F	I	1	1.00	Somatic	Forbes *et al.*, 2015
271	F	S	4	1.25	Somatic	Forbes *et al.*, 2015
272	H	P	2	1.00	Somatic	Forbes *et al.*, 2015
272	H	Y	2	1.50	Somatic	Forbes *et al.*, 2015
272	H	R	2	1.50	Somatic	Forbes *et al.*, 2015
273	F	S	1	1.00	Somatic	Forbes *et al.*, 2015
273	F	L	1	1.00	Somatic	Forbes *et al.*, 2015
274	W	L	5	2.40	Autism	McBride *et al.*, 2010
274	W	G	3	1.00	Somatic	Forbes *et al.*, 2015
274	W	R	1	1.00	Somatic	Forbes *et al.*, 2015
275	V	A	1	3.00	Somatic	Forbes *et al.*, 2015
275	V	L	2	2.50	Somatic	Forbes *et al.*, 2015
276	N	S	1	1.00	Autism	Orrico *et al.*, 2009
276	N	K	2	2.00	Somatic	Forbes *et al.*, 2015
277	T	S	1	2.00	Somatic	Forbes *et al.*, 2015
277	T	I	4	2.00	Somatic	Forbes *et al.*, 2015
277	T	A	2	1.00	Somatic	Forbes *et al.*, 2015
277	T	R			PHTS	Banneau *et al.*, 2010
284	E	K	1	2.00	Somatic	Forbes *et al.*, 2015
284	E	G	7	3.71	Somatic	Forbes *et al.*, 2015
286	T	N			Null	Sequence Alignment
287	S	L	2	2.00	Somatic	Forbes *et al.*, 2015
287	S	P	2	3.00	Somatic	Forbes *et al.*, 2015
288	E	K	2	2.50	Null	Rodríguez-Escudero *et al.*, 2014
288	E	D			Null	Sequence Alignment
289	K	E			PHTS	Chi *et al.*, 1998
291	E	G	2	2.00	Somatic	Forbes *et al.*, 2015
291	E	K	3	2.33	Somatic	Forbes *et al.*, 2015
293	G	V	1	2.00	Somatic	Forbes *et al.*, 2015
293	G	R	1	4.00	Somatic	Forbes *et al.*, 2015
294	S	N	1	1.00	Somatic	Forbes *et al.*, 2015
296	C	V			Null	Sequence Alignment
298	Q	R	1	3.00	Somatic	Forbes *et al.*, 2015
299	E	D	1	5.00	Somatic	Forbes *et al.*, 2015
299	E	G	2	2.50	Somatic	Forbes *et al.*, 2015
304	C	S	1	1.00	Somatic	Forbes *et al.*, 2015
304	C	R	1	3.00	Somatic	Forbes *et al.*, 2015
304	C	G	1	1.00	Somatic	Forbes *et al.*, 2015
304	C	F			Null	Sequence Alignment
305	S	N	1	1.00	Somatic	Forbes *et al.*, 2015

306	I	T			Null	Sequence Alignment
307	E	K	4	1.00	Somatic	Forbes *et al.*, 2015
307	E	G	2	2.00	Somatic	Forbes *et al.*, 2015
308	R	C	2	1.00	Somatic	Forbes *et al.*, 2015
308	R	H	1	1.00	Somatic	Forbes *et al.*, 2015
309	A	S			Null	Sequence Alignment
310	D	G	1	1.00	Somatic	Forbes *et al.*, 2015
314	E	K	1	1.00	Somatic	Forbes *et al.*, 2015
317	V	I			Null	Sequence Alignment
318	L	P	4	2.50	Somatic	Forbes *et al.*, 2015
318	L	F	1	3.00	Somatic	Forbes *et al.*, 2015
320	L	V	1	3.00	Somatic	Forbes *et al.*, 2015
320	L	S	1	7.00	Somatic	Forbes *et al.*, 2015
322	K	E	1	1.00	Somatic	Forbes *et al.*, 2015
323	N	T	1	3.00	Somatic	Forbes *et al.*, 2015
323	N	K	2	4.00	Somatic	Forbes *et al.*, 2015
325	L	F	1	4.00	Somatic	Forbes *et al.*, 2015
325	L	R	2	1.50	Somatic	Forbes *et al.*, 2015
325	L	P	3	1.33	Somatic	Forbes *et al.*, 2015
325	L	H	2	2.00	Somatic	Forbes *et al.*, 2015
325	L	V	1	1.00	Somatic	Forbes *et al.*, 2015
326	D	N			Autism	Buxbaum *et al.*, 2007
326	D	Y	1	5.00	Somatic	Forbes *et al.*, 2015
326	D	G	3	2.00	Somatic	Forbes *et al.*, 2015
328	A	V			Null	Rodríguez-Escudero *et al.*, 2014
329	N	A			Null	Rodríguez-Escudero *et al.*, 2014
331	D	A			Null	Rodríguez-Escudero *et al.*, 2014
331	D	G			Null	Rodríguez-Escudero *et al.*, 2014
331	D	H	1	1.00	Somatic	Forbes *et al.*, 2015
332	K	A			Null	Rodríguez-Escudero *et al.*, 2014
333	A	V			Null	Rodríguez-Escudero *et al.*, 2014
334	N	D	1	2.00	Somatic	Forbes *et al.*, 2015
334	N	A			Null	Rodríguez-Escudero *et al.*, 2014
334	N	Y	1	1.00	Somatic	Forbes *et al.*, 2015
335	R	G	1	3.00	Somatic	Forbes *et al.*, 2015
335	R	Q	1	6.00	Somatic	Forbes *et al.*, 2015
335	R	A			Null	Rodríguez-Escudero *et al.*, 2014
335	R	L			PHTS	Sawada *et al.*, 2000
336	Y	F	1	4.00	Somatic	Forbes *et al.*, 2015
336	Y	C	1	1.00	Somatic	Forbes *et al.*, 2015
336	Y	H	1	4.00	Somatic	Forbes *et al.*, 2015
336	Y	A			Null	Rodríguez-Escudero *et al.*, 2014

337	F	L	1	1.00	Somatic	Forbes *et al.*, 2015
337	F	S			PHTS	Lachlan *et al.*, 2007
338	S	T	1	3.00	Somatic	Forbes *et al.*, 2015
338	S	F	1	2.00	Somatic	Forbes *et al.*, 2015
338	S	A			Null	Rodríguez-Escudero *et al.*, 2014
339	P	S	3	2.00	Somatic	Forbes *et al.*, 2015
339	P	L	3	2.33	Somatic	Forbes *et al.*, 2015
339	P	A			Null	Rodríguez-Escudero *et al.*, 2014
341	F	C	1	3.00	Somatic	Forbes *et al.*, 2015
341	F	V	6	2.17	Somatic	Forbes *et al.*, 2015
341	F	A			Null	Rodríguez-Escudero *et al.*, 2014
342	K	N	2	1.00	Somatic	Forbes *et al.*, 2015
342	K	R	3	4.00	Somatic	Forbes *et al.*, 2015
342	K	A			Null	Rodríguez-Escudero *et al.*, 2014
343	V	G	1	2.00	Somatic	Forbes *et al.*, 2015
343	V	E			PHTS	Lynch *et al.*, 1997
344	K	E	4	3.50	Somatic	Forbes *et al.*, 2015
344	K	R	5	2.60	Somatic	Forbes *et al.*, 2015
344	K	A			Null	Rodríguez-Escudero *et al.*, 2014
345	L	Q	2	1.50	Somatic	Forbes *et al.*, 2015
345	L	P	1	3.00	Somatic	Forbes *et al.*, 2015
345	L	A			Null	Rodríguez-Escudero *et al.*, 2014
345	L	V			Null	Rodríguez-Escudero *et al.*, 2014
346	Y	C	1	1.00	Somatic	Forbes *et al.*, 2015
346	Y	D	1	3.00	Somatic	Forbes *et al.*, 2015
346	Y	F			Null	Sequence Alignment
347	F	L	1	1.00	PHTS	Lynch *et al.*, 1997
348	T	K	1	4.00	Somatic	Forbes *et al.*, 2015
348	T	A	3	2.33	Somatic	Forbes *et al.*, 2015
348	T	I	1	3.00	Somatic	Forbes *et al.*, 2015
352	E	G	11	4.45	Somatic	Forbes *et al.*, 2015
354	P	Q			PHTS	M.-H. Tan *et al.*, 2011
356	N	D			PHTS	M.-H. Tan *et al.*, 2011
357	P	S	2	1.00	Somatic	Forbes *et al.*, 2015
364	S	C	2	1.00	Somatic	Forbes *et al.*, 2015
364	S	P	1	4.00	Somatic	Forbes *et al.*, 2015
365	V	I	1	2.00	Somatic	Forbes *et al.*, 2015
365	V	E	1	5.00	Somatic	Forbes *et al.*, 2015
369	V	A	1	1.00	Somatic	Forbes *et al.*, 2015
369	V	G	1	1.00	Somatic	Forbes *et al.*, 2015
373	E	K	1	1.00	Somatic	Forbes *et al.*, 2015
375	D	G	1	4.00	Somatic	Forbes *et al.*, 2015

375	D	N	3	1.00	Somatic	Forbes *et al.*, 2015
382	T	A	1	2.00	Somatic	Forbes *et al.*, 2015
382	T	S	1	3.00	Somatic	Forbes *et al.*, 2015
383	T	I	1	1.00	Somatic	Forbes *et al.*, 2015
384	D	G	1	1.00	Somatic	Forbes *et al.*, 2015
384	D	N	1	1.00	Somatic	Forbes *et al.*, 2015
397	H	Y	2	1.00	Somatic	Forbes *et al.*, 2015
397	H	Q	1	4.00	Somatic	Forbes *et al.*, 2015
397	H	R	2	3.50	Somatic	Forbes *et al.*, 2015
398	T	S	1	3.00	Null	Sequence Alignment
401	T	I	2	1.00	Somatic	Forbes *et al.*, 2015

Bibliography

Adzhubei I. A., Schmidt S., Peshkin L., Ramensky V. E., Gerasimova A., Bork P., Kondrashov A. S., and Sunyaev S. R. (2010). A method and server for predicting damaging missense mutations. *Nat. Methods* **7**, 248–249.

Alimonti A., Carracedo A., Clohessy J. G., Trotman L. C., Nardella C., Egia A., Salmena L., Sampieri K., Haveman W. J., Brogi E., Richardson A. L., Zhang J., and Pandolfi P. P. (2010). Subtle variations in Pten dose determine cancer susceptibility. *Nat. Genet.* **42**, 454–U136.

Andersen J. F. and Ribeiro J. M. C. (2006). A secreted salivary inositol polyphosphate 5-phosphatase from a blood-feeding insect: Allosteric activation by soluble phosphoinositides and phosphatidylserine. *Biochemistry* **45**, 5450–5457.

Asperger H. (1944). Die "autistischen psychopathen" im kindesalter. *Arch. Psychiatr. Nervenkr.* **117**, 76–136.

Baker S. J. (2007). PTEN enters the nuclear age. *Cell* **128**, 25–28.

Baldwin R. L. (1996). How Hofmeister ion interactions affect protein stability. *Biophys. J.* **71**, 2056–2063.

Banneau G., Guedj M., MacGrogan G., Mascarel I. de, Velasco V., Schiappa R., Bonadona V., David A., Dugast C., Gilbert-Dussardier B., Ingster O., Vabres P., Caux F., Reynies A. de, Iggo R., Sevenet N., Bonnet F., and Longy M. (2010). Molecular apocrine differentiation is a common feature of breast cancer in patients with germline PTEN mutations. *Breast Cancer Res.* **12**, R63.

Bassi C., Ho J., Srikumar T., Dowling R. J. O., Gorrini C., Miller S. J., Mak T. W., Neel B. G., Raught B., and Stambolic V. (2013). Nuclear PTEN controls DNA repair and sensitivity to genotoxic stress. *Science* **341**, 395–399.

Beck M., Schmidt A., Malmstroem J., Claassen M., Ori A., Szymborska A., Herzog F., Rinner O., Ellenberg J., and Aebersold R. (2011). The quantitative proteome of a human cell line. *Mol. Syst. Biol.* **7**, 549.

Berman H. M., Coimbatore Narayanan B., Di Costanzo L., Dutta S., Ghosh S., Hudson B. P., Lawson C. L., Peisach E., Prlić A., Rose P. W., Shao C., Yang H., Young J., and Zardecki C. (2013). Trendspotting in the Protein Data Bank. *FEBS Lett.* **587**, 1036–1045.

Biesecker L. G., Happle R., Mulliken J. B., Weksberg R., Graham J. M., Viljoen D. L., and Cohen M. M. (1999). Proteus syndrome: diagnostic criteria, differential diagnosis, and patient evaluation. *Am. J. Med. Genet.* **84**, 389–395.

Bigner S. H., Mark J., Mahaley M. S., and Bigner D. D. (1984). Patterns of the early, gross chromosomal changes in malignant human gliomas. *Hereditas* **101**, 103–113.

Bishop C. M. (2006). *Pattern Recognition and Machine Learning*. New York, Springer Verlag.

Boccone L., Dessì V., Zappu A., Piga S., Piludu M. B., Rais M., Massidda C., De Virgiliis S., Cao A., and Loudianos G. (2006). Bannayan-Riley-Ruvalcaba syndrome with reactive nodular lymphoid hyperplasia and autism and a PTEN mutation. *Am. J. Med. Genet. A.* **140**, 1965–1969.

Bradford M. M. (1976). A rapid and sensitive method for the quantitation of microgram quantities of protein utilizing the principle of protein-dye binding. *Anal. Biochem.* **72**, 248–254.

Brandt T., Kaar J. L., Fersht A. R., and Veprintsev D. B. (2012). Stability of p53 homologs. *PLoS One* **7**, e47889.

Bullock A. N., Henckel J., DeDecker B. S., Johnson C. M., Nikolova P. V., Proctor M. R., Lane D. P., and Fersht A. R. (1997). Thermodynamic stability of wild-type and mutant p53 core domain. *Proc. Natl. Acad. Sci. U.S.A.* **94**, 14338–14342.

Bussaglia E., Pujol R. M., Gil M. J., Martí R. M., Tuneu A., Febrer M. I., Garcia-Patos V., Ruiz E. M., Barnadas M., Alegre M., Serrano S., and Matias-Guiu X. (2002). PTEN mutations in eight Spanish families and one Brazilian family with Cowden syndrome. *J. Invest. Dermatol.* **118**, 639–644.

Butler M. G., Dasouki M. J., Zhou X. P., Talebizadeh Z., Brown M., Takahashi T. N., Miles J. H., Wang C. H., Stratton R., Pilarski R., and Eng C. (2005). Subset of individuals with autism spectrum disorders and extreme macrocephaly associated with germline PTEN tumour suppressor gene mutations. *J. Med. Genet.* **42**, 318–321.

Buxbaum J. D., Cai G., Chaste P., Nygren G., Goldsmith J., Reichert J., Anckarsater H., Rastam M., Smith C. J., Silverman J. M., Hollander E., Leboyer M., Gillberg C., Verloes A., and Betancur C. (2007). Mutation screening of the PTEN gene in patients with autism spectrum disorders and macrocephaly. *Am. J. Med. Genet. B Neuropsychiatr. Genet.* **144B**, 484–491.

Campbell N. A. and Reece J. B. (2004). *Biology, 7th Edition*. San Francisco, Benjamin Cummings.

Campbell R. B., Liu F. H., and Ross A. H. (2003). Allosteric activation of PTEN phosphatase by phosphatidylinositol 4,5-bisphosphate. *J. Biol. Chem.* **278**, 33617–33620.

Cantley L. C. (2002). The phosphoinositide 3-kinase pathway. *Science* **296**, 1655–1657.

Capriotti E. and Altman R. B. (2011). Improving the prediction of disease-related variants using protein three-dimensional structure. *BMC Bioinform.* **12 Suppl 4**, S3.

Cargill M., Altshuler D., Ireland J., Sklar P., Ardlie K., Patil N., Shaw N., Lane C. R., Lim E. P., Kalyanaraman N., Nemesh J., Ziaugra L., Friedland L., Rolfe A., Warrington J., Lipshutz R., Daley G. Q., and Lander E. S. (1999). Characterization of single-nucleotide polymorphisms in coding regions of human genes. *Nat. Genet.* **22**, 231–238.

Cariaso M. and Lennon G. (2012). SNPedia: a wiki supporting personal genome annotation, interpretation and analysis. *Nucleic Acids Res.* **40**, D1308–D1312.

Caronna E. B., Milunsky J. M., and Tager-Flusberg H. (2008). Autism spectrum disorders: Clinical and research frontiers. *Arch. Dis. Child.* **93**, 518–523.

Celebi J. T., Chen F. F., Zhang H., Ping X. L., Tsou H. C., and Peacocke M. (1999). Identification of PTEN mutations in five families with Bannayan-Zonana syndrome. *Exp. Dermatol.* **8**, 134–139.

Celebi J. T., Ping X. L., Zhang H., Remington T., Sulica V. I., Tsou H. C., and Peacocke M. (2000). Germline PTEN mutations in three families with Cowden syndrome. *Exp. Dermatol.* **9**, 152–156.

Chaffer C. L. and Weinberg R. A. (2011). A perspective on cancer cell metastasis. *Science* **331**, 1559–1564.

Chan P. A., Duraisamy S., Miller P. J., Newell J. A., McBride C., Bond J. P., Raevaara T., Ollila S., Nystrom M., Grimm A. J., Christodoulou J., Oetting W. S., and Greenblatt M. S. (2007). Interpreting missense variants: comparing computational methods

in human disease genes CDKN2A, MLH1, MSH2, MECP2, and tyrosinase (TYR). *Hum. Mutat.* **28**, 683–693.

Chang C.-C. and Lin C.-J. (2011). LIBSVM: A library for support vector machines. *ACM Trans. Intell. Syst. Technol.* **2**, 27–27.

Chi S. G., Kim H. J., Park B. J., Min H. J., Park J. H., Kim Y. W., Dong S. H., Kim B. H., Lee J. I., Chang Y. W., Chang R., Kim W. K., and Yang M. H. (1998). Mutational abrogation of the PTEN/MMAC1 gene in gastrointestinal polyps in patients with Cowden disease. *Gastroenterology* **115**, 1084–1089.

Choi Y., Sims G. E., Murphy S., Miller J. R., and Chan A. P. (2012). Predicting the functional effect of amino acid substitutions and indels. *PLoS One* **7**, e46688.

Cordes M. H., Davidson A. R., and Sauer R. T. (1996). Sequence space, folding and protein design. *Curr. Opin. Struct. Biol.* **6**, 3–10.

Cornish-Bowden A. (2014). Understanding allosteric and cooperative interactions in enzymes. *FEBS J.* **281**, 621–632.

Crabtree B., Thiyagarajan N., Prior S. H., Wilson P., Iyer S., Ferns T., Shapiro R., Brew K., Subramanian V., and Acharya K. R. (2007). Characterization of human angiogenin variants implicated in amyotrophic lateral sclerosis. *Biochemistry* **46**, 11810–11818.

Das S., Dixon J. E., and Cho W. W. (2003). Membrane-binding and activation mechanism of PTEN. *Proc. Natl. Acad. Sci. U.S.A.* **100**, 7491–7496.

De Vivo I., Gertig D. M., Nagase S., Hankinson S. E., O'Brien R., Speizer F. E., Parsons R., and Hunter D. J. (2000). Novel germline mutations in the PTEN tumour suppressor gene found in women with multiple cancers. *J. Med. Genet.* **37**, 336–341.

Delatycki M. B., Danks A., Churchyard A., Zhou X. P., and Eng C. (2003). De novo germline PTEN mutation in a man with Lhermitte-Duclos disease which arose on the paternal chromosome and was transmitted to his child with polydactyly and Wormian bones. *J. Med. Genet.* **40**, e92.

Denu J. M. and Dixon J. E. (1995). A catalytic mechanism for the dual-specific phosphatases. *Proc. Natl. Acad. Sci. U.S.A.* **92**, 5910–5914.

Denu J. M., Stuckey J. A., Saper M. A., and Dixon J. E. (1996). Form and function in protein dephosphorylation. *Cell* **87**, 361–364.

Derrey S., Proust F., Debono B., Langlois O., Layet A., Layet V., Longy M., Fréger P., and Laquerrière A. (2004). Association between Cowden syndrome and Lhermitte-Duclos disease: report of two cases and review of the literature. *Surg. Neurol.* **61**, 447–454.

Dhar A., Girdhar K., Singh D., Gelman H., Ebbinghaus S., and Gruebele M. (2011). Protein stability and folding kinetics in the nucleus and endoplasmic reticulum of eucaryotic cells. *Biophys. J.* **101**, 421–430.

Downey A., Elkner J., and Meyers C. (2002). *How to Think Like a Computer Scientist.* Learning with Python, Green Tea Press, Wellesley, Massachusetts.

Eisenhaber F. and Argos P. (1993). Improved strategy in analytic surface calculation for molecular systems: Handling of singularities and computational efficiency. *J. Comput. Chem.* **14**, 1272–1280.

Elcock A. H. (2010). Models of macromolecular crowding effects and the need for quantitative comparisons with experiment. *Curr. Opin. Struct. Biol.* **20**, 196–206.

Ellis R. J. (2001). Macromolecular crowding: Obvious but underappreciated. *Trends Biochem. Sci.* **26**, 597–604.

Ellison J. and Driscoll D. (2010). Novel human pathological mutations. Gene symbol: PTEN. Disease: PTEN Hamartoma Tumour Syndrome. *Hum. Genet.* **127**, 124.

Eng C. (2003). PTEN: One gene, many syndromes. *Hum. Mutat.* **22**, 183–198.

Faraggi E., Zhang T., Yang Y., Kurgan L., and Zhou Y. (2012). SPINE X: improving protein secondary structure prediction by multistep learning coupled with prediction of solvent accessible surface area and backbone torsion angles. *J. Comput. Chem.* **33**, 259–267.

Fayard E., Xue G., Parcellier A., Bozulic L., and Hemmings B. A. (2010). Protein Kinase B (PKB/Akt), a Key Mediator of the PI3K Signaling Pathway. *Curr. Top. Microbiol. Immunol.* **346**, 31–56.

Figer A., Kaplan A., Frydman M., Lev D., Paswell J., Papa M. Z., Goldman B., and Friedman E. (2002). Germline mutations in the PTEN gene in Israeli patients with

Bannayan-Riley-Ruvalcaba syndrome and women with familial breast cancer. *Clin. Genet.* **62**, 298–302.

Forbes S. A., Beare D., Gunasekaran P., Leung K., Bindal N., Boutselakis H., Ding M., Bamford S., Cole C., Ward S., Kok C. Y., Jia M., De T., Teague J. W., Stratton M. R., McDermott U., and Campbell P. J. (2015). COSMIC: Exploring the world's knowledge of somatic mutations in human cancer. *Nucleic Acids Res.* **43**, D805–D811.

Frishman D. and Argos P. (1995). Knowledge-based protein secondary structure assignment. *Proteins* **23**, 566–579.

Fuchs S. M. and Raines R. T. (2005). Polyarginine as a multifunctional fusion tag. *Protein Sci.* **14**, 1538–1544.

Fuchs S. M. and Raines R. T. (2007). Arginine grafting to endow cell permeability. *ACS Chem. Biol.* **2**, 167–170.

Fuchs S. M., Rutkoski T., Kung V., Groeschl R., and Raines R. T. (2007). Increasing the potency of a cytotoxin with an arginine graft. *Protein Eng. Des. Sel.* **20**, 505–509.

Funamoto S., Meili R., Lee S., Parry L., and Firtel R. A. (2002). Spatial and temporal regulation of 3-phosphoinositides by PI 3-kinase and PTEN mediates chemotaxis. *Cell* **109**, 611–623.

Gernsbacher M. A., Dawson M., and Goldsmith H. H. (2005). Three Reasons Not to Believe in an Autism Epidemic. *Curr. Dir. Psychol.* **14**, 55–58.

Gibson D. G., Young L., Chuang R. Y., Venter J. C., Hutchison C. A., and Smith H. O. (2009). Enzymatic assembly of DNA molecules up to several hundred kilobases. *Nat. Methods* **6**, 343–345.

Gicquel J.-J., Vabres P., Bonneau D., Mercié M., Handiri L., and Dighiero P. (2003). Retinal angioma in a patient with Cowden disease. *Am. J. Ophthalmol.* **135**, 400–402.

Goffin A., Hoefsloot L. H., Bosgoed E., Swillen A., and Fryns J. P. (2001). PTEN mutation in a family with Cowden syndrome and autism. *Am. J. Med. Genet.* **105**, 521–524.

Gu T., Zhang Z., Wong A. C., Wang J., Guo J., Shen W. H., and Yin Y. (2011). CREB is a Novel Nuclear Target of PTEN Phosphatase. *Cancer Res.* **71**, 2821–2825.

Hanahan D. and Weinberg R. A. (2000). The hallmarks of cancer. *Cell* **100**, 57–70.

Hanahan D. and Weinberg R. A. (2011). Hallmarks of cancer: the next generation. *Cell* **144**, 646–674.

Hanson R. M., Prilusky J., Renjian Z., Nakane T., and Sussman J. L. (2013). JSmol and the Next-Generation Web-Based Representation of 3D Molecular Structure as Applied to Proteopedia. *Isr. J. Chem.* **53**, 207–216.

Heffernan R., Paliwal K., Lyons J., Dehzangi A., Sharma A., Wang J., Sattar A., Yang Y., and Zhou Y. (2015). Improving prediction of secondary structure, local backbone angles, and solvent accessible surface area of proteins by iterative deep learning, Submitted.

Henikoff S. and Henikoff J. G. (1992). Amino acid substitution matrices from protein blocks. *Proc. Natl. Acad. Sci. U.S.A.* **89**, 10915–10919.

Heron M. (2013). Deaths: leading causes for 2010. *Natl. Vital Stat. Rep.* **62**, 1–96.

Hess H. H. and Derr J. E. (1975). Assay of inorganic and organic phosphorus in the 0.1-5 nanomole range. *Anal. Biochem.* **63**, 607–613.

Hobert J. A., Embacher R., Mester J. L., Frazier T. W., and Eng C. (2014). Biochemical screening and PTEN mutation analysis in individuals with autism spectrum disorders and macrocephaly. *Eur. J. Hum. Genet.* **22**, 273–276.

Hobert J. A., Mester J. L., Moline J., and Eng C. (2012). Elevated plasma succinate in PTEN, SDHB, and SDHD mutation-positive individuals. *Genet. Med.* **14**, 616–619.

Hopkins B. D., Fine B., Steinbach N., Dendy M., Rapp Z., Shaw J., Pappas K., Yu J. S., Hodakoski C., Mense S., Klein J., Pegno S., Sulis M.-L., Goldstein H., Amendolara B., Lei L., Maurer M., Bruce J., Canoll P., Hibshoosh H., and Parsons R. (2013). A secreted PTEN phosphatase that enters cells to alter signaling and survival. *Science* **341**, 399–402.

Hopkins B. D., Hodakoski C., Barrows D., Mense S. M., and Parsons R. E. (2014). PTEN function: The long and the short of it. *Trends Biochem. Sci.* **39**, 183–190.

Hunter J. D. (2007). Matplotlib: A 2D Graphics Environment. *Comput. Sci. Eng.* **9**, 90–95.

Imai K., Kricka L. J., and Fortina P. (2011). Concordance study of 3 direct-to-consumer genetic-testing services. *Clin. Chem.* **57**, 518–521.

Johnston S. B. (2015). Unpublished observations.

Johnston S. B. and Raines R. T. (2015a). Catalysis by the tumor-suppressor enzymes PTEN and PTEN-L. *PLoS One* **10**, e0116898.

Johnston S. B. and Raines R. T. (2015b). Conformational Stability and Catalytic Activity of PTEN Variants Linked to Cancers and Autism Spectrum Disorders. *Biochemistry* **54**, 1576–1582.

Jones D. S., Podolsky S. H., and Greene J. A. (2012). The burden of disease and the changing task of medicine. *N. Engl. J. Med.* **366**, 2333–2338.

Kanner L. (1943). Autistic disturbances of affective contact. *Nerv Child* **2**, 217–250.

Katsonis P., Koire A., Wilson S. J., Hsu T.-K., Lua R. C., Wilkins A. D., and Lichtarge O. (2014). Single nucleotide variations: biological impact and theoretical interpretation. *Protein Sci.* **23**, 1650–1666.

Kim D.-K., Myung S.-J., Yang S.-K., Hong S. S., Kim K. J., Byeon J.-S., Lee G. H., Kim J.-H., Min Y. I., Lee S. M., Jeong J.-Y., Song K., and Jung S.-A. (2005). Analysis of PTEN gene mutations in Korean patients with Cowden syndrome and polyposis syndrome. *Dis. Colon Rectum* **48**, 1714–1722.

Kirches E., Steiner J., Schneider T., Vorwerk C. K., Scherlach C., Holtkamp N., Keilhoff G., Eng C., and Mawrin C. (2010). Lhermitte-Duclos disease caused by a novel

germline PTEN mutation R173P in a patient presenting with psychosis. *Neuropathol. Appl. Neurobiol.* **36**, 86–89.

Knerr S., Personnaz L., and Dreyfus G. (1990). Single-layer learning revisited: a stepwise procedure for building and training a neural network. *Neurocomputing*. Berlin, Heidelberg, Springer Berlin Heidelberg, pp. 41–50.

Knowles J. R. (1987). Tinkering with enzymes: What are we learning? *Science* **236**, 1252–1258.

Kohno T., Takahashi M., Fukutomi T., Ushio K., and Yokota J. (1998). Germline mutations of the PTEN/MMAC1 gene in Japanese patients with Cowden disease. *Jpn. J. Cancer Res.* **89**, 471–474.

Kreis P., Leondaritis G., Lieberam I., and Eickholt B. J. (2014). Subcellular targeting and dynamic regulation of PTEN: Implications for neuronal cells and neurological disorders. *Front. Mol. Neurosci.* **7**, 23.

Kubo Y., Urano Y., Hida Y., Ikeuchi T., Nomoto M., Kunitomo K., and Arase S. (2000). A novel PTEN mutation in a Japanese patient with Cowden disease. *Br. J. Dermatol.* **142**, 1100–1105.

Kurose K., Araki T., Matsunaka T., Takada Y., and Emi M. (1999). Variant manifestation of Cowden disease in Japan: hamartomatous polyposis of the digestive tract with mutation of the PTEN gene. *Am. J. Hum. Genet.* **64**, 308–310.

Kwon C. H., Luikart B. W., Powell C. M., Zhou J., Matheny S. A., Zhang W., Li Y. J., Baker S. J., and Parada L. F. (2006). Pten regulates neuronal arborization and social interaction in mice. *Neuron* **50**, 377–388.

Kwon J., Lee S.-R., Yang K.-S., Ahn Y., Kim Y. J., Stadtman E. R., and Rhee S. G. (2004). Reversible oxidation and inactivation of the tumor suppressor PTEN in cells stimulated with peptide growth factors. *Proc. Natl. Acad. Sci. U.S.A.* **101**, 16419–16424.

Lachlan K. L., Lucassen A. M., Bunyan D., and Temple I. K. (2007). Cowden syndrome and Bannayan-Riley-Ruvalcaba syndrome represent one condition with variable expression and age-related penetrance: results of a clinical study of PTEN mutation carriers. *J. Med. Genet.* **44**, 579–585.

Lavery P., Brown M. J., and Pope A. J. (2001). Simple absorbance-based assays for ultra-high throughput screening. *J. Biomol. Screen.* **6**, 3–9.

Lee J.-O., Yang H., Georgescu M.-M., Di Cristofano A., Maehama T., Shi Y., Dixon J. E., Pandolfi P., and Pavletich N. P. (1999). Crystal structure of the PTEN tumor suppressor: Implications for its phosphoinositide phosphatase activity and membrane association. *Cell* **99**, 323–334.

Lee S.-R., Yang K.-S., Kwon J., Lee C., Jeong W., and Rhee S. G. (2002). Reversible inactivation of the tumor suppressor PTEN by H2O2. *J. Biol. Chem.* **277**, 20336–20342.

Levine M. N., Hoang T. T., and Raines R. T. (2013). Fluorogenic probe for constitutive cellular endocytosis. *Chem. Biol.* **20**, 614–618.

Li D. M. and Sun H. (1997). TEP1, encoded by a candidate tumor suppressor locus, is a novel protein tyrosine phosphatase regulated by transforming growth factor beta. *Cancer Res.* **57**, 2124–2129.

Li J., Yen C., Liaw D., Podsypanina K., Bose S., Wang S., Puc J., Miliaresis C., Rodgers L., McCombie R., Bigner S., Giovanella B., Ittmann M., Tycko B., Hibshoosh H., Wigler M., and Parsons R. (1997). PTEN, a putative protein tyrosine phosphatase gene mutated in human brain, breast, and prostate cancer. *Science* **275**, 1943–1947.

Liang H., He S., Yang J., Jia X., Wang P., Chen X., Zhang Z., Zou X., McNutt M., Shen W. H., and Yin Y. (2014). PTENα, a PTEN isoform translated through alternative initiation, regulates mitochondrial function and energy metabolism. *Cell Metab.* **19**, 836–848.

Liaw D., Marsh D. J., Li J., Dahia P. L., Wang S. I., Zheng Z., Bose S., Call K. M., Tsou H. C., Peacocke M., Eng C., and Parsons R. (1997). Germline mutations of the PTEN gene in Cowden disease, an inherited breast and thyroid cancer syndrome. *Nat. Genet.* **16**, 64–67.

Liliental J., Moon S. Y., Lesche R., Mamillapalli R., Li D., Zheng Y., Sun H., and Wu H. (2000). Genetic deletion of the Pten tumor suppressor gene promotes cell motility by activation of Rac1 and Cdc42 GTPases. *Curr. Biol.* **10**, 401–404.

Lobo G. P., Waite K. A., Planchon S. M., Romigh T., Nassif N. T., and Eng C. (2009). Germline and somatic cancer-associated mutations in the ATP-binding motifs of PTEN influence its subcellular localization and tumor suppressive function. *Hum. Mol. Genet.* **18**, 2851–2862.

Loffeld A., McLellan N. J., Cole T., Payne S. J., Fricker D., and Moss C. (2006). Epidermal naevus in Proteus syndrome showing loss of heterozygosity for an inherited PTEN mutation. *Br. J. Dermatol.* **154**, 1194–1198.

Lukesh J. C. I., Palte M., and Raines R. T. (2012). A potent, versatile disulfide-reducing agent from aspartic acid. *J. Am. Chem. Soc.* **134**, 4057–4059.

Lv J.-W., Cheng T.-L., Qiu Z.-L., and Zhou W.-H. (2013). Role of the PTEN signaling pathway in autism spectrum disorder. *Neurosci. Bull.* **29**, 773–778.

Lynch E. D., Ostermeyer E. A., Lee M. K., Arena J. F., Ji H., Dann J., Swisshelm K., Suchard D., MacLeod P. M., Kvinnsland S., Gjertsen B. T., Heimdal K., Lubs H., Møller P., and King M. C. (1997). Inherited mutations in PTEN that are associated with breast cancer, cowden disease, and juvenile polyposis. *Am. J. Hum. Genet.* **61**, 1254–1260.

Maehama T. and Dixon J. E. (1998). The tumor suppressor, PTEN/MMAC1, dephosphorylates the lipid second messenger, phosphatidylinositol 3,4,5-trisphosphate. *J. Biol. Chem.* **273**, 13375–13378.

Maehama T., Taylor G. S., Slama J. T., and Dixon J. E. (2000). A sensitive assay for phosphoinositide phosphatases. *Anal. Biochem.* **279**, 248–250.

Malaney P., Uversky V. N., and Davé V. (2013). The PTEN Long N-tail is intrinsically disordered: Increased viability for PTEN therapy. *Mol. BioSyst.* **9**, 2877–2888.

Manning B. D. and Cantley L. C. (2007). AKT/PKB signaling: Navigating downstream. *Cell* **129**, 1261–1274.

Marsh D. J., Dahia P. L., Zheng Z., Liaw D., Parsons R., Gorlin R. J., and Eng C. (1997). Germline mutations in PTEN are present in Bannayan-Zonana syndrome. *Nat. Genet.* **16**, 333–334.

Marsh D. J., Kum J. B., Lunetta K. L., Bennett M. J., Gorlin R. J., Ahmed S. F., Bodurtha J., Crowe C., Curtis M. A., Dasouki M., Dunn T., Feit H., Geraghty M. T., Graham J. M., Hodgson S. V., Hunter A., Korf B. R., Manchester D., Miesfeldt S., Murday V. A., Nathanson K. L., Parisi M., Pober B., Romano C., and Eng C. (1999). PTEN mutation spectrum and genotype-phenotype correlations in Bannayan-Riley-Ruvalcaba syndrome suggest a single entity with Cowden syndrome. *Hum. Mol. Genet.* **8**, 1461–1472.

Marsh D., Coulon V., Lunetta K., Rocca-Serra P., Dahia P., Zheng Z., Liaw D., Caron S., Duboue B., Lin A., Richardson A., Bonnetblanc J., Bressieux J., Cabarrot-Moreau A., Chompret A., Demange L., Eeles R., Yahanda A., Fearon E., Fricker J., Gorlin R., Hodgson S., Huson S., Lacombe D., LePrat F., Odent S., Toulouse C., Olopade O., Sobol H., Tishler S., Woods C., Robinson B., Weber H., Parsons R., Peacocke M.,

Longy M., and Eng C. (1998). Mutation spectrum and genotype-phenotype analyses in Cowden disease and Bannayan-Zonana syndrome, two hamartoma syndromes with germline PTEN mutation. *Hum. Mol. Genet.* **7**, 507–515.

Martin T. F. J. (1998). Phosphoinositide lipids as signaling molecules: Common themes for signal transduction, cytoskeletal regulation, and membrane trafficking. *Annu. Rev. Cell Dev. Biol.* **14**, 231–264.

Martin-Belmonte F., Gassama A., Datta A., Yu W., Rescher U., Gerke V., and Mostov K. (2007). PTEN-mediated apical segregation of phosphoinositides controls epithelial morphogenesis through Cdc42. *Cell* **128**, 383–397.

McBride K. L., Varga E. A., Pastore M. T., Prior T. W., Manickam K., Atkin J. F., and Herman G. E. (2010). Confirmation study of PTEN mutations among individuals with autism or developmental delays/mental retardation and macrocephaly. *Autism Res.* **3**, 137–141.

McConnachie G., Pass I., Walker S. M., and Downes C. P. (2003). Interfacial kinetic analysis of the tumour suppressor phosphatase, PTEN: Evidence for activation by anionic phospholipids. *Biochem. J.* **371**, 947–955.

Melander W. and Horvath C. (1977). Salt effects on hydrophobic interactions in precipitation and chromatography of proteins: An interpretation of the lyotropic series. *Arch. Biochem. Biophys.* **183**, 200–215.

Mester J. L., Tilot A. K., Rybicki L. A., Frazier Thomas W I., and Eng C. (2011). Analysis of prevalence and degree of macrocephaly in patients with germline PTEN mutations and of brain weight in Pten knock-in murine model. *Eur. J. Hum. Genet.* **19**, 763–768.

Miller P. J., Duraisamy S., Newell J. A., Chan P. A., Tie M. M., Rogers A. E., Ankuda C. K., Walstrom G. M. von, Bond J. P., and Greenblatt M. S. (2011). Classifying Variants of CDKN2A Using Computational and Laboratory Studies. *Hum. Mutat.* **32**, 900–911.

Molina Martinez D., Jafari R., Ignatushchenko M., Seki T., Larsson E., Dan C., Sreekumar L., Cao Y., and Nordlund P. (2013). Monitoring drug target engagement in cells and tissues using the cellular thermal shift assay. *Science* **341**, 84–87.

Monod J., Wyman J., and Changeux J. (1965). On the nature of allosteric transitions: A plausible model. *J. Mol. Biol.* **12**, 88–118.

Mosca R., Céol A., and Aloy P. (2013). Interactome3D: adding structural details to protein networks. *Nature* **10**, 47–53.

Myers M. P., Stolarov J. P., Eng C., Li J., Wang S. I., Wigler M. H., Parsons R., and Tonks N. K. (1997). P-TEN, the tumor suppressor from human chromosome 10q23, is a dual-specificity phosphatase. *Proc. Natl. Acad. Sci. U.S.A.* **94**, 9052–9057.

Nagy R., Ganapathi S., Comeras I., Peterson C., Orloff M., Porter K., Eng C., Ringel M. D., and Kloos R. T. (2011). Frequency of germline PTEN mutations in differentiated thyroid cancer. *Thyroid* **21**, 505–510.

Nelen M. R., Kremer H., Konings I. B., Schoute F., Essen A. J. van, Koch R., Woods C. G., Fryns J. P., Hamel B., Hoefsloot L. H., Peeters E. A., and Padberg G. W. (1999). Novel PTEN mutations in patients with Cowden disease: absence of clear genotype-phenotype correlations. *Eur. J. Hum. Genet.* **7**, 267–273.

Nelen M. R., Staveren W. C. van, Peeters E. A., Hassel M. B., Gorlin R. J., Hamm H., Lindboe C. F., Fryns J. P., Sijmons R. H., Woods D. G., Mariman E. C., Padberg G. W., and Kremer H. (1997). Germline mutations in the PTEN/MMAC1 gene in patients with Cowden disease. *Hum. Mol. Genet.* **6**, 1383–1387.

Nelson D. L. and Cox M. M. (2008). *Principles of Biochemistry.*

Newschaffer C. J., Croen L. A., Daniels J., Giarelli E., Grether J. K., Levy S. E., Mandell D. S., Miller L. A., Pinto-Martin J., Reaven J., Reynolds A. M., Rice C. E., Schendel D., and Windham G. C. (2007). The epidemiology of autism spectrum disorders. *Annu. Rev. Public Health* **28**, 235–258.

Ng P. C. and Henikoff S. (2001). Predicting deleterious amino acid substitutions. *Genome Res.* **11**, 863–874.

Ng P. C. and Henikoff S. (2003). SIFT: Predicting amino acid changes that affect protein function. *Nucleic Acids Res.* **31**, 3812–3814.

Ngeow J. and Eng C. (2014). PTEN Hamartoma Tumor Syndrome: Clinical Risk Assessment and Management Protocol. *Methods*, 10.1016/j.ymeth.2014.10.011.

Nielsen H., Engelbrecht J., Brunak S., and Heijne G. von. (1997). Identification of prokaryotic and eukaryotic signal peptides and prediction of their cleavage sites. *Protein Eng.* **10**, 1–6.

Nielsen H. and Krogh A. (1998). Prediction of signal peptides and signal anchors by a hidden Markov model. *Proc. Int. Conf. Intell. Syst. Mol. Biol.* **6**, 122–130.

Niesen F. H., Berglund H., and Vedadi M. (2007). The use of differential scanning fluorimetry to detect ligand interactions that promote protein stability. *Nat. Protoc.* **2**, 2212–2221.

Olschwang S., Serova-Sinilnikova O. M., Lenoir G. M., and Thomas G. (1998). PTEN germ-line mutations in juvenile polyposis coli. *Nat. Genet.* **18**, 12–14.

Orrico A., Galli L., Buoni S., Orsi A., Vonella G., and Sorrentino V. (2009). Novel PTEN mutations in neurodevelopmental disorders and macrocephaly. *Clin. Genet.* **75**, 195–198.

O'Sullivan C. and Tompson F. W. (1890). LX.—Invertase: A contribution to the history of an enzyme or unorganised ferment. *J. Chem. Soc.* **57**, 834–931.

Papa A., Wan L., Bonora M., Salmena L., Song M. S., Hobbs R. M., Lunardi A., Webster K., Ng C., Newton R. H., Knoblauch N., Guarnerio J., Ito K., Turka L. A., Beck A. H., Pinton P., Bronson R. T., Wei W., and Pandolfi P. P. (2014). Cancer-associated PTEN

mutants act in a dominant-negative manner to suppress PTEN protein function. *Cell* **157**, 595–610.

Pappalardo M. and Wass M. N. (2014). VarMod: modelling the functional effects of non-synonymous variants. *Nucleic Acids Res.* **42**, W331–W336.

Parisi M. A., Dinulos M. B., Leppig K. A., Sybert V. P., Eng C., and Hudgins L. (2001). The spectrum and evolution of phenotypic findings in PTEN mutation positive cases of Bannayan-Riley-Ruvalcaba syndrome. *J. Med. Genet.* **38**, 52–58.

Park C. and Marqusee S. (2005). Pulse proteolysis: A simple method for quantitative determination of protein stability and ligand binding. *Nat. Methods* **2**, 307–312.

Park C. and Raines R. T. (2001). Quantitative analysis of the effect of salt concentration on enzymatic catalysis. *J. Am. Chem. Soc.* **123**, 11472–11479.

Paulsen C. E., Truong T. H., Garcia F. J., Homann A., Gupta V., Leonard S. E., and Carroll K. S. (2012). Peroxide-dependent sulfenylation of the EGFR catalytic site enhances kinase activity. *Nat. Chem. Biol.* **8**, 57–64.

Pedregosa F., Varoquaux G., Gramfort A., Michel V., Thirion B., Grisel O., Blondel M., Prettenhofer P., Weiss R., Dubourg V., Vanderplas J., Passos A., Cournapeau D., Brucher M., Perrot M., and Duchesnay E. (2011). Scikit-learn: Machine Learning in Python. *J. Mach. Learn. Res.* **12**, 2825–2830.

Perren A., Komminoth P., Saremaslani P., Matter C., Feurer S., Lees J., Heitz P., and Eng C. (2000). Mutation and expression analyses reveal differential subcellular compartmentalization of PTEN in endocrine pancreatic tumors compared to normal islet cells. *Am. J. Pathol.* **157**, 1097–1103.

Petersen T. N., Brunak S., Heijne G. von, and Nielsen H. (2011). SignalP 4.0: discriminating signal peptides from transmembrane regions. *Nature* **8**, 785–786.

Pierce A. J., Stark J. M., Araujo F. D., Moynahan M. E., Berwick M., and Jasin M. (2001). Double-strand breaks and tumorigenesis. *Trends Cell Biol.* **11**, S52–S59.

Porter C. M. and Miller B. G. (2012). Cooperativity in monomeric enzymes with single ligand-binding sites. *Bioorg. Chem.* **43**, 44–50.

Powers D. M. W. (2011). Evaluation: from Precision, Recall and F-measure to ROC, Informedness, Markedness and Correlation. *J. Mach. Learn. Tech.* **2**, 37–63.

Pulido R., Baker S. J., Barata J. T., Carracedo A., Cid V. J., Chin-Sang I. D., Davé V., Hertog J. den, Devreotes P., Eickholt B. J., Eng C., Furnari F. B., Georgescu M.-M., Gericke A., Hopkins B., Jiang X., Lee S.-R., Lösche M., Malaney P., Matias-Guiu X., Molina M., Pandolfi P. P., Parsons R., Pinton P., Rivas C., Rocha R. M., Rodríguez M. S., Ross A. H., Serrano M., Stambolic V., Stiles B., Suzuki A., Tan S.-S., Tonks N. K., Trotman L. C., Wolff N., Woscholski R., Wu H., and Leslie N. R. (2014). A unified nomenclature and amino acid numbering for human PTEN. *Sci. Signal.* **7**, pe15.

Raftopoulou M., Etienne-Manneville S., Self A., Nicholls S., and Hall A. (2004). Regulation of cell migration by the C2 domain of the tumor suppressor PTEN. *Science* **303**, 1179–1181.

Ramensky V., Bork P., and Sunyaev S. (2002). Human non-synonymous SNPs: server and survey. *Nucleic Acids Res.* **30**, 3894–3900.

Reardon W., Zhou X.-P., and Eng C. (2001). A novel germline mutation of the PTEN-gene in a patient with macrocephaly, ventricular dilatation, and features of VATER association. *J. Med. Genet.* **38**, 820–823.

Reddie K. G., Seo Y. H., Muse Iii W. B., Leonard S. E., and Carroll K. S. (2008). A chemical approach for detecting sulfenic acid-modified proteins in living cells. *Mol. BioSyst.* **4**, 521–531.

Redfern R. E., Daou M. C., Li L., Munson M., Gericke A., and Ross A. H. (2010). A mutant form of PTEN linked to autism. *Protein Sci.* **19**, 1948–1956.

Redfern R. E., Redfern D., Furgason M. L. M., Munson M., Ross A. H., and Gericke A. (2008). PTEN phosphatase selectively binds phosphoinositides and undergoes structural changes. *Biochemistry* **47**, 2162–2171.

Reumers J., Schymkowitz J., Ferkinghoff-Borg J., Stricher F., Serrano L., and Rousseau F. (2005). SNPeffect: a database mapping molecular phenotypic effects of human non-synonymous coding SNPs. *Nucleic Acids Res.* **33**, D527–D532.

Roach J. C., Glusman G., Smit A. F. A., Huff C. D., Hubley R., Shannon P. T., Rowen L., Pant K. P., Goodman N., Bamshad M., Shendure J., Drmanac R., Jorde L. B., Hood L., and Galas D. J. (2010). Analysis of genetic inheritance in a family quartet by whole-genome sequencing. *Science* **328**, 636–639.

Rodríguez-Escudero I., Oliver M. D., Andres-Pons A., Molina M., Cid V. J., and Pulido R. (2011). A comprehensive functional analysis of PTEN mutations: implications in tumor- and autism-related syndromes. *Hum. Mol. Genet.* **20**, 4132–4142.

Rodríguez-Escudero I., Fernández-Acero T., Bravo I., Leslie N. R., Pulido R., Molina M., and Cid V. J. (2014). Yeast-based methods to assess PTEN phosphoinositide phosphatase activity in vivo. *Methods*.

Rüegg M., Moor U., and Blanc B. (1977). A calorimetric study of the thermal denaturation of whey proteins in simulated milk ultrafiltrate. *J. Dairy Res.* **44**, 509–520.

Rutkoski T. J. and Raines R. T. (2008). Evasion of ribonuclease inhibitor as a determinant of ribonuclease cytotoxicity. *Curr. Pharm. Biotechnol.* **9**, 185–189.

Salmena L., Carracedo A., and Pandolfi P. P. (2008). Tenets of PTEN tumor suppression. *Cell* **133**, 403–414.

Sawada T., Hamano N., Satoh H., Okada T., Takeda Y., and Mabuchi H. (2000). Mutation analysis of the PTEN / MMAC1 gene in Japanese patients with Cowden disease. *Jpn. J. Cancer Res.* **91**, 700–705.

Sawada T., Okada T., Miwa K., Satoh H., Asano A., and Mabuchi H. (2004). Two novel mutations of PTEN gene in Japanese patients with Cowden syndrome. *Am. J. Med. Genet. A.* **128A**, 12–14.

Scala S., Bruni P., Lo Muzio L., Mignogna M., Viglietto G., and Fusco A. (1998). Novel mutation of the PTEN gene in an Italian Cowden's disease kindred. *Int. J. Oncol.* **13**, 665–668.

Schaletzky J., Dove S. K., Short B., Lorenzo O., Clague M. J., and Barr F. A. (2003). Phosphatidylinositol-5-phosphate activation and conserved substrate specificity of the myotubularin phosphatidylinositol 3-phosphatases. *Curr. Biol.* **13**, 504–509.

Schellman J. A. (1975). Macromolecular binding. *Biopolymers* **14**, 999–1018.

Schwarze S. R., Ho A., Vocero-Akbani A., and Dowdy S. F. (1999). In vivo protein transduction: delivery of a biologically active protein into the mouse. *Science* **285**, 1569–1572.

Shabalina S. A., Ogurtsov A. Y., Kondrashov V. A., and Kondrashov A. S. (2001). Selective constraint in intergenic regions of human and mouse genomes. *Trends Genet.* **17**, 373–376.

Shen W. H., Balajee A. S., Wang J., Wu H., Eng C., Pandolfi P. P., and Yin Y. (2007). Essential role for nuclear PTEN in maintaining chromosomal integrity. *Cell* **128**, 157–170.

Sherry S. T., Ward M. H., Kholodov M., Baker J., Phan L., Smigielski E. M., and Sirotkin K. (2001). dbSNP: the NCBI database of genetic variation. *Nucleic Acids Res.* **29**, 308–311.

Silva A., Yunes J. A., Cardoso B. A., Martins L. R., Jotta P. Y., Abecasis M., Nowill A. E., Leslie N. R., Cardoso A. A., and Barata J. T. (2008). PTEN posttranslational inactivation and hyperactivation of the PI3K/Akt pathway sustain primary T cell leukemia viability. *J. Clin. Invest.* **118**, 3762–3774.

Song M. S., Carracedo A., Salmena L., Song S. J., Egia A., Malumbres M., and Pandolfi P. P. (2011). Nuclear PTEN regulates the APC-CDH1 tumor-suppressive complex in a phosphatase-independent manner. *Cell* **144**, 187–199.

Song M. S., Salmena L., and Pandolfi P. P. (2012). The functions and regulation of the PTEN tumour suppressor. *Nat. Rev. Mol. Cell Biol.* **13**, 283–296.

Spinelli L., Black F. M., Berg J. N., Eickholt B. J., and Leslie N. R. (2015). Functionally distinct groups of inherited PTEN mutations in autism and tumour syndromes. *J. Med. Genet.* **52**, 128–134.

Staal F. J. T., Luijt R. B. van der, Baert M. R. M., Drunen J. van, Bakel H. van, Peters E., Valk I. de, Amstel H. K. P. van, Taphoorn M. J. B., Jansen G. H., Veelen C. W. M. van, Burgering B., and Staal G. E. J. (2002). A novel germline mutation of PTEN associated with brain tumours of multiple lineages. *Br. J. Cancer* **86**, 1586–1591.

Stambolic V., Suzuki A., Pompa J. L. de la, Brothers G. M., Mirtsos C., Sasaki T., Ruland J., Penninger J., Siderovski D., and Mak T. (1998). Negative regulation of PKB/Akt-dependent cell survival by the tumor suppressor PTEN. *Cell* **95**, 29–39.

Steck P. A., Pershouse M. A., Jasser S. A., Yung W. K., Lin H., Ligon A. H., Langford L. A., Baumgard M. L., Hattier T., Davis T., Frye C., Hu R., Swedlund B., Teng D. H., and Tavtigian S. V. (1997). Identification of a candidate tumour suppressor gene, MMAC1, at chromosome 10q23.3 that is mutated in multiple advanced cancers. *Nat. Genet.* **15**, 356–362.

Stenson P. D., Mort M., Ball E. V., Shaw K., Phillips A., and Cooper D. N. (2014). The Human Gene Mutation Database: building a comprehensive mutation repository for clinical and molecular genetics, diagnostic testing and personalized genomic medicine. *Hum. Genet.* **133**, 1–9.

Stone E. A. and Sidow A. (2005). Physicochemical constraint violation by missense substitutions mediates impairment of protein function and disease severity. *Genome Res.* **15**, 978–986.

Supek F., Miñana B., Valcárcel J., Gabaldón T., and Lehner B. (2014). Synonymous mutations frequently act as driver mutations in human cancers. *Cell* **156**, 1324–1335.

Tamura M., Gu J. G., Danen E. H. J., Takino T., Miyamoto S., and Yamada K. M. (1999). PTEN interactions with focal adhesion kinase and suppression of the extracellular matrix-dependent phosphatidylinositol 3-kinase/Akt cell survival pathway. *J. Biol. Chem.* **274**, 20693–20703.

Tamura M., Gu J., Matsumoto K., Aota S., Parsons R., and Yamada K. M. (1998). Inhibition of cell migration, spreading, and focal adhesions by tumor suppressor PTEN. *Science* **280**, 1614–1617.

Tan M.-H., Mester J., Peterson C., Yang Y., Chen J.-L., Rybicki L. A., Milas K., Pederson H., Remzi B., Orloff M. S., and Eng C. (2011). A clinical scoring system for selection of patients for PTEN mutation testing is proposed on the basis of a prospective study of 3042 probands. *Am. J. Hum. Genet.* **88**, 42–56.

Tan W.-H., Baris H. N., Burrows P. E., Robson C. D., Alomari A. I., Mulliken J. B., Fishman S. J., and Irons M. B. (2007). The spectrum of vascular anomalies in patients with PTEN mutations: implications for diagnosis and management. *J. Med. Genet.* **44**, 594–602.

Tate G., Suzuki T., Endo Y., and Mitsuya T. (2008). A novel mutation of the PTEN gene in a Japanese patient with Cowden syndrome and bilateral breast cancer. *Cancer Genet. Cytogenet.* **184**, 67–71.

Taylor G. S. and Dixon J. E. (2003). PTEN and myotubularins: Families of phosphoinositide phosphatases. *Methods Enzymol.* **366**, 43–56.

Tekin M., Hişmi B. O., Fitoz S., Yalçinkaya F., Ekim M., Kansu A., Ertem M., Deda G., Tutar E., Arsan S., Zhou X.-P., Pilarski R., Eng C., and Akar N. (2006). A germline PTEN mutation with manifestations of prenatal onset and verrucous epidermal nevus. *Am. J. Med. Genet. A.* **140**, 1472–1475.

Thiffault I., Schwartz C. E., Der Kaloustian V., and Foulkes W. D. (2004). Mutation analysis of the tumor suppressor PTEN and the glypican 3 (GPC3) gene in patients diagnosed with Proteus syndrome. *Am. J. Med. Genet. A.* **130A**, 123–127.

Thompson B. A., Greenblatt M. S., Vallee M. P., Herkert J. C., Tessereau C., Young E. L., Adzhubey I. A., Li B., Bell R., Feng B., Mooney S. D., Radivojac P., Sunyaev S. R., Frebourg T., Hofstra R. M., Sijmons R. H., Boucher K., Thomas A., Goldgar D. E., Spurdle A. B., and Tavtigian S. V. (2012). Calibration of Multiple In Silico Tools for Predicting Pathogenicity of Mismatch Repair Gene Missense Substitutions. *Hum. Mutat.*

Tipton K. F. (2002). *Enzyme Assays: A Practical Approach, 2nd ed.* Ed. by R. Eisenthal and M. Danson. New York, NY, Oxford University Press, 1–48.

Topham C. M., Srinivasan N., and Blundell T. L. (1997). Prediction of the stability of protein mutants based on structural environment-dependent amino acid substitution and propensity tables. *Protein Eng.* **10**, 7–21.

Torre L. A., Bray F., Siegel R. L., Ferlay J., Lortet-Tieulent J., and Jemal A. (2015). Global cancer statistics, 2012. *CA. Cancer J. Clin.* **65**, 87–108.

Trotman L. C., Wang X., Alimonti A., Chen Z., Teruya-Feldstein J., Yang H., Pavletich N. P., Carver B. S., Cordon-Cardo C., Erdjument-Bromage H., Tempst P., Chi S.-G., Kim H.-J., Misteli T., Jiang X., and Pandolfi P. P. (2007). Ubiquitination regulates PTEN nuclear import and tumor suppression. *Cell* **128**, 141–156.

Tsou H. C., Ping X. L., Xie X. X., Gruener A. C., Zhang H., Nini R., Swisshelm K., Sybert V., Diamond T. M., Sutphen R., and Peacocke M. (1998). The genetic basis of Cowden's syndrome: three novel mutations in PTEN/MMAC1/TEP1. *Hum. Genet.* **102**, 467–473.

Turner T., Van Epps-Fung M., Kassis J., and Wells A. (1997). Molecular inhibition of phospholipase Cγ signaling abrogates DU-145 prostate tumor cell invasion. *Clin. Cancer Res.* **3**, 2275–2282.

Varga E. A., Pastore M., Prior T., Herman G. E., and McBride K. L. (2009). The prevalence of PTEN mutations in a clinical pediatric cohort with autism spectrum disorders, developmental delay, and macrocephaly. *Genet. Med.* **11**, 111–117.

Vazquez F., Grossman S. R., Takahashi Y., Rokas M. V., Nakamura N., and Sellers W. R. (2001). Phosphorylation of the PTEN tail acts as an inhibitory switch by preventing its recruitment into a protein complex. *J. Biol. Chem.* **276**, 48627–48630.

Vega A., Torres J., Torres M., Cameselle-Teijeiro J., Macia M., Carracedo A., and Pulido R. (2003). A novel loss-of-function mutation (N48K) in the PTEN gene in a Spanish patient with Cowden disease. *J. Invest. Dermatol.* **121**, 1356–1359.

Webb M. R. (1992). A continuous spectrophotometric assay for inorganic phosphate and for measuring phosphate release kinetics in biological systems. *Proc. Natl. Acad. Sci. U.S.A.* **89**, 4884–4887.

Whiteman D. C., Zhou X.-P., Cummings M. C., Pavey S., Hayward N. K., and Eng C. (2002). Nuclear PTEN expression and clinicopathologic features in a population-based series of primary cutaneous melanoma. *Int. J. Cancer* **99**, 63–67.

Willsey A. J. and State M. W. (2015). Autism spectrum disorders: from genes to neurobiology. *Curr. Opin. Neurobiol.* **30**, 92–99.

Worby C. and Dixon J. E. (2014). PTEN. *Annu. Rev. Biochem.* **83**, 641–669.

Xue Y., Liu Z., Cao J., Ma Q., Gao X., Wang Q., Jin C., Zhou Y., Wen L., and Ren J. (2011). GPS 2.1: Enhanced prediction of kinase-specific phosphorylation sites with an algorithm of motif length selection. *Protein Eng. Des. Sel.* **24**, 255–260.

Yates C. M., Filippis I., Kelley L. A., and Sternberg M. J. E. (2014). SuSPect: enhanced prediction of single amino acid variant (SAV) phenotype using network features. *J. Mol. Biol.* **426**, 2692–2701.

Zhong S., Hsu F., Stefan C. J., Wu X., Patel A., Cosgrove M. S., and Mao Y. (2012). Allosteric activation of the phosphoinositide phosphatase Sac1 by anionic phospholipids. *Biochemistry* **51**, 3170–3177.

Zhou H.-X., Rivas G., and Minton A. P. (2008). Macromolecular crowding and confinement: Biochemical, biophysical, and potential physiological consequences. *Annu. Rev. Biophys.* **2008**, 375–397.

Zhou X., Hampel H., Thiele H., Gorlin R., Hennekam R., Parisi M., Winter R., and Eng C. (2001). Association of germline mutation in the PTEN tumour suppressor gene and Proteus and Proteus-like syndromes. *Lancet* **358**, 210–211.

Zori R. T., Marsh D. J., Graham G. E., Marliss E. B., and Eng C. (1998). Germline PTEN mutation in a family with Cowden syndrome and Bannayan-Riley-Ruvalcaba syndrome. *Am. J. Med. Genet.* **80**, 399–402.